Modular and Automated Synthesis of Oligonucleotide-Small Molecule Conjugates for Cathepsin B Mediated Traceless Release of Payloads

Cheng Jin[1,2]*, Siqi Li[1,3], Katherine A. Vallis[3], Afaf H. El-Sagheer[1,4] and Tom Brown[1]*

1. Department of Chemistry, Chemistry Research Laboratory, University of Oxford, 12 Mansfield Road, Oxford, OX1 3TA, United Kingdom

2. Hangzhou Institute of Medicine (HIM), Chinese Academy of Sciences, Zhejiang Cancer Hospital, Hangzhou, Zhejiang 310022, China

3. Medical Research Council, Oxford Institute for Radiation Oncology, Department of Oncology, University of Oxford, Oxford, OX3 7DQ, United Kingdom

4. Department of Science and Mathematics, Suez University, Faculty of Petroleum and Mining Engineering, Suez, 43721, Egypt

*Corresponding authors: jincheng@him.cas.cn (C.J.) and tom.brown@chem.ox.ac.uk (T.B.)

ABSTRACT

Attachment of small molecules to oligonucleotides is a versatile tool in the development of therapeutic oligonucleotides. However, cleavable linkers in the oligonucleotide field are scarce, particularly with respect to the requirement of traceless release of payload *in vivo*. Herein, a cathepsin B-cleavable dipeptide phosphoramidite, Val-Ala(NB), is developed for the automated synthesis of oligonucleotide-small molecule conjugates. Val-Ala(NB) was protected by photolabile 2-nitrobenzyl to improve stability of the peptide linker during DNA synthesis. After photolysis, intracellular cathepsin B digests the dipeptide efficiently, releasing the payload-phosphate which is converted to the free payload by endogenous phosphatase enzymes. With the advantages of modular synthesis and stimuli-responsive drug release, we believe Val-Ala(NB) will be a commonly used cleavable linker in the development of oligonucleotide-drug conjugates.

INTRODUCTION

Solid-phase synthesis of oligonucleotides is well known as an example of automated and modular molecular synthesis. This technology enables the programmable synthesis of oligonucleotides by iterative assembly of nucleosides phosphoramidites on resins.[1] In addition to nucleosides, other

small molecules can also covalently attach to oligonucleotides through solid-phase phosphoramidite chemistry in high yield. These well-defined oligonucleotide-small molecule conjugates combine the functionality of small molecules and the sequence-specific target recognition of nucleic acids, expanding their potential practical uses. Fluorescence dyes/probes, hydrophobic molecules, targeting molecules and therapeutic reagents have all been conjugated with oligonucleotides for bioanalytical sensing,[2, 3] molecular assembly[4-6] and drug development.[7-10] In general, linkers between oligonucleotides and small molecules are non-cleavable and provide a stable connection. However, for oligonucleotide-drug conjugates in which small-molecule drugs should be conditionally released after entering into the target cells, cleavable linkers are needed between the two entities.[11, 12]

Cleavable linkers are molecules that join two functional moieties through a cleavable bond.[13] Incorporation of cleavable linkers into therapeutic molecules confers advantages of site-specific and stimuli-responsive cleavage.[14-17] This enables the controllable release of payload which can lower side effects and provide precision medicines. However, commonly used cleavable linkers in oligonucleotides field, photocleavage (PC) and disulfide linkers, have drawbacks for in vivo applications. For example, limited tissue penetration of ultraviolet light for cleavage of the PC linker and poor stability of disulfide linker during blood circulation. Inspired by the cathepsin B-sensitive dipeptide linkers in FDA-approved antibody-drug conjugates (ADCs),[18-20] we recently reported the development of Val-Ala-02 dipeptide linker phosphoramidite for the automated synthesis of enzyme-cleavable oligonucleotides.[21] In the Val-Ala-02 structure p-aminophenethyl alcohol, instead of self-immolative p-aminobenzyl alcohol, was conjugated with the dipeptide moiety. Val-Ala-02 shows excellent stability during DNA synthesis but cannot be used for the traceless release of payloads.

Herein, therefore, we overcome this problem by developing a novel dipeptide linker phosphoramidite for the automated and modular synthesis of oligonucleotide-small molecule conjugates. As shown in Figure 1, we synthesized Val-Ala(NB) dipeptide phosphoramidite in which the dipeptide is protected by a photolabile 2-nitrobenzyl group to enhance stability during DNA

synthesis. After DNA synthesis, deprotection and photolysis, cathepsin B is able to cleave the Val-Ala dipeptide of oligonucleotide-payload conjugates. As a result, payload-phosphate is released which is further converted to the dephosphorylated small molecule by phosphatase enzymes. ODN7UV, a DNA conjugate with the microtubule destabilizing reagent combretastatin A-4 (CA4) attached via Val-Ala linker, was delivered to HCT116 cells by lipofectamine. After transfection, we found a clear decline of cell viability which can be attribute to the release of CA4 via intracellular cathepsin B-mediated cleavage of the dipeptide. In addition, payloads containing an amino group can conjugate with Val-Ala(NB) via a carbamate linkage through a two-step solid-phase process, expanding the general utility of Val-Ala(NB) phosphoramidite in the facile synthesis of oligonucleotide-small molecule conjugates.

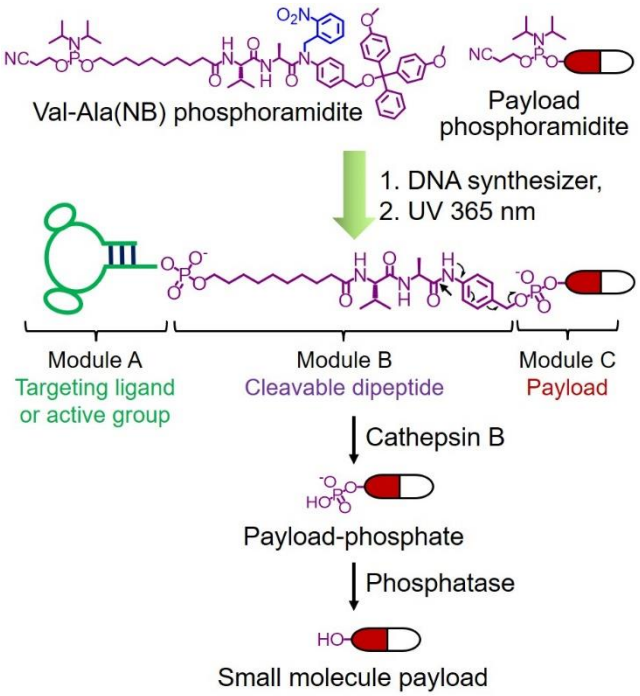

Figure 1. Schematic illustration of modular and automated synthesis of targeting ligands-small molecule conjugates using of Val-Ala(NB) phosphoramidite on DNA synthesizer, and the release of payload-phosphate after cathepsin B-mediated enzymatic cleavage. Photolabile 2-nitrobenzyl on Val-Ala(NB) monomer stabilizes the dipeptide during DNA synthesis. The released payload-phosphate can be designed as a prodrug or probe which is converted to the dephosphorylated small molecule by phosphatase enzymes.

Results and Discussion

In solid-phase oligonucleotide synthesis, phosphoramidite monomers are iteratively and efficiently assembled on solid support. Using this principle, almost any small molecule can be covalently attached to oligonucleotides provided that the corresponding phosphoramidite is available and the small molecule is stable during oligonucleotide synthesis and deprotection.[22] To develop a cathepsin B-cleavable dipeptide phosphoramidite for traceless release of payload after enzymatic cleavage, a self-immolative spacer was designed to link to the dipeptide on one side, and a small molecule on the other side via a phosphodiester linkage. p-Aminobenzyl alcohol is a typical self-immolative linker that has been used in ADCs such as Adcetris.[23, 24] However, we previously reported that the p-acetamidobenzyl(PAB)-phosphodiester structure has poor stability during oligonucleotide synthesis/deprotection.[21] We speculate that the acetamido group at the para-position leads to degradation of the PAB-phosphodiester during oligonucleotide synthesis/deprotection. To evaluate this hypothesis, benzyl, PAB and N-methylated PAB (mPAB) phosphoramidites were synthesized and conjugated to DNA (Figure 2). After oligonucleotide synthesis, the DNA conjugates were deprotected with concentrated aqueous ammonia at room temperature for two hours. As shown in Figures 2b and S3, consistent with the previous report, DNA-PAB conjugate (ODN2) was completely degraded, and was even unstable to ultra-mild deprotection by 50 mM K_2CO_3 in methanol at room temperature for 4 hours (Figure S4). However, DNA-benzyl (ODN1) and DNA-mPAB (ODN3) conjugates have better stability compared to ODN2, with 40.8% degradation for ODN1 and 56.2% degradation for ODN3 (Figures 2a, 2c). These results indicate that PAB-phosphodiester structure has poor stability during oligonucleotide synthesis/deprotection while N-methylation of PAB-phosphodiester improves the stability.

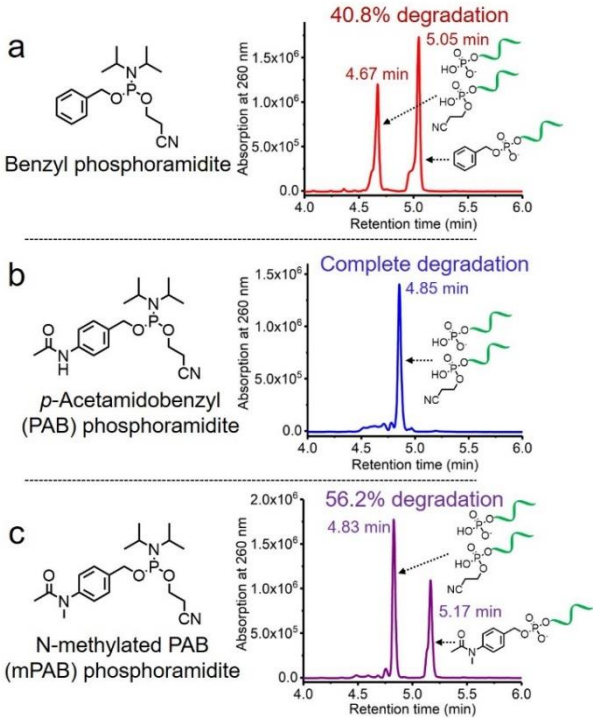

Figure 2. HPLC traces of (**a**) DNA-benzyl conjugate (ODN1), (**b**) DNA-PAB conjugate (ODN2) and (**c**) DNA-mPAB conjugate (ODN3) after deprotection by ammonia at room temperature for two hours. The percentages of degradation of ODN1, ODN2 and ODN3 are 40.8%, almost 100% and 56.2%, respectively, demonstrating that N-methylation of PAB-phosphodiester enhances stability during oligonucleotide synthesis and deprotection.

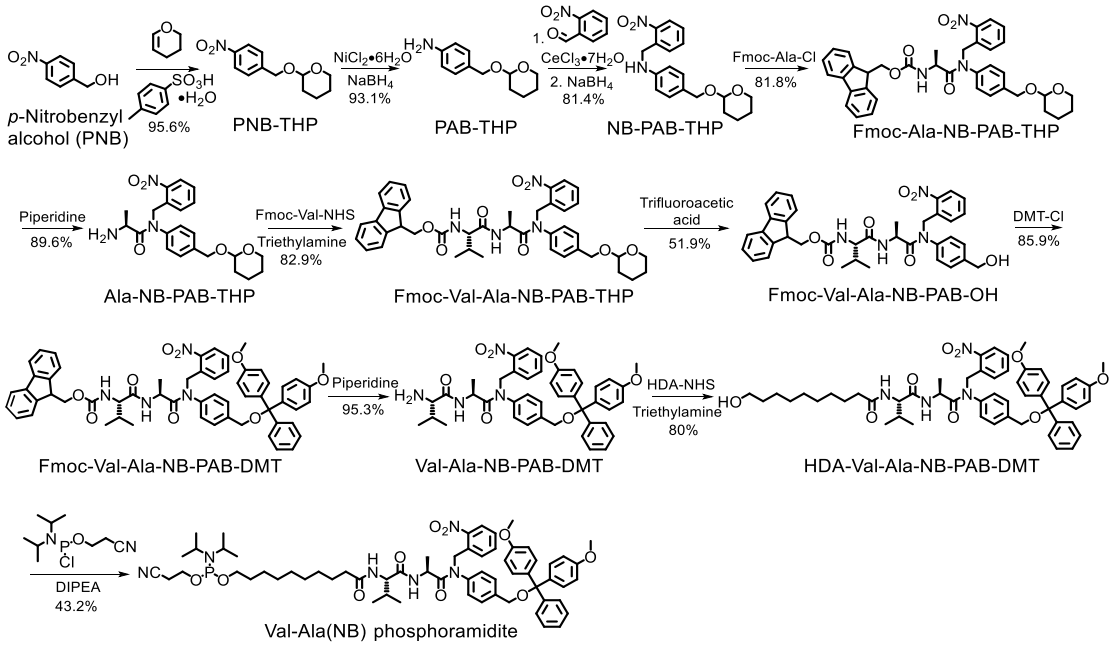

Figure 3. Synthesis of Val-Ala(NB) phosphoramidite. Fmoc-Ala-Cl: Fmoc-L-alanyl

chloride. DMT-Cl: 4,4'-dimethoxytrityl chloride. HDA-NHS: NHS-protected 10-hydroxydecanoic acid. DIPEA: N,N-diisopropylethylamine.

Encouraged by these results, we designed Val-Ala(NB) phosphoramidite in which the dipeptide is protected by a photolabile 2-nitrobenzyl group to enhance stability. As shown in Figure 3, p-nitrobenzyl alcohol (PNB) was protected with tetrahydropyranyl (THP) in 95.6% yield, and the resulted PNB-THP was reduced to PAB-THP by $NaBH_4$ and nickel (II) chloride hexahydrate in an acetonitrile-water mixture. PAB-THP was then reacted with 2-nitrobenzaldehyde and then reduced with $NaBH_4$ to provide NB-PAB-THP in 81.4% yield. The obtained NB-PAB-THP was coupled with Fmoc-L-alanyl chloride (Fmoc-Ala-Cl) to provide Fmoc-Ala-NB-PAB-THP in 81.8% yield, followed by the deprotection of the Fmoc group with 20% piperidine in DMF. After reaction between Ala-NB-PAB-THP and NHS-protected Fmoc-Val-OH (Fmoc-Val-NHS), Fmoc-Val-Ala-NB-PAB-THP was obtained in 82.9% yield. The THP group of Fmoc-Val-Ala-NB-PAB-THP was deprotected in 50% trifluoroacetic acid in dichloromethane, and then the hydroxyl group of the purified Fmoc-Val-Ala-NB-PAB-OH was protected with 4,4'-dimethoxytrityl (DMT) in anhydrous pyridine in 85.9% yield. After purification, Fmoc-Val-Ala-NB-PAB-DMT was treated with 20% piperidine in DMF, and the resultant Val-Ala-NB-PAB-DMT was further reacted with NHS-protected 10-hydroxydecanoic acid (HDA-NHS). HDA-Val-Ala-NB-PAB-DMT was finally converted into Val-Ala(NB) phosphoramidite for oligonucleotide synthesis (Figures S71, S72).

Next, an oligonucleotide with one Val-Ala(NB) incorporation (ODN4) was synthesized (Table S1). After synthesis, ODN4 was deprotected with concentrated ammonia at room temperature for two hours, followed by HPLC purification. As shown in Figure S6, 86.9% Val-Ala(NB) remained intact, demonstrating that the 2-nitrobenzyl protection group indeed improves the stability of the dipeptide. To study if the Val-Ala(NB) could be degraded after longer deprotection times, Val-Ala(NB) incorporated into DNA (ODN5) was deprotected with ammonia at 55 °C for 5 and 10 hours. Results indicate that

the dipeptide shows good tolerance to both deprotection conditions, 85.1% for 5 hours and 86.1% for 10 hours (Figures S7, S8). This means that Val-Ala(NB) is stable during deprotection, and the slight degradation most likely occurs during DNA synthesis.

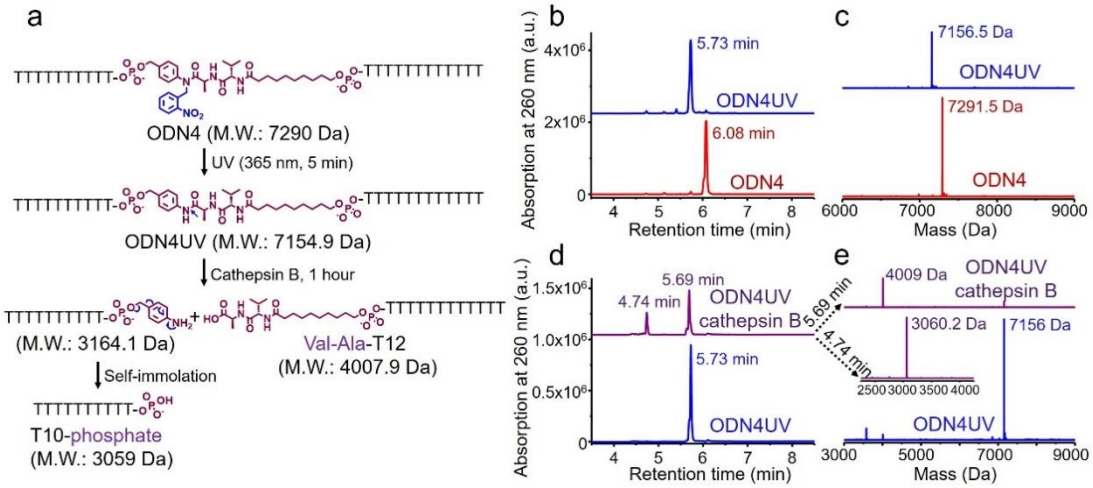

Figure 4. Photolysis of ODN4 and cathepsin B-mediated cleavage of the dipeptide in ODN4UV. (**a**) Reaction scheme for photolysis of ODN4 and cathepsin B-mediated cleavage of ODN4UV. (**b**) HPLC traces of ODN4 before (red line) and after (blue line) treatment with 365 nm UV light for 5 minutes. (**c**) Mass spectra of ODN4 before (red line) and after (blue line) treatment with 365 nm UV light for 5 minutes. (**d**) HPLC traces of 10 μM ODN4UV after incubation with (purple line) and without (blue line) 0.2 U/mL cathepsin B in buffer A for one hour at 37 °C. (**e**) Mass spectra of 10 μM ODN4UV after incubation with (purple lines) and without (blue line) 0.2 U/mL cathepsin B in buffer A for one hour at 37 °C.

Photolabile 2-nitrobenzyl is sensitive to exposure to ultraviolet (UV) light at 365 nm.[25] Therefore, a 365 nm LED light was used to remove the 2-nitrobenzyl group from ODN4 in water. As shown in Figure 4b, after treatment with UV light for 5 minutes, ODN4 peak at 6.08 min completely disappeared, instead, a new DNA peak at 5.73 min was observed (Figure 4b, blue line). The molecular weight of the new peak at 5.73 min is 7156.5 Da which is consistent with the molecular weight of ODN4 without the 2-nitrobenzyl group (ODN4UV) (Figure 4c), confirming that the 2-nitrobenzyl group had been removed from ODN4. We then incubated 10 μM of ODN4UV with 0.2 U/mL cathepsin B in 25 mM sodium acetate, 5 mM dithiothreitol (DTT) at pH 5.0

(buffer A) at 37 °C for 1 hour to investigate the enzymatic cleavage of the Val-Ala dipeptide in ODN4UV. After incubation, the oligonucleotide was desalted and analyzed by mass spectrometry. As shown in Figures 4d and 4e, ODN4UV shows excellent stability in buffer A after 1 hour of incubation (blue lines). However, after incubation with cathepsin B for 1 hour, ODN4UV was converted to T10-phosphate and Val-Ala-T12 (Figures 4d and 4e, purple lines). These results demonstrate that cathepsin B cleaves ODN4UV into T10-phosphate and Val-Ala-T12. We further investigated the enzymatic cleavage kinetics of 2 μM Val-Ala dipeptide in FAM-labeled ODN4UV by 0.2 U/mL cathepsin B, and found that almost all the dipeptide was cleaved within two hours (Figure S9).

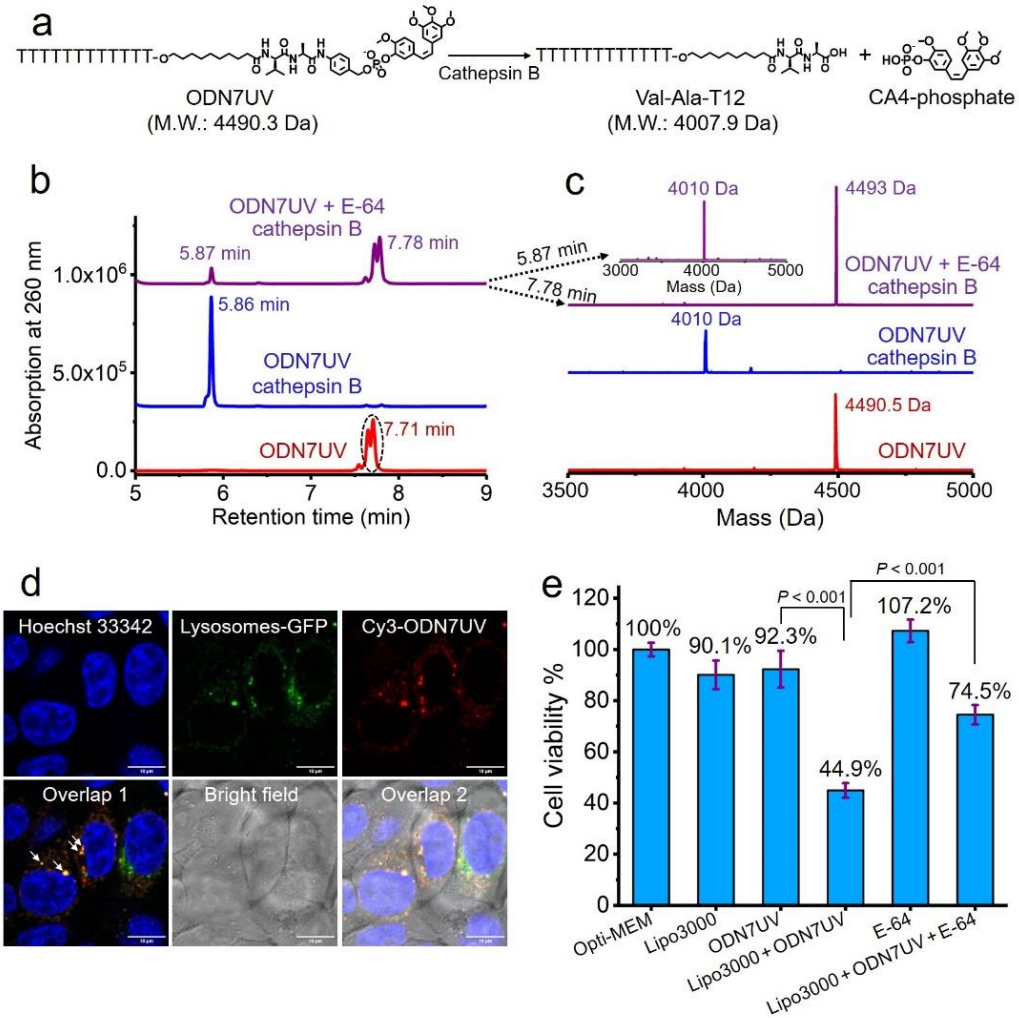

Figure 5. Intracellular cathepsin B-mediated cleavage of the dipeptide in ODN7UV. (**a**) Enzymatic cleavage reaction of ODN7UV by cathepsin B. (**b**) HPLC traces of 10

μM ODN7UV after incubation without cathepsin B (red line), with 0.2 U/mL cathepsin B (blue line) or with 0.2 U/mL cathepsin B and 1 μM E-64 (purple line) in buffer A at 37 °C for 1 hour. (**c**) Mass spectra of 10 μM ODN7UV after incubation without cathepsin B (red line), with 0.2 U/mL cathepsin B (blue line) or with 0.2 U/mL cathepsin B and 1 μM E-64 (purple line) in buffer A at 37 °C for 1 hour. After one hour of incubation, 10 μM ODN7UV was completely cleaved by 0.2 U/mL cathepsin B in buffer A. (**d**) Fluorescence co-localization imaging of HCT116 cells after incubation with Hoechst 33342 (blue color), CellLight™ lysosomes-GFP (green color) and Lipo3000-transfected Cy3-ODN7UV (red color) in Opti-MEM culture medium for 6 hours. The white arrows in Overlap 1 indicate co-localization of Cy3-ODN7UV with Lysosomes-GFP. Scale bar: 10 μm. (**e**) Cell viability of HCT116 cells treated with Lipo3000, 1 μM ODN7UV, Lipo3000-transfected ODN7UV (1 μM), 50 μM E-64 and Lipo3000-transfected ODN7UV (1 μM) + 50 μM E-64 in Opti-MEM culture medium for 48 hours.

Having confirmed the release of T10-phosphate from ODN4UV after enzymatic cleavage, we proceeded to construct oligonucleotide-small molecule conjugates with a cleavable dipeptide linkage. Various small molecules phosphoramidites can be quickly and efficiently attached to the Val-Ala(NB) linker and oligonucleotide sequences on a DNA synthesizer instead of resorting to complicated organic synthesis, and this is a key advantage of the automated modular synthesis.[26, 27] CA4 is a microtubule destabilizing small-molecule drug[28] (Figure S10), and its phosphate derivative is a prodrug which converts into dephosphorylated compound by intracellular phosphatase. We synthesized CA4 phosphoramidite (Figure S34) and covalently conjugated it to the dipeptide on ODN7 (Table S1). 10 μM ODN7UV was incubated with 0.2 U/mL cathepsin B in buffer A at 37 °C for 1 hour (Figure 5a). After incubation with cathepsin B, the DNA peak of ODN7UV disappeared, and instead, a new DNA peak at 5.86 min was observed which corresponds to Val-Ala-T12 (Figures 5b and 5c), demonstrating the enzymatic cleavage of ODN7UV by cathepsin B. E-64, a commercial protease inhibitor, was used to inhibit the activity of cathepsin B.[29] As shown in Figure 5b, 0.2 U/mL cathepsin B failed to efficiently cut 10 μM ODN7UV in buffer A containing 1 μM E-64 (purple line), suggesting again, cathepsin B is responsible for the enzymatic

cleavage of the dipeptide in ODN7UV. To investigate if the released payload-phosphate was further converted to dephosphorylated compound by phosphatase, we conjugate 4-methylumbelliferone (4MU) with peptide. 4MU is a coumarin fluorescent dye, and its phosphate derivative is a commercial fluorescent probe for phosphatase enzymes.[30] As shown in Figure S11d, an obvious fluorescence emission at 454 nm was observed if 0.2 U/mL cathepsin B and 0.2 U/mL acid phosphatase were added, indicating the conversion of 4MU-posphate to 4MU. To investigate if the dipeptide is cleavable by cathepsin B in biological fluids, 5 μM ODN6UV was treated with HCT116 cell lysate (final protein concentration is 100 μg/mL) in buffer A at 37 °C. After the addition of cell lysate, an obvious increase of fluorescence intensity was observed (Figure S11e), indicating the cleavage of dipeptide by the cathepsin B which comes from the cell lysate. ODN6UV shows negligible cleavage in the buffer solution containing cell lysate if E-64 was added (Figure S11e, cyan line), suggesting the good biological stability of phosphodiester linkage between peptide and payload. These experiments support the conclusion that the successive cleavage of dipeptide-small molecule conjugates by cathepsin B and phosphatase resulting in the release of payloads.

Next, we investigated if the Val-Ala dipeptide attached to DNA can be cleaved by intracellular cathepsin B. ODN7UV was transfected by lipofectamine into HCT116 cells, and the cell viability of the HCT116 cells was measured. Lipofectamine delivered the Cy3-labeled ODN7UV into cellular lysosomes after 6 hours of transfection (Figure 5d). Since intracellular cathepsin B largely localizes in lysosomes, intracellular delivery of ODN7UV to lysosomes by lipofectamine enables enzymatic cleavage of the dipeptide. As shown in Figure 5e, after 48 hours incubation, the cell viability of HCT116 cells treated with lipofectamine-transfected ODN7UV (1 μM) is 44.9%, demonstrating the release of the microtubule destabilizing drug CA4-phosphate (Figure S14). To further study if the intracellular release of CA4-phosphate from ODN7UV is dependent on the cathepsin B-mediated cleavage of the dipeptide, 50 μM cell-penetrable E-64 was added to inhibit the activity of intracellular cathepsin B. As shown in Figure 5e, the cell viability of HCT116 cells incubated with lipofectamine + ODN7UV + E-64 (50 μM) is 74.5%

which much greater than lipofectamine + ODN7UV (44.9%). This result indicates that the intracellular release of CA4-phosphate from ODN7UV is dependent on the activity of intracellular cathepsin B.

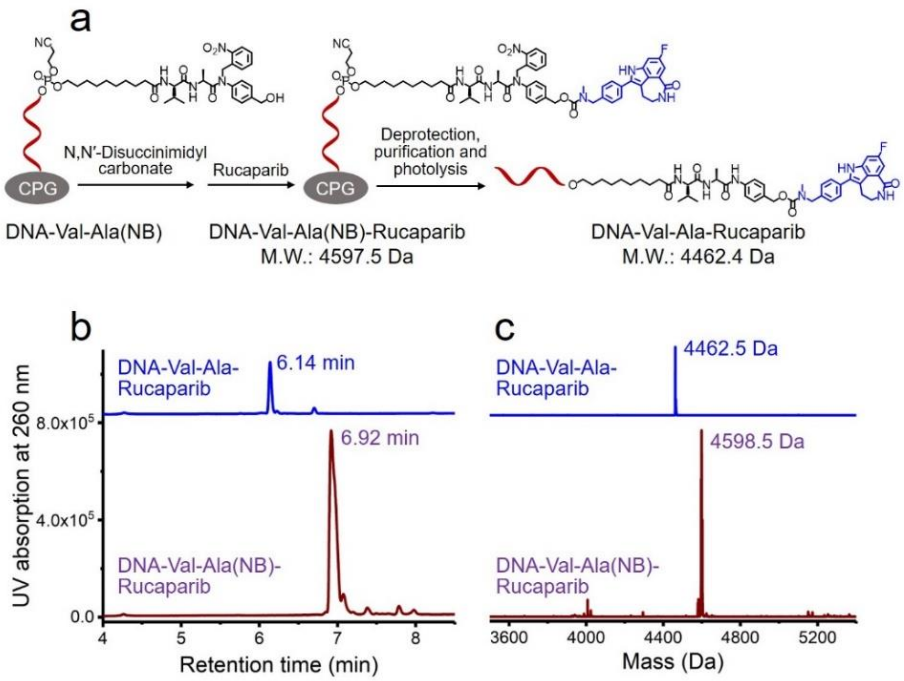

Figure 6. Solid-phase conjugation of small-molecule anticancer drug Rucaparib with Val-Ala(NB) dipeptide linker through a carbamate linkage. (**a**) Schematic of activation of DNA-Val-Ala(NB) and then conjugation with Rucaparib on resins, and the deprotection, purification and photolysis of DNA-Val-Ala(NB)-Rucaparib. (**b**) HPLC traces of DNA-Val-Ala(NB)-Rucaparib (purple line) and DNA-Val-Ala-Rucaparib (blue line). (**c**) Mass spectra of DNA-Val-Ala(NB)-Rucaparib (purple line) and DNA-Val-Ala-Rucaparib (blue line).

Covalent conjugation of small molecules with Val-Ala(NB) linker through phosphoramidite chemistry is limited to those small molecules containing a hydroxy group. To expand the general utility of Val-Ala(NB) dipeptide linker in the facile synthesis of oligonucleotide-small molecule conjugates, we studied the solid-phase conjugation of Val-Ala(NB) linker with payloads containing an amino group via a carbamate linker. As shown in Figure 6a, hydroxy group of Val-Ala(NB) was activated by N,N'-disuccinimidyl carbonate at 37 °C overnight, followed by reaction with the secondary amino group of Rucaparib.[31] After washing, deprotection and purification, DNA-Val-Ala(NB)-

Rucaparib was obtained (Figures 6b, 6c). The dipeptide in DNA-Val-Ala-Rucaparib can be cleavable by cathepsin B, resulting in the traceless release of Rucaparib. These experiments support the conclusion that covalent conjugation of small molecules containing an amino group with Val-Ala(NB) can proceed on solid supports.

Many small-molecule drug candidates fail to advance since their poor pharmacokinetics or unmanageable toxicities. One method to overcome these barriers is to covalently conjugate small-molecule drugs with targeting ligands for targeted delivery. There are examples of ADCs, aptamer-drug conjugates (ApDCs) and small molecule-drug conjugates (SMDCs). By using of Val-Ala(NB) monomer and DNA synthesizer, sgc8-CA4, GalNAc-CA4 and NH_2-DNA-CA4 conjugates are readily obtained (Figure S16). NH_2-DNA-CA4 conjugate contains an active amino group which are able to connect with antibody via crosslinker to synthesize ADCs (Figure S17). These results suggest the promising of Val-Ala(NB) in the development of various of targeting ligands-drug conjugates.

Conclusion

In summary, Val-Ala(NB) phosphoramidite has been developed for the modular and automated synthesis of oligonucleotide-small molecule conjugates. After DNA synthesis, deprotection and photolysis, oligonucleotide-small molecule conjugates with a cathepsin B-cleavable Val-Ala linker were obtained. Cathepsin B cleaves the dipeptide efficiently and thus releases small molecule-phosphate which is further converted to the free small molecule by phosphatase enzymes. Cell experiments demonstrate that CA4-phosphate is released from ODN7UV after intracellular cathepsin B-mediated cleavage of the dipeptide if the DNA is delivered into lysosomes. These results are encouraging in the context of developing therapeutic oligonucleotides containing the dipeptide linker for stimuli-responsive therapeutics, including targeting ligands-drug conjugates for targeted cancer therapy, and traceless release of siRNA or ASOs from nanocarriers.

The attachment of small molecules to oligonucleotides via the Val-Ala(NB) linker reported in this work is modular and automated. This means any

functional small molecule phosphoramidite can be quickly and efficiently conjugated to oligonucleotides via the Val-Ala(NB) linker on a DNA synthesizer, instead of resorting to complex organic synthesis. In addition, solid-phase conjugation of small molecules containing amino group with the Val-Ala(NB) linker through a carbamate linkage was achieved, expanding the general utility of this dipeptide in the construction of oligonucleotide-small molecule conjugates.

Author Contributions

C.J. and T.B. designed the experiments. C.J. performed the experiments and collected the experimental data. A.H.E.-S. and C.J. synthesized oligonucleotides. S.L. and C.J. performed confocal fluorescence microscopy imaging experiments. C.J. and T. B. analyzed the data. C.J. wrote the manuscript, and T.B., A.H.E.-S., and K.A.V. revised the manuscript.

Conflicts of interest

The authors declare no competing financial interest.

Acknowledgements

This work was supported by UK BBSRC grant BB/S018794/1, UK Medical research council grants MR/X008029/1 (TransNAT) and CiC123/11578 (MC_PC_19049#4050789009), Natural Science Foundation of China Grant No. 23CAA00865 and Huadong Medicine Joint Funds of the Zhejiang Provincial Natural Science Foundation of China under Grant No. LHDMZ24H300004.

References

1. G. Alvaradourbina, G. M. Sathe, W. C. Liu, M. F. Gillen, P. D. Duck, R. Bender and K. K. Ogilvie, *Science*, 1981, 214, 270-274.

2. J. Q. Qiu, A. Wilson, A. H. El-Sagheer and T. Brown, *Nucleic Acids Res.*, 2016, 44, e138.

3. K. M. Wang, Z. W. Tang, C. Y. J. Yang, Y. M. Kim, X. H. Fang, W. Li, Y. R. Wu, C. D. Medley, Z. H. Cao, J. Li, P. Colon, H. Lin and W. H. Tan, *Angew. Chem. Int. Ed.*, 2009, 48, 856-870.

4. H. P. Liu, Z. Zhu, H. Z. Kang, Y. R. Wu, K. Sefan and W. H. Tan, *Chem. Eur. J.* 2010, 16, 3791-3797.

5. J. Gorman, S. R. E. Orsborne, A. Sridhar, R. Pandya, P. Budden, A. Ohmann, N. A. Panjwani, Y. Liu, J. L. Greenfield, S. Dowland, V. Gray, S. T. J. Ryan, S. De Ornellas, A. H. El-Sagheer, T. Brown, J. R. Nitschke, J. Behrends, U. F. Keyser, A. Rao, R. Collepardo-Guevara, E. Stulz, R. H. Friend and F. Auras, *J. Am. Chem. Soc.*, 2022, 144, 368-376.

6. T. G. W. Edwardson, K. M. M. Carneiro, C. J. Serpell and H. F. Sleiman, *Angew. Chem. Int. Ed.*, 2014, 53, 4567-4571.

7. J. K. Nair, J. L. S. Willoughby, A. Chan, K. Charisse, M. R. Alam, Q. F. Wang, M. Hoekstra, P. Kandasamy, A. V. Kel'in, S. Milstein, N. Taneja, J. O'Shea, S. Shaikh, L. G. Zhang, R. J. van der Sluis, M. E. Jung, A. Akinc, R. Hutabarat, S. Kuchimanchi, K. Fitzgerald, T. Zimmermann, T. J. C. van Berkel, M. A. Maier, K. G. Rajeev and M. Manoharan, *J. Am. Chem. Soc.*, 2014, 136, 16958-16961.

8. T. Nagata, C. A. Dwyer, K. Yoshida-Tanaka, K. Ihara, M. Ohyagi, H. Kaburagi, H. Miyata, S. Ebihara, K. Yoshioka, T. Ishii, K. Miyata, K. Miyata, B. Powers, T. Igari, S. Yamamoto, N. Arimura, H. Hirabayashi, T. Uchihara, R. I. Hara, T. Wada, C. F. Bennett, P. P. Seth, F. Rigo and T. Yokota, *Nat. Biotechnol.*, 2021, 39, 1529-1533.

9. G. Z. Zhu, G. Niu and X. Y. Chen, Bioconjugate Chem., 2015, 26, 2186-2197.

10. H. P. Liu, K. D. Moynihan, Y. R. Zheng, G. L. Szeto, A. V. Li, B. Huang, D. S. Van Egeren, C. Park and D. J. Irvine, *Nature*, 2014, 507, 519-522.

11. F. F. Li, J. Lu, J. Liu, C. Liang, M. L. Wang, L. Y. Wang, D. F. Li, H. Z. Yao, Q. L. Zhang, J. Wen, Z. K. Zhang, J. Li, Q. X. Lv, X. J. He, B. S. Guo, D. G. Guan, Y. Y. Yu, L. Dang, X. H. Wu, Y. S. Li, G. F. Chen, F. Jiang, S. G. Sun, B. T. Zhang, A. P. Lu and G. Zhang, *Nat. Commun.*, 2017, 8,1390.

12. A. Mrcher, M. A. D. Nijenhuis and K. V. Gothelf, *Angew. Chem. Int. Ed.*, 2021, 60, 21691-21696.

13. G. Leriche, L. Chisholm and A. Wagner, *Bioorg. Med. Chem.*, 2012, 20, 571-582.

14. K. Skakuj, S. Y. Wang, L. Qin, A. Lee, B. Zhang and C. A. Mirkin, *J. Am. Chem. Soc.*, 2018, 140, 1227-1230.

15. J. L. Yang, C. M. Chen and X. J. Tang, *Bioconjugate Chem.*, 2018, 29, 1010-1015.

16. K. Darrah, J. Wesalo, B. Lukasak, M. Tsang, J. K. Chen and A. Deiters, *J. Am. Chem. Soc.*, 2021, 143, 18665-18671.

17. X. Y. Tan, B. B. Li, X. G. Lu, F. Jia, C. Santori, P. Menon, H. Li, B. H. Zhang, J.

J. Zhao and K. Zhang, *J. Am. Chem. Soc.*, 2015, 137, 6112-6115.

18. Q. X. Yang, Z. Y. Deng, D. Wang, J. X. He, D. L. Zhang, Y. Tan, T. H. Peng, X. Q. Wang and W. H. Tan, *J. Am. Chem. Soc.*, 2020, 142, 2532-2540.

19. L. R. Saunders, A. J. Bankovich, W. C. Anderson, M. A. Aujay, S. Bheddah, K. Black, R. Desai, P. A. Escarpe, J. Hampl, A. Laysang, D. Liu, J. Lopez-Molina, M. Milton, A. Park, M. A. Pysz, H. Shao, B. Slingerland, M. Torgov, S. A. Williams, O. Foord, P. Howard, J. Jassem, A. Badzio, P. Czapiewski, D. H. Harpole, A. Dowlati, P. P. Massion, W. D. Travis, M. C. Pietanza, J. T. Poirier, C. M. Rudin, R. A. Stull and S. J. Dylla, *Sci. Transl. Med.*, 2015, 7, 302ra136.

20. J. C. Kern, D. Dooney, R. Zhang, L. D. Liang, P. E. Brandish, M. G. Cheng, G. Feng, A. Beck, D. Bresson, J. Firdos, D. Gately, N. Knudsen, A. Manibusan, Y. Sun and R. M. Garbaccio, *Bioconjugate Chem.*, 2016, 27, 2081-2088.

21. C. Jin, A. H. Ei-Sagheer, S. Q. Li, K. A. Vallis, W. H. Tan and T. Brown, *Angew. Chem. Int. Ed.*, 2022, 61, e202114016.

22. C. Jin, H. Zhang, J. M. Zou, Y. Liu, L. Zhang, F. J. Li, R. W. Wang, W. J. Xuan, M. Ye and W. H. Tan, *Angew. Chem. Int. Ed.*, 2018, 57, 8994-8997.

23. P. D. Senter and E. L. Sievers, Nat. Biotechnol., 2012, 30, 631-637.

24. A. Younes, U. Yasothan and P. Kirkpatrick, *Nat. Rev. Drug Discov.*, 2012, 11, 19-20.

25. P. Klan, T. Solomek, C. G. Bochet, A. Blanc, R. Givens, M. Rubina, V. Popik, A. Kostikov and J. Wirz, *Chem. Rev.*, 2013, 113, 119-191.

26. L. J. Zhu, J. P. Yang, Y. Ma, X. Y. Zhu and C. Zhang, *J. Am. Chem. Soc.*, 2022, 144, 1493-1497.

27. R. W. Wang, G. Z. Zhu, L. Mei, Y. Xie, H. B. Ma, M. Ye, F. L. Qing and W. H. Tan, *J. Am. Chem. Soc.*, 2014, 136, 2731-2734.

28. G. C. Tron, T. Pirali, G. Sorba, F. Pagliai, S. Busacca and A. A. Genazzani, *J. Med. Chem.*, 2006, 49, 3033-3044.

29. D. P. Dickinson, *Crit. Rev. Oral Bio. Med.*, 2002, 13, 238-275.

30. K. Bednarska, M. Klink and Z. Sulowska, *Mediators of Inflamm.*, 2006, 2006, 019307.

31. M. I. Meschaninova, D. S. Novopashina, O. A. Semikolenova, V. N. Silnikov and A. G. Venyaminova, *Molecules*, 2019, 24, 4266.

Modular and Automated Synthesis of Oligonucleotide-Small Molecule Conjugates for Cathepsin B Mediated Traceless Release of Payloads

Cheng Jin[1,2]*, Siqi Li[1,3], Katherine A. Vallis[3], Afaf H. El-Sagheer[1,4] and Tom Brown[1]*

1 Department of Chemistry, Chemistry Research Laboratory, University of Oxford, 12 Mansfield Road, Oxford, OX1 3TA, United Kingdom

2 Hangzhou Institute of Medicine (HIM), Chinese Academy of Sciences, Zhejiang Cancer Hospital, Hangzhou, Zhejiang 310022, China

3 Department of Oncology, University of Oxford, Oxford, OX3 7DQ, United Kingdom

4 Department of Science and Mathematics, Suez University, Faculty of Petroleum and Mining Engineering, Suez, 43721, Egypt

*Corresponding authors: jincheng@him.cas.cn (C.J.) and tom.brown@chem.ox.ac.uk (T.B.)

Contents

1. Materials

All chemicals for organic synthesis were purchased commercially without further treatment. Combretastatin A-4 (CA4) was purchased from Fluorochem. 5'-GalNAc C3 phosphoramidite and 3'-amino modifier C7 CPG were purchased from Glen Research. Cathepsin B from human placenta, E-64 protease inhibitor, acid phosphatase from potato, cell counting kit-8 (CCK-8), Rucaparib camsylate and 4-methylumbelliferone (4MU) were purchased from Sigma-Aldrich. CellLight™ Lysosomes-GFP BacMam 2.0, Lipofectamine™ 3000 Transfection Reagent and Opti-MEM™ I Reduced Serum Medium were purchased from Thermo Fisher Scientific.

2. Experimental section

2.1 Oligonucleotide synthesis

All oligonucleotides were synthesized on an ABI 394 DNA/RNA synthesizer with standard protocol. Val-Ala(NB) phosphoramidite was dissolved in anhydrous dichloromethane in concentration of 0.1 mol/L. Benzyl, PAB, mPAB, CA4, 4MU and GalNAc phosphoramidites were dissolved in anhydrous acetonitrile in concentration of 0.1 mol/L, respectively. After oligonucleotide synthesis, DNA were deprotected in concentrated aqueous ammonia at room temperature for 2 hours. For sgc8-CA4 conjugate, DNA were deprotected in concentrated aqueous ammonia at 55 °C for 10 hours. After deprotection, the ammonia was removed under high vacuum, and the DNA was purified using of high-performance liquid chromatography (HPLC). For ODN4 and ODN5 (Table S1), 80% aqueous acetic acid was used to remove 4,4'-dimethoxytrityl (DMT) group from DNA after HPLC purification. Then, the purified DNA was freeze dried and desalted, and quantitated by detecting their absorbance at 260 nm.

2.2 Photolysis

365 nm LED light (Thorlabs M365LP1) was used to remove 2-nitrobenzyl group from DNA. The desalted DNA was exposure to 365 nm LED light for 5 minutes at room temperature in water. Then, DNA was subjected to HPLC for further purification.

2.3 Enzymatic cleavage of dipeptide by cathepsin B

Cathepsin B from human placenta (2 U) (Sigma-Aldrich) was dissolved in 200 μL activation buffer (25 mM sodium acetate, 5 mM dithiothreitol (DTT), 1 mM ethylenediaminetetraacetic acid (EDTA), pH 5.0) to the final concentration of 10 U/mL. For enzymatic cleavage, 10 μM DNA was dissolved with 200 μL buffer A (25 mM sodium acetate, 5 mM DTT, pH 5.0) and incubated with 0.2 U/mL cathepsin B at 37 °C for one hour. After incubation, the DNA solution was desalted using of NAP columns (GE Healthcare), and the desalted DNA was analyzed by electrospray mass spectrometry (ES-).

2.4 Fluorescence spectra experiments

ODN6UV was dissolved in buffer A and then incubated with cathepsin B and acid phosphatase for enzymatic cleavage study. ODN6UV (2 μM) was incubated with 0.2 U/mL cathepsin B in buffer A at 37 °C for 1 hour. Then, 0.2 U/mL acid phosphatase was added, and the mixture was incubated at 37 °C for 1 hour. Then, the mixture was subjected to fluorescence spectra detection (PerkinElmer LS-50B Luminescence Spectrophotometer). Excitation wavelength: 360 nm, slit width: 7 nm; emission wavelength: 380 to 650 nm, slit width: 7 nm.

2.5 Fluorescence analysis of ODN6UV in cell lysate

Preparation of HCT116 cell lysate. HCT116 cells were cultured in 6-well cell culture plate to about 90% confluency. The DMEM culture medium was removed, and cells were washed with 1 mL Dulbecco's phosphate-buffered saline (DPBS) twice. After washing, 600 μL cell lysis buffer (10 mM Tris-HCl buffer, 50 mM KCl, 1.5 mM $MgCl_2$, 0.45% Tween 20 and 0.45% Triton X-100, pH 8.5) was added to the each well, followed by vibration at 400 rpm for 5 min. The mixture was collected and centrifuged at 8000 rpm for 5 min. The supernatant was collected, and the protein was quantitated by Pierce™ BCA protein assay kit (Thermo Fisher Scientific). The protein concentration of the supernatant is 1993.2 μg/mL.

5 μM ODN6UV was incubated with HCT116 cell lysate (the final protein concentration is 100 μg/mL) in buffer A at 37 °C for various time intervals. For the control group, 5 μM ODN6UV was incubated with HCT116 cell lysate and 10 μM E-64 in buffer A at 37 °C. The fluorescence intensity was measured at 450 nm on a microplate reader (INFINITE M1000 PRO). Excitation wavelength: 360 nm, emission wavelength: 450 nm, both slit widths were set as 20 nm.

2.6 Cell viability assay

HCT116 cells were cultured in DMEM culture media with 10% FBS, and 0.1 U/mL penicillin and 0.1 mg/mL streptomycin under 5% CO_2 atmosphere. For cell viability assay, 3000 HCT116 cells were cultured in the each well of 96-well cell culture plate and were grew for 24 hours in complete DMEM medium before incubation. Then, DMEM medium was removed, and 100 μL DPBS was added to wash cells. Then, cells were incubated with lipofectamine-transfected ODN7UV in Opti-MEM cell culture medium for 48 hours. After incubation, 10 μL cell counting kit-8 (CCK-8) was added. The cell viability was measured by detecting their absorbance at 450 nm on a microplate reader (INFINITE M1000 PRO).

Preparation of lipofectamine-ODN7UV transfection complex. 0.6 μL lipofectamine 3000 was diluted with 50 μL Opti-MEM cell culture medium (solution A), and 0.1 nmol ODN7UV was diluted with another 50 μL Opti-MEM cell culture medium and 0.4 μL P3000 reagent was added (solution B). Solutions A and B were mixed, and the mixture was stand at room temperature for 15 minutes before incubation with HCT116 cells.

2.7 Confocal fluorescence microscopy imaging

HCT116 cells were cultured in 10-wells microscope slide in 200 μL complete DMEM culture medium, and CellLight™ Lysosomes-GFP (8 μL) was added. After 24 hours, DMEM culture medium was removed, and the cells were washed twice with DPBS. Then, cells were incubated with Cy3-ODN7UV (1 μM) or lipofectamine-transfected Cy3-ODN7UV (1 μM) in Opti-MEM culture medium for 6 hours. Hoechst 33342 (1 μg/ml) was incubated with cells for 10 minutes to stain the cell nucleus. After incubation, Opti-MEM culture medium was removed, and the cells were washed twice with DPBS and then subjected to confocal fluorescence microscopy imaging.

Preparation of lipofectamine/Cy3-ODN7UV transfection complex. Lipofectamine 3000 (0.6 μL) was diluted with 100 μL Opti-MEM culture medium (solution C). 0.2 nmol Cy3-ODN7UV was dissolved with 100 μL Opti-MEM culture medium and 0.4 μL P3000 reagent was added (solution D). Solutions C and D were mixed, and the mixture was stand for 15 minutes at room temperature before incubation with HCT116 cells.

2.8 Solid-phase conjugation of Val-Ala(NB) with amino compound

Resins of DNA-Val-Ala(NB) (DMT-off, 5' Val-Ala(NB)-TTTTTTTTTTTT 3') were dried with argon gas before conjugation reaction. Then, DNA-Val-Ala(NB) (0.5 μmol) resins were reacted with N,N'-disuccinimidyl carbonate (65 mg, 250 μmol) dissolved in 2.7 mL anhydrous CH_3CN and 0.3 mL anhydrous DIPEA at 37 °C for 5 hours. After washing with anhydrous CH_3CN, the resins were further reacted with 6-amino-1-hexanol (14 mg, 120 μmol) dissolved in 1.8 mL CH_3CN, 0.3 mL DMSO and 0.2 mL DIPEA at 37 °C overnight. Then, the resins were washed with CH_3CN and dried by argon gas. The oligonucleotide was deprotected by 50 mM K_2CO_3 in methanol (3 mL) at 25 °C for 4 hours. After deprotection, 18 μL acetic acid was added to neutralize the solution. The solvents were removed under high vacuum, and the DNA was purified by HPLC and analyzed by electrospray mass spectrometry (ES-).

After activation with N,N'-disuccinimidyl carbonate, 0.5 μmol DNA-Val-Ala(NB) resins were reacted with Rucaparib camsylate (3 mg, 5.4 μmol) dissolved in 1.5 mL DMSO, 0.5 mL anhydrous CH_3CN and 0.1 mL DIPEA at 37 °C overnight. Then, the resins were washed with CH_3CN and dried by argon gas, and the DNA was deprotected. After purification and photolysis, DNA-Val-Ala(NB)-Rucaparib and DNA-Val-Ala-Rucaparib were analyzed by electrospray mass spectrometry (ES-).

3. Figures and Tables

Table S1. Designed oligonucleotides in this work

Name	Sequences (from 5' to 3')
ODN1	Benzyl-TTT TTT TTT TTT
ODN2	PAB-TTT TTT TTT TTT
ODN3	mPAB-TTT TTT TTT TTT
ODN4	TTT TTT TTT T-Val-Ala(NB)-TTT TTT TTT TTT
ODN4UV	TTT TTT TTT T-Val-Ala-TTT TTT TTT TTT
FAM-ODN4	FAM-TTT TTT TTT T-Val-Ala(NB)-TTT TTT TTT TTT
FAM-ODN4UV	FAM-TTT TTT TTT T-Val-Ala-TTT TTT TTT TTT
ODN5	T-Val-Ala(NB)-TTT TTT TTT TTT
ODN5UV	T-Val-Ala-TTT TTT TTT TTT
ODN6	4MU-Val-Ala(NB)-TTT TTT TTT TTT
ODN6UV	4MU-Val-Ala-TTT TTT TTT TTT
ODN7	CA4-Val-Ala(NB)-TTT TTT TTT TTT
ODN7UV	CA4-Val-Ala-TTT TTT TTT TTT
Cy3-ODN7	CA4-Val-Ala(NB)-TTT TTT TTT TTT-Cy3
Cy3-ODN7UV	CA4-Val-Ala-TTT TTT TTT TTT-Cy3
Sgc8-CA4	CA4-Val-Ala-TTT ATC TAA CTG CTG CGC CGC CGG GAA AAT ACT GTA CGG TTA GA
GalNAc-CA4	CA4-Val-Ala-$U_{OMe}U_{OMe}U_{OMe}U_{OMe}U_{OMe}U_{OMe}$-GalNAc-GalNAc-GalNAc-T
NH_2-DNA-CA4	CA4-Val-Ala-TTT TTT TTT TTT TTT-NH_2

Note: Val-Ala indicates dipeptide without 2-nitrobenzyl protection. U_{OMe} indicates 2'-OMe-U. NH_2 indicates 3'-amino C7 modification. GalNAc indicates 5'-GalNAc C3 modification.

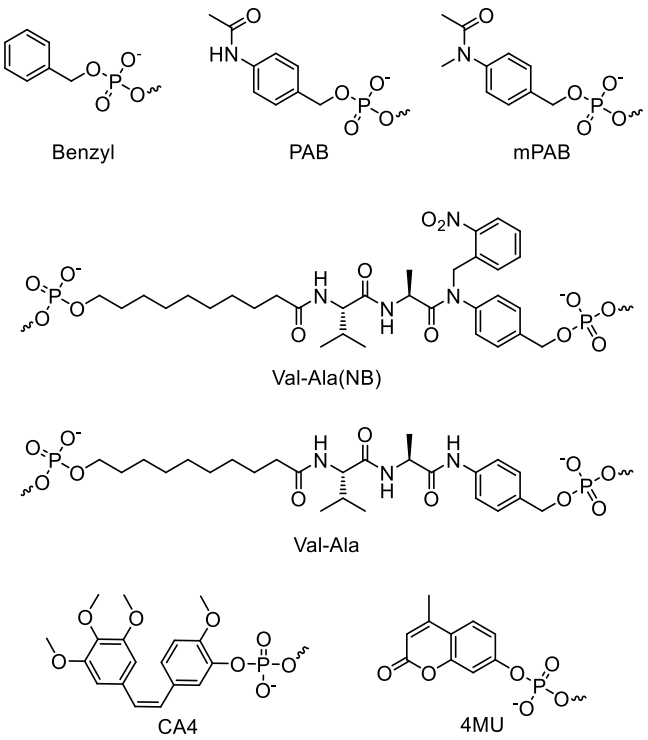

Figure S1. Chemical structures of Benzyl, PAB, mPAB, Val-Ala(NB), Val-Ala, CA4 and 4MU modifications on oligonucleotides.

Table S2. Calculated and found mass of DNA

Name	Calculated mass (Da)	Found mass (Da)
ODN4	7290	7291.5
ODN4UV	7154.9	7156.5
FAM-ODN4	7826.7	7827.4
FAM-ODN4UV	7692.5	7693
ODN5	4552.3	4553
ODN5UV	4417.2	4419
ODN6	4486.2	4489.5
ODN6UV	4351.1	4353.5
ODN7	4625.4	4626
ODN7UV	4490.3	4491
Cy3-ODN7	5132	5133.6
Cy3-ODN7UV	4998.9	5000
Sgc8-CA4	14448.7	14450.5
GalNAc-CA4	4880.5	4881
NH_2-DNA-CA4	5614.6	5613.1

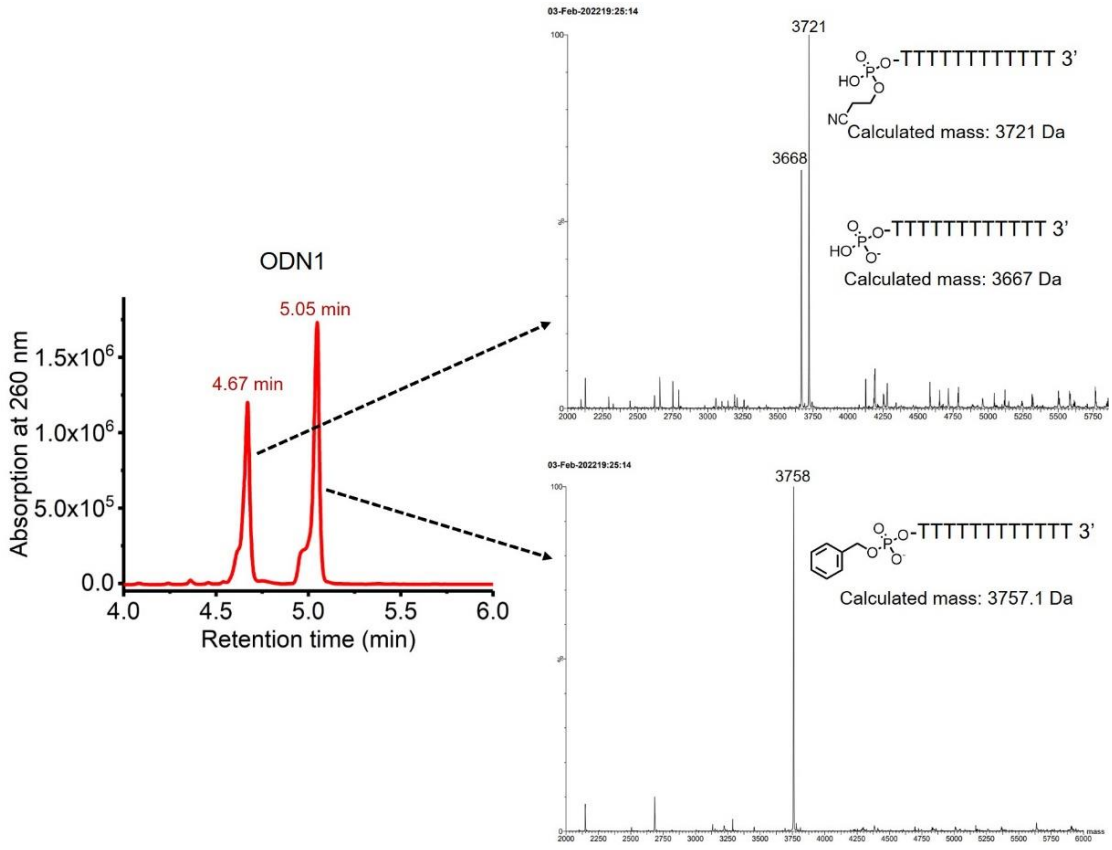

Figure S2. HPLC trace (left) and mass spectra (right) of ODN1 after deprotection by concentrated aqueous ammonia at room temperature for two hours. DNA peaks at 4.67 and 5.05 minutes are degraded and successful DNA, respectively.

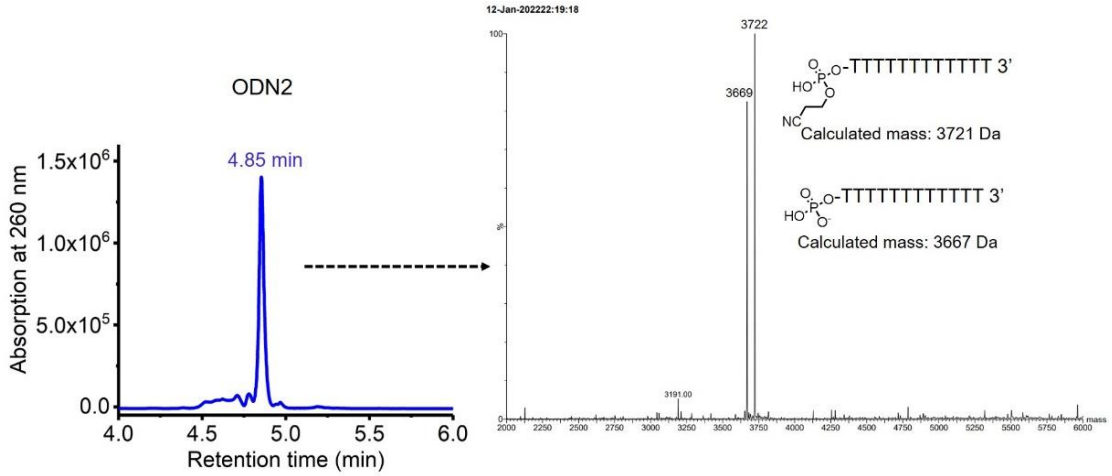

Figure S3. HPLC trace (left) and mass spectrum (right) of ODN2 after deprotection by concentrated aqueous ammonia at room temperature for two hours. ODN2 was completely degraded during oligonucleotide synthesis and deprotection.

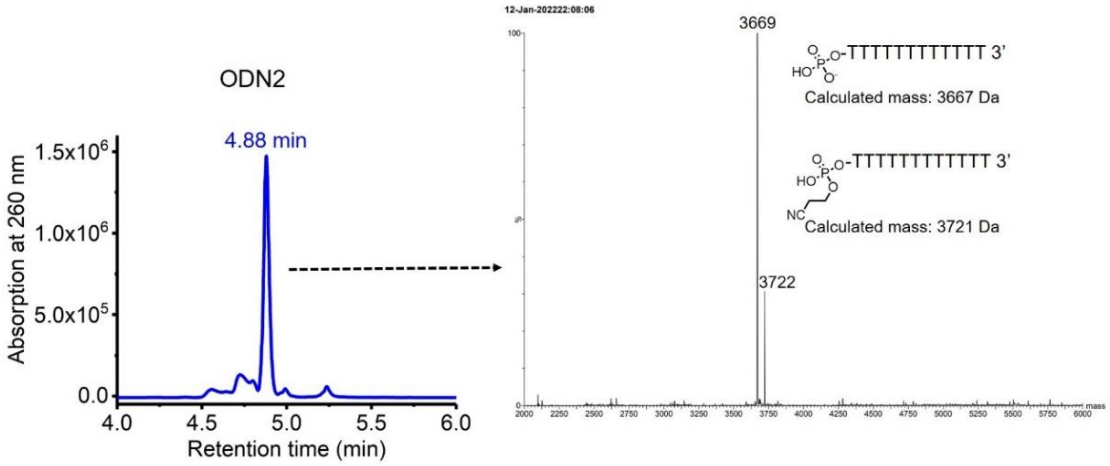

Figure S4. HPLC trace (left) and mass spectrum (right) of ODN2 after deprotection by 50 mM anhydrous K_2CO_3 in methanol at room temperature for 4 hours. After deprotection by 50 mM K_2CO_3 in methanol (2 mL), 12 µL of acetic acid were added to neutralize the solution. Then, the solvent was removed under high vacuum. ODN2 was completely degraded during oligonucleotide synthesis and deprotection.

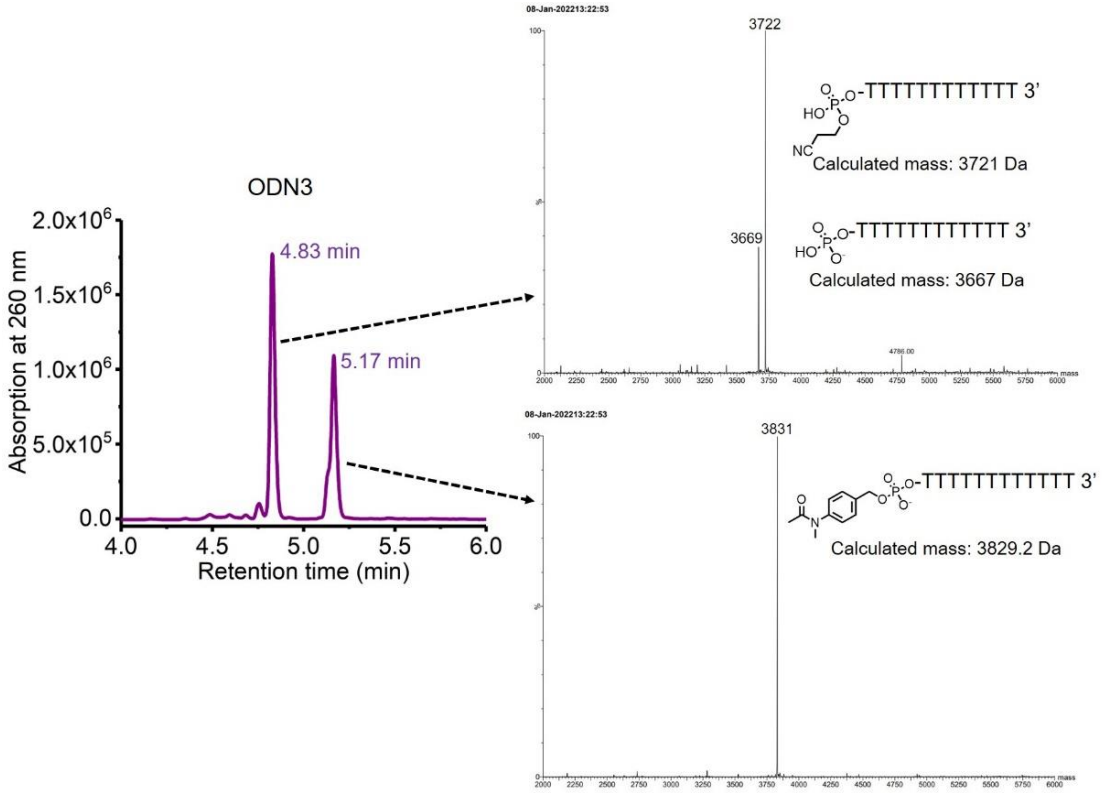

Figure S5. HPLC trace (left) and mass spectra (right) of ODN3 after deprotection by concentrated aqueous ammonia at room temperature for two hours. DNA peaks at 4.83 and 5.17 minutes are degraded and successful DNA, respectively.

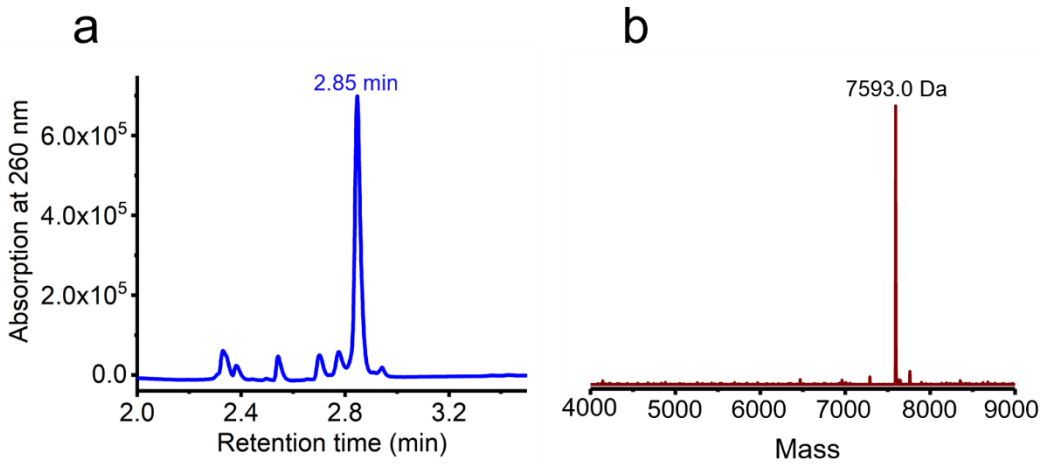

Figure S6. HPLC trace and mass spectrum of DMT-protected ODN4 after deprotection. (**a**) HPLC trace of DMT-protected ODN4 after deprotection by concentrated aqueous ammonia at room temperature for two hours. DNA peak at 2.85 min is the successful DMT-protected ODN4: 5' DMT-TTTTTTTTTT-Val-Ala(NB)-TTTTTTTTTTTT 3'. After calculation, 86.9% Val-Ala(NB) on ODN4 remained intact after deprotection. (**b**) Mass spectrum of DNA peak at 2.85 min in Figure S6a. The calculated molecular weight is 7593 Da, and the observed molecular weight is 7593 Da.

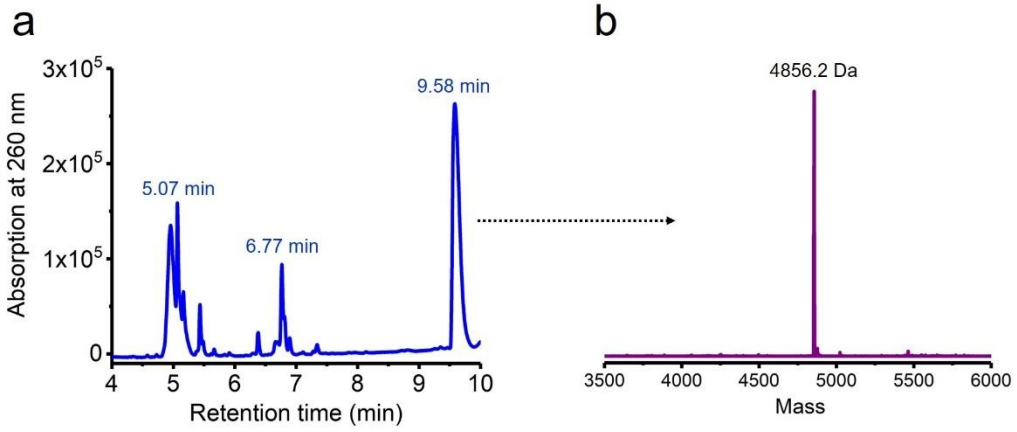

Figure S7. HPLC trace and mass spectrum of DMT-protected ODN5 (5' DMT-T-Val-Ala(NB)-TTTTTTTTTTTT 3') after 5 hours of deprotection. (**a**) HPLC trace of DMT-protected ODN5 after deprotection by concentrated aqueous ammonia at 55 °C for 5 hours. DNA peak around 5.07 min is DNA without peptide (5' TTTTTTTTTTTT 3'). DNA peak at 6.77min is DNA with degraded peptide (5' phosphite-Val-Ala(NB)-TTTTTTTTTTTT 3'). DNA peak at 9.58 min is the successfully synthesized DNA (5' DMT-T-Val-Ala(NB)-TTTTTTTTTTTT 3'). Calculating the peak area of DNA at 6.77 and 9.58 min, 85.1% Val-Ala(NB) remained intact after deprotection. (**b**) Mass spectrum of DNA peak at 9.58 min in Figure S7a. The calculated molecular weight is 4854.7 Da, and the observed molecular weight is 4856.2 Da.

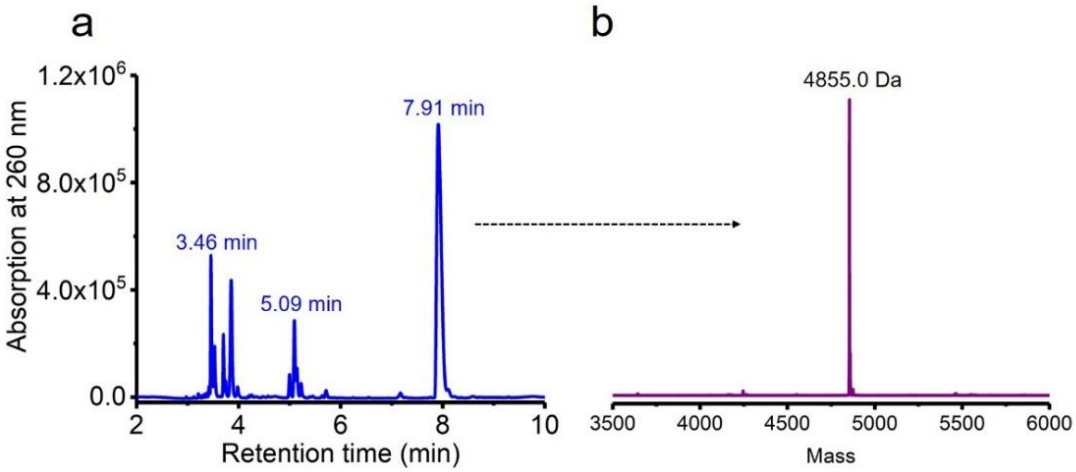

Figure S8. HPLC trace and mass spectrum of DMT-protected ODN5 (5' DMT-T-Val-Ala(NB)-TTTTTTTTTTTT 3') after 10 hours of deprotection. (**a**) HPLC trace of DMT-protected ODN5 after deprotection by concentrated aqueous ammonia at 55 °C for 10 hours. DNA peak around 3.46 min is the DNA without peptide (TTTTTTTTTTTT). DNA peak at 5.09 min is the DNA with degraded peptide (5' phosphite-Val-Ala(NB)-TTTTTTTTTTTT). DNA peak at 7.91 min is the successfully synthesized DNA (5' DMT-T-Val-Ala(NB)-TTTTTTTTTTTT 3'). Calculating the peak area of DNA at 5.09 and 7.91 min, 86.1% Val-Ala(NB) on ODN5 remained intact after deprotection. (**b**) Mass spectrum of DNA peak at 7.91 min in Figure S8a. The calculated molecular weight is 4854.7 Da, and the observed molecular weight is 4855.0 Da.

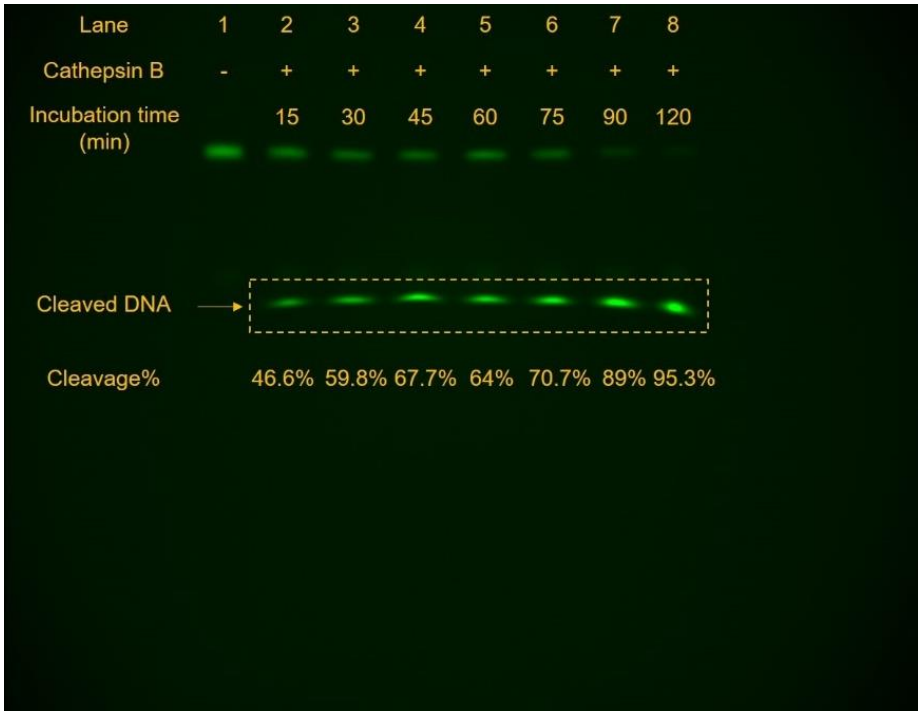

Figure S9. 12% Native PAGE gel analysis of cathepsin B-mediated enzymatic cleavage kinetics of FAM-ODN4UV (5' FAM-TTTTTTTTTT-Val-Ala-TTTTTTTTTTTT 3'). 2 μM FAM-ODN4UV was incubated with 0.2 U/mL cathepsin B in buffer A at 37 °C for various incubation intervals. After incubation, the mixture was subjected to electrophoresis gel analysis. The gel was run for one hour at room temperature and the power was set at 20 W. 2 μM FAM-ODN4UV was completely cleaved by 0.2 U/mL cathepsin B within two hours of incubation in buffer A.

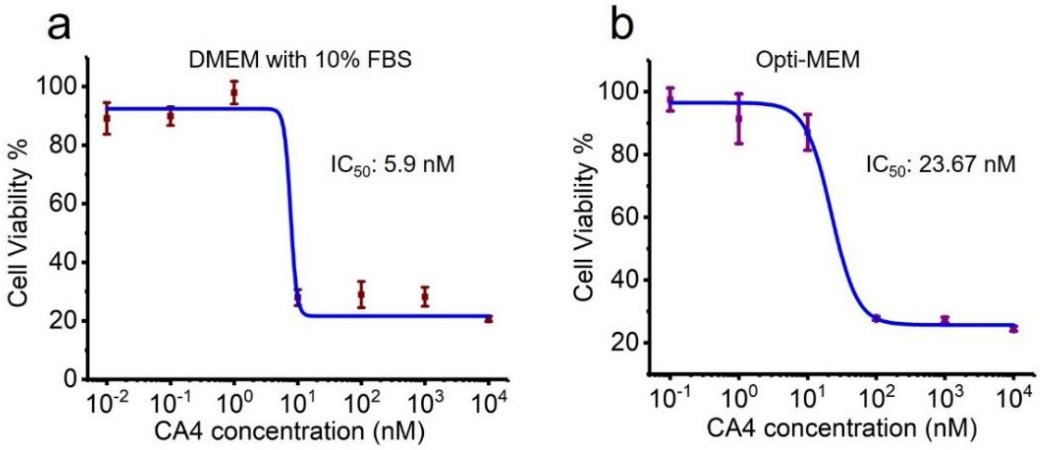

Figure S10. Cell viability of HCT116 cells after incubation with CA4 in DMEM cell culture medium supplemented with10% FBS (**a**) and Opti-MEM cell culture medium (**b**) for 48 hours.

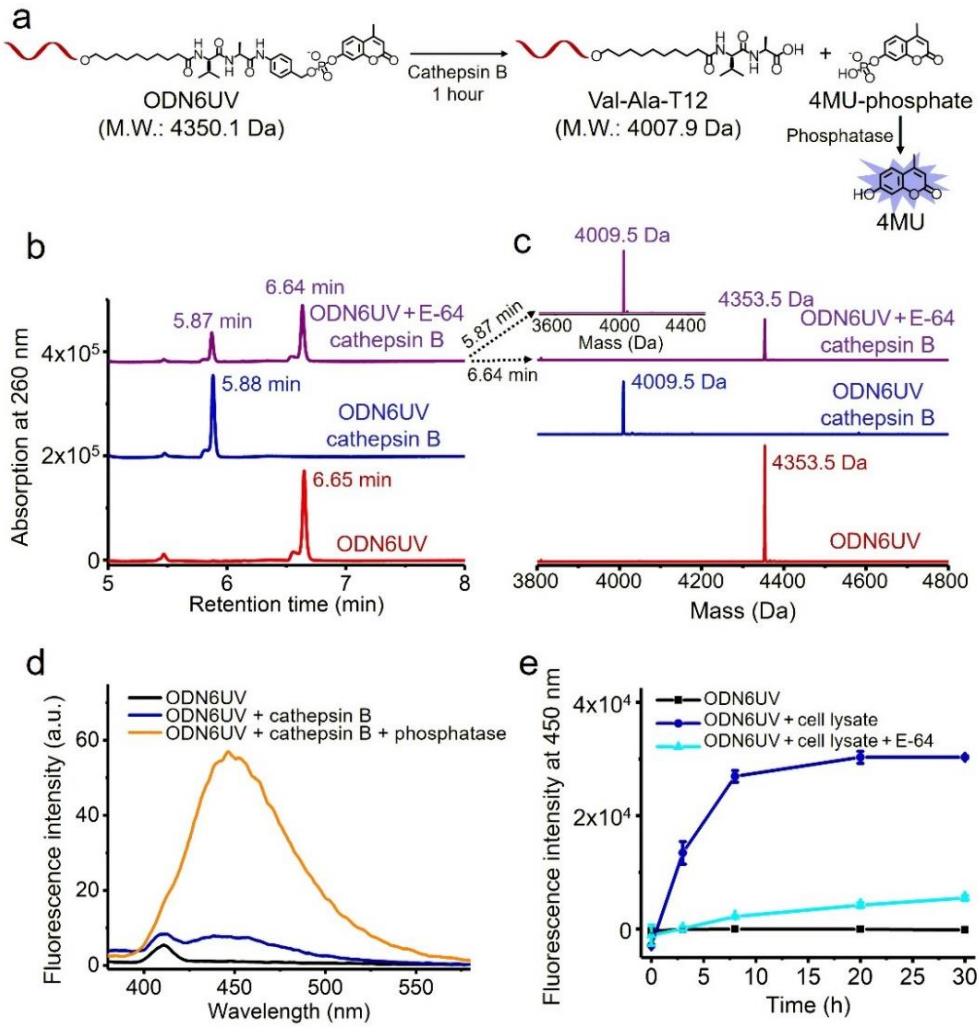

Figure S11. Cathepsin B-mediated cleavage of ODN6UV. (**a**) Cathepsin B-mediated cleavage reaction and conversion of 4MU-phosphate to 4MU by phosphatase. (**b**) HPLC traces of 10 μM ODN6UV after incubation without cathepsin B (red line), with 0.2 U/mL cathepsin B (blue line) or with 0.2 U/mL cathepsin B and 1 μM E-64 (purple line) in buffer A at 37 °C for 1 hour. (**c**) Mass spectra of 10 μM ODN6UV after incubation without cathepsin B (red line), with 0.2 U/mL cathepsin B (blue line) or with 0.2 U/mL cathepsin B and 1 μM E-64 (purple line) in buffer A at 37 °C for 1 hour. After incubation in buffer A at 37 °C for 1 hour, Val-Ala dipeptide in ODN6UV was completely cleaved by cathepsin B. (**d**) Fluorescence spectra of 2 μM ODN6UV before and after treatment with 0.2 U/mL cathepsin B and 0.2 U/mL acid phosphatase in buffer A at 37 °C for 1 hour. Black line: ODN6UV. Blue line: ODN6UV incubated with cathepsin B. Orange line: ODN6UV incubated with cathepsin B and then incubated with acid phosphatase. Excitation wavelength: 360 nm, emission wavelength: 380 to 650 nm. (**e**) Fluorescence intensity of 5 μM ODN6UV at 450 nm after incubation with 100 μg/mL HCT116 cell lysate in buffer A with (cyan line) or without (blue line) 10 μM E-64 at 37 °C for various times. The fluorescence intensity was measured on a microplate reader (INFINITE M1000 PRO). Excitation wavelength: 360 nm, emission wavelength: 450 nm, both slit widths were set as 20 nm.

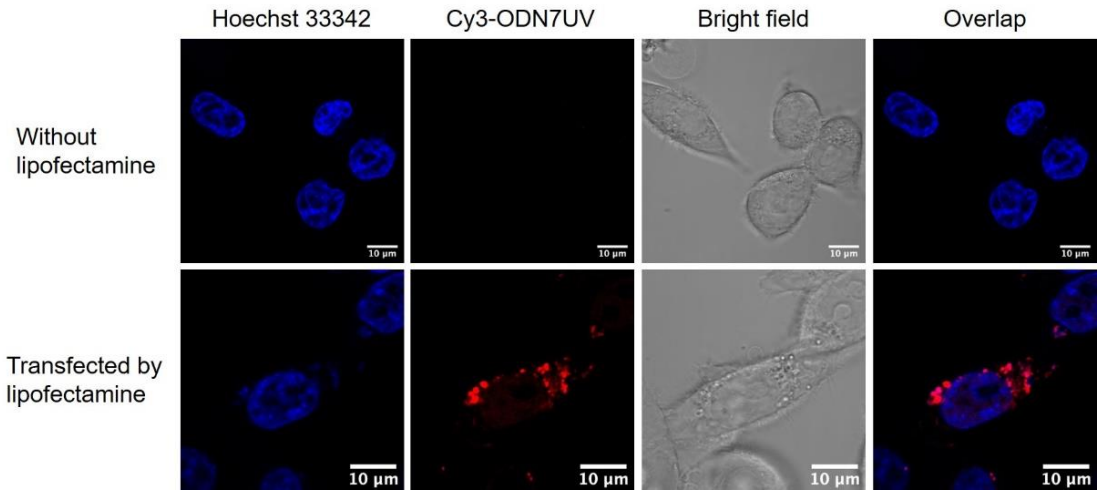

Figure S12. Confocal fluorescence microscopy imaging of HCT116 cells treated with Cy3-ODN7UV (1 μM) with or without transfection by lipofectamine in Opti-MEM culture medium at 37 °C for 6 hours. Cy3-ODN7UV: 5' CA4-Val-Ala-TTTTTTTTTTTT-Cy3 3'. Scale bar: 10 μm.

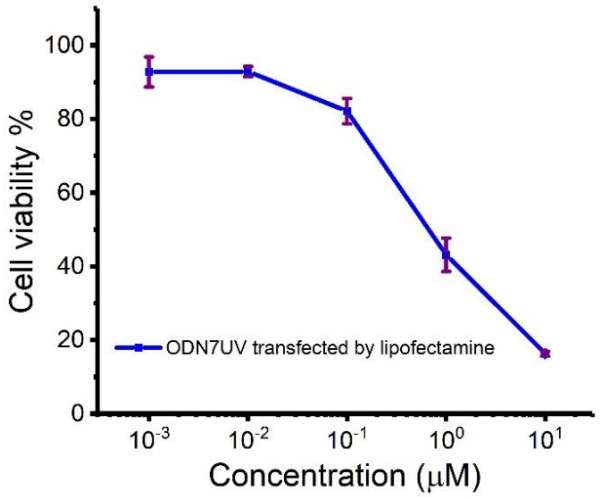

Figure S13. Cell viability of HCT116 cells after incubation with lipofectamine-transfected ODN7UV in Opti-MEM culture medium at 37 °C for 48 hours. The IC_{50} value of lipofectamine/ODN7UV complex to HCT116 cells after 48 hours of incubation in Opti-MEM culture medium is 0.79±0.4 μM.

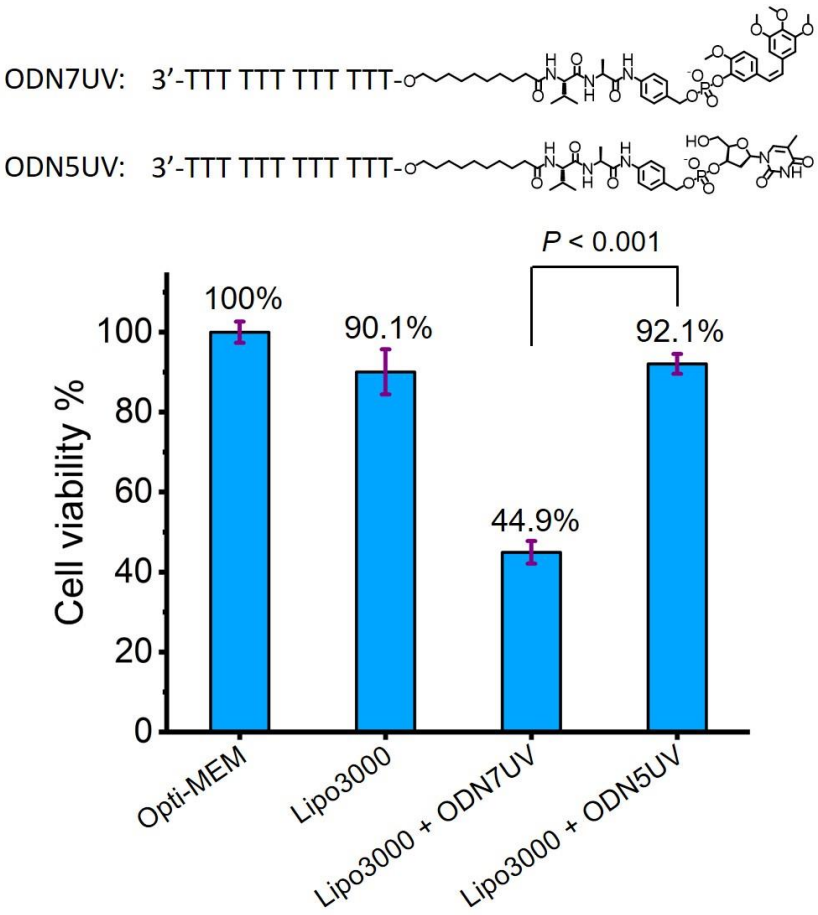

Figure S14. Cell viability of HCT116 cells after incubation with lipofectamine-transfected ODN7UV (1 μM) or lipofectamine-transfected ODN5UV (1 μM) in Opti-MEM cell culture medium at 37 °C for 48 hours.

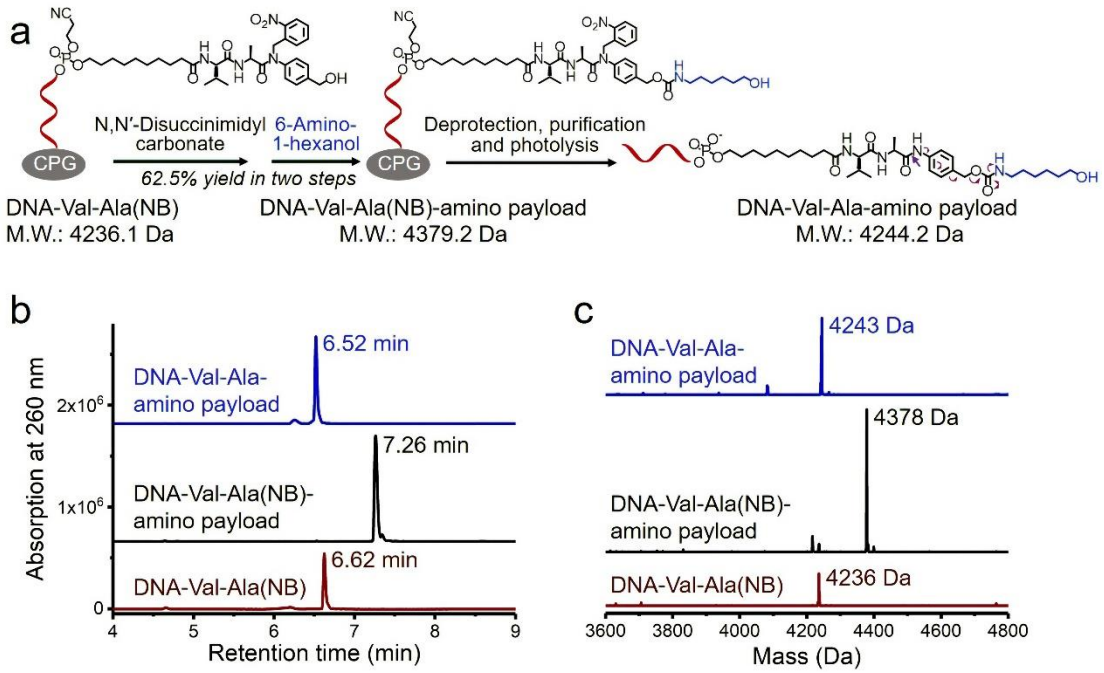

Figure S15. Solid-phase conjugation of small molecules containing an amino group with Val-Ala(NB) dipeptide linker through a carbamate linkage. (**a**) Schematic of activation and conjugation with 6-amino-1-hexanol of DNA-Val-Ala(NB) on resins, and the deprotection, purification and photolysis of DNA-Val-Ala(NB)-amino payload. (**b**) HPLC traces of DNA-Val-Ala(NB) (purple line), DNA-Val-Ala(NB)-amino payload (black line) and DNA-Val-Ala-amino payload (blue line). (**c**) Mass spectra of DNA-Val-Ala(NB) (purple line), DNA-Val-Ala(NB)-amino payload (black line) and DNA-Val-Ala-amino payload (blue line).

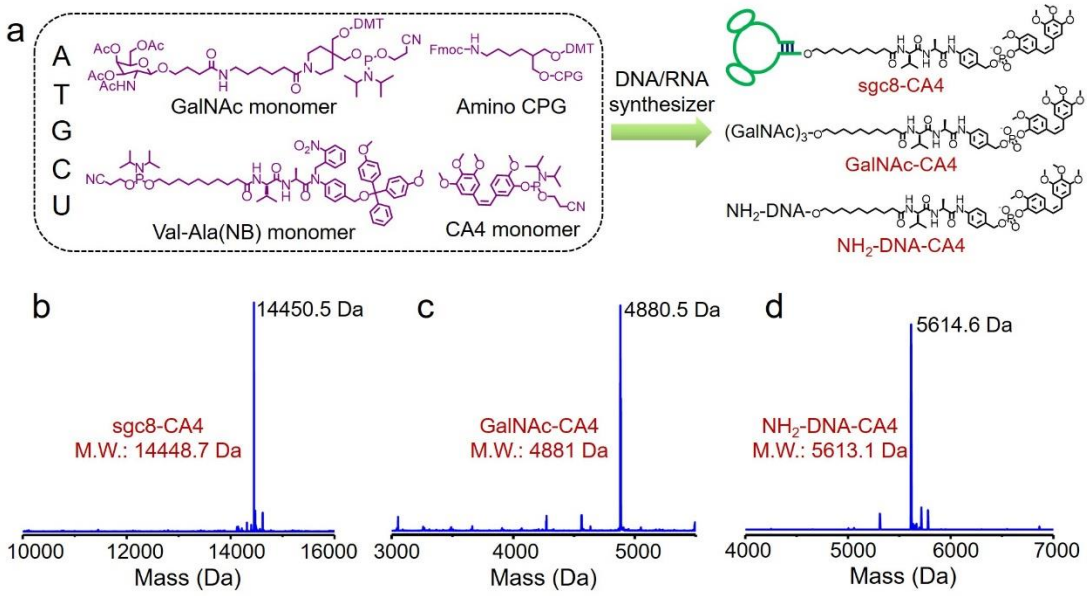

Figure S16. Automated conjugation of drug with targeted ligands or active groups through cleavable dipeptide linker. (**a**) Schematic of automated modular synthesis of sgc8-CA4, GalNAc-CA4 and NH_2-DNA-CA4 through DNA solid-phase synthesis. (**b**) Mass spectrum of sgc8-CA4 conjugate. (**c**) Mass spectrum of GalNAc-CA4 conjugate. (**d**) Mass spectrum of NH_2-DNA-CA4 conjugate.

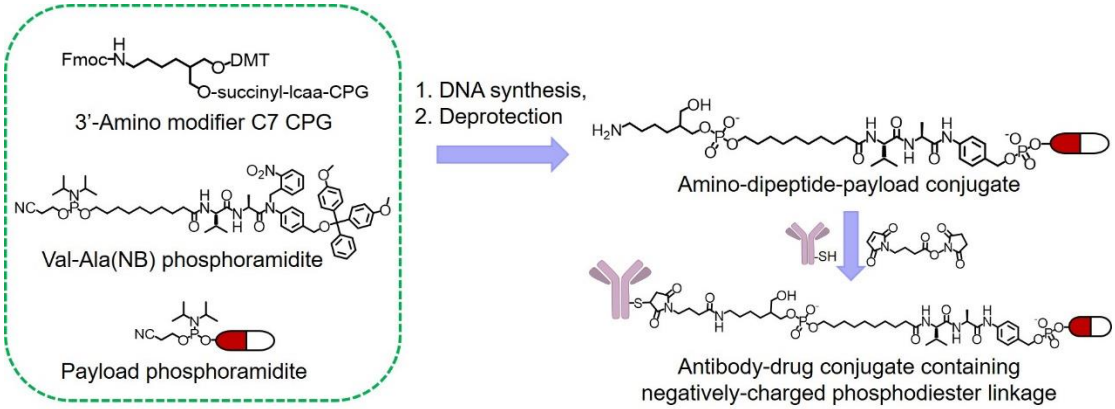

Figure S17. Automated synthesis of amino-dipeptide-payload conjugate through DNA solid-phase synthesis using of 3'-amino CPG and Val-Ala(NB) and payload phosphoramidites. The amino-dipeptide-payload and 4-maleimidobutyric acid N-hydroxysuccinimide ester enable the facile conjugation with antibody via Miachel addition reaction between thiol and maleimide groups.

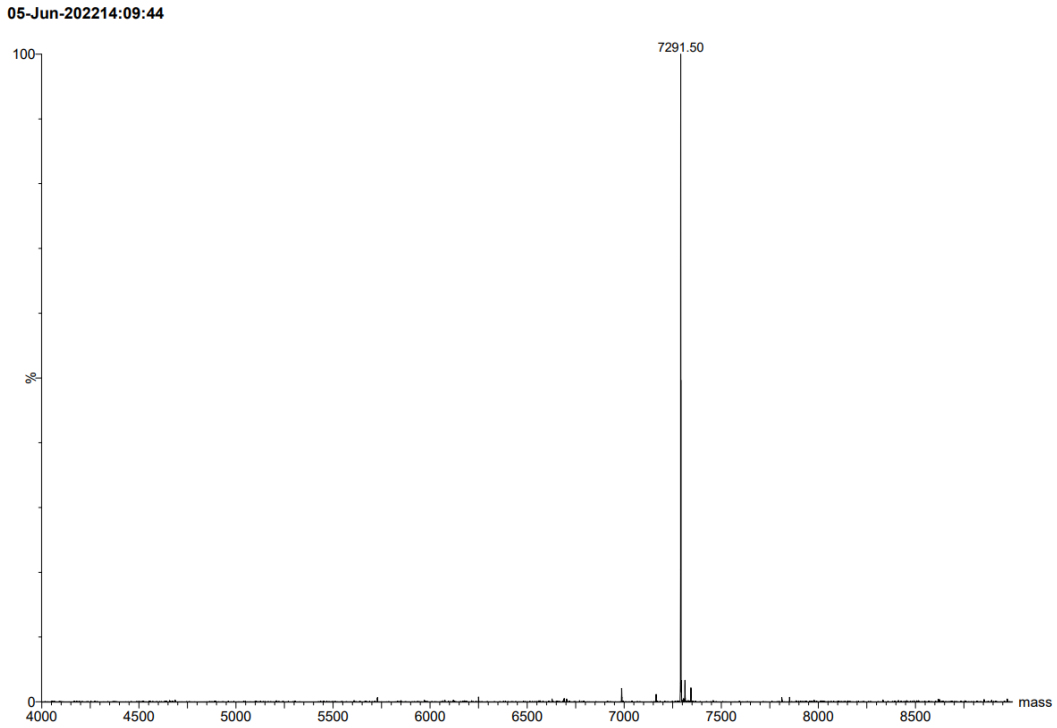

Figure S18. Mass spectrum of ODN4. The calculated molecular weight is 7290 Da, and observed molecular weight is 7291.5 Da.

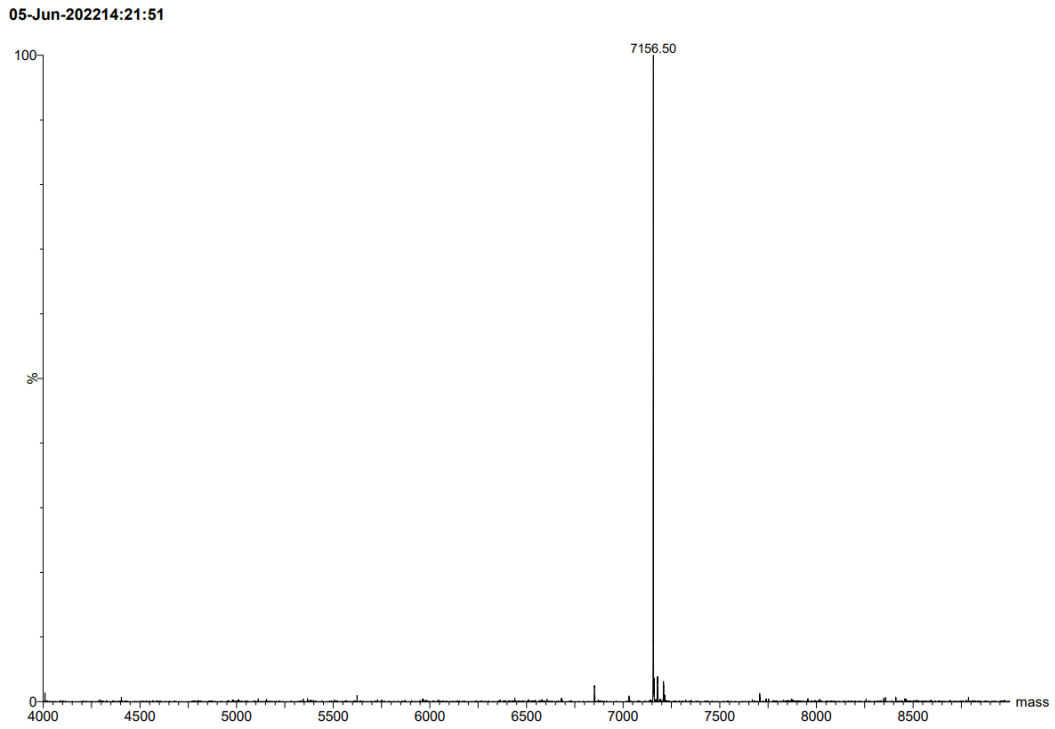

Figure S19. Mass spectrum of ODN4UV. The calculated molecular weight is 7154.9 Da, and observed molecular weight is 7156.5 Da.

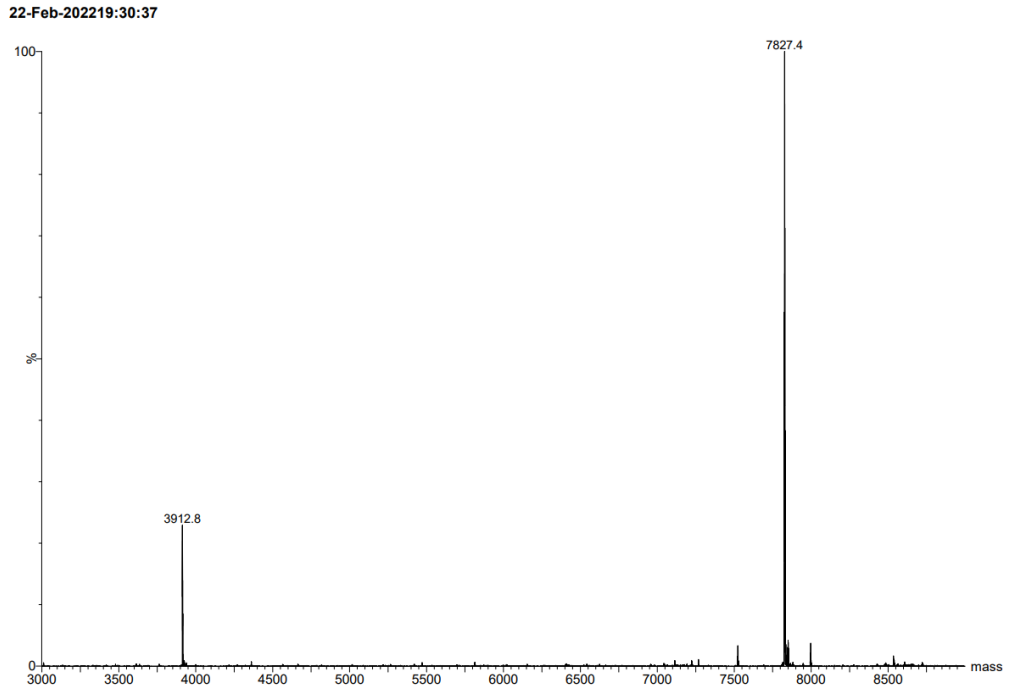

Figure S20. Mass spectrum of FAM-ODN4. The calculated molecular weight is 7826.7 Da, and observed molecular weight is 7827.4 Da. The DNA peak of 3912.8 Da is due to the half molecular weight of FAM-ODN4.

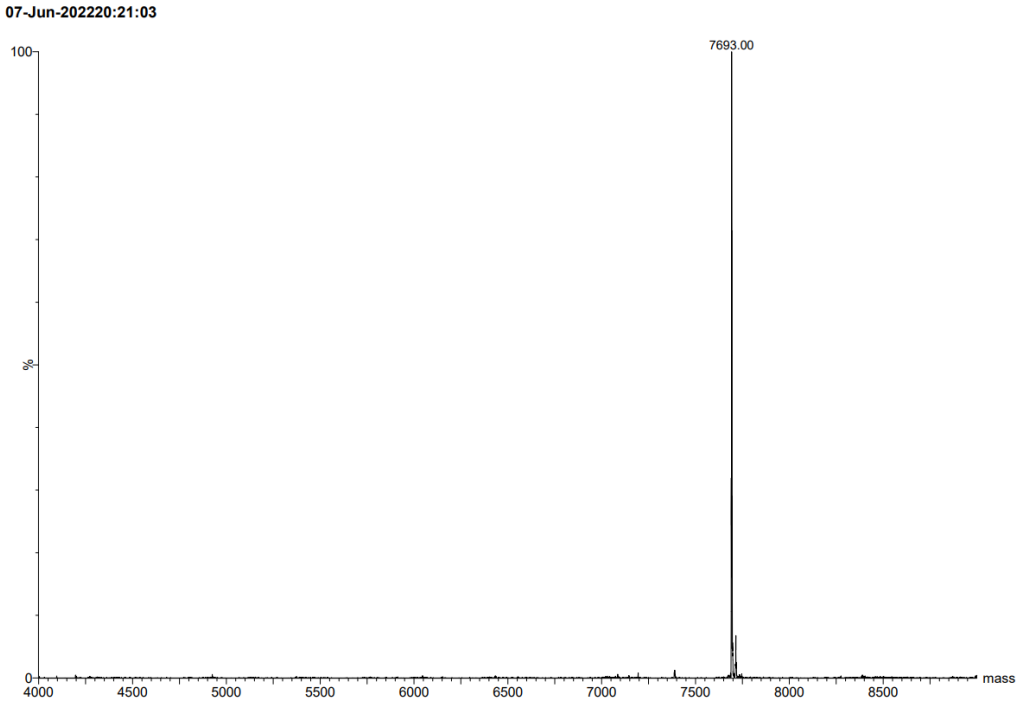

Figure S21. Mass spectrum of FAM-ODN4UV. The calculated molecular weight is 7692.5 Da, and observed molecular weight is 7693 Da.

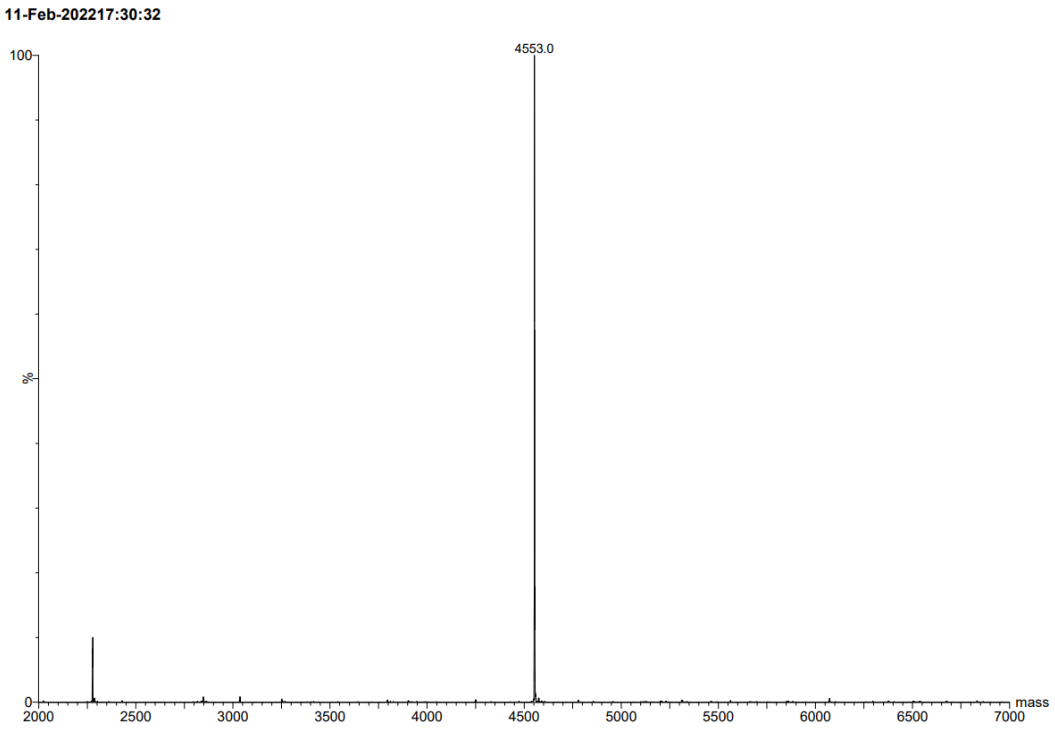

Figure S22. Mass spectrum of ODN5. The calculated molecular weight is 4552.3 Da, and observed molecular weight is 4553 Da. The DNA peak of 2276.5 Da is due to the half molecular weight of ODN5.

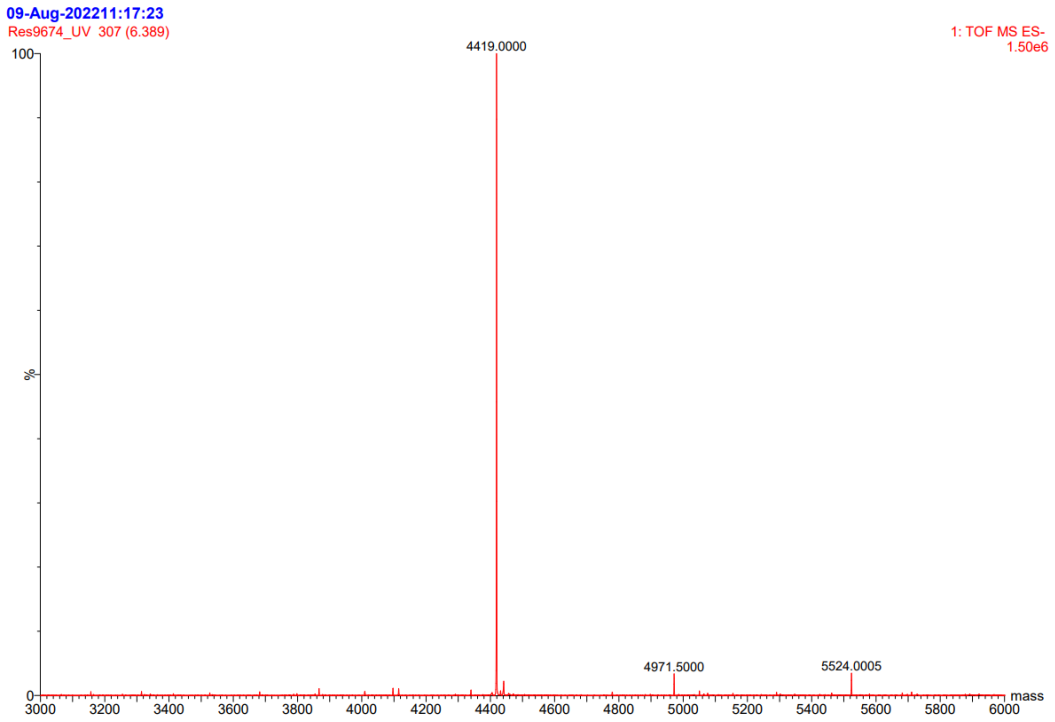

Figure S23. Mass spectrum of ODN5UV. The calculated molecular weight is 4417.2 Da, and observed molecular weight is 4419 Da.

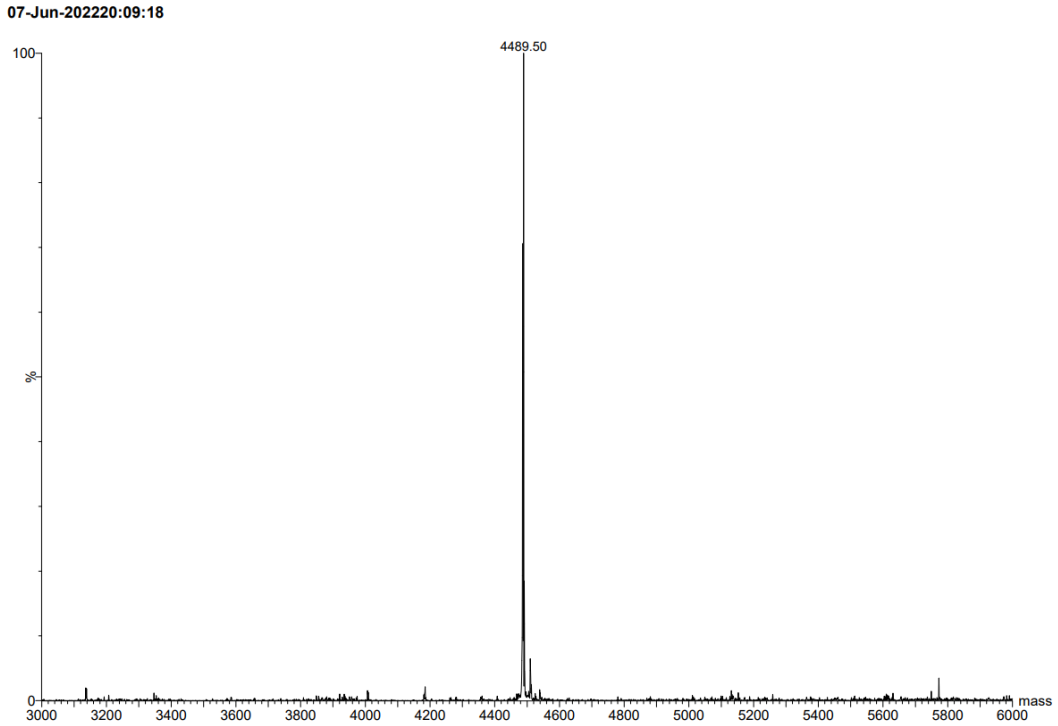

Figure S24. Mass spectrum of ODN6. The calculated molecular weight is 4486.2 Da, and observed molecular weight is 4489.5 Da.

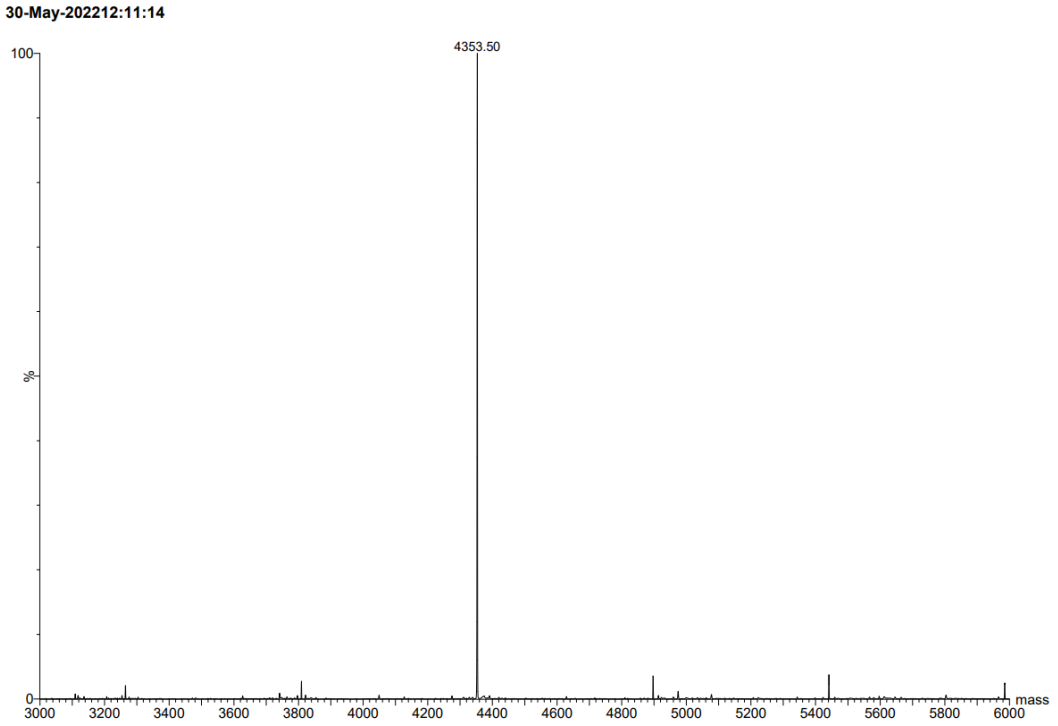

Figure S25. Mass spectrum of ODN6UV. Calculated molecular weight is 4351.1 Da, and observed molecular weight is 4353.5 Da.

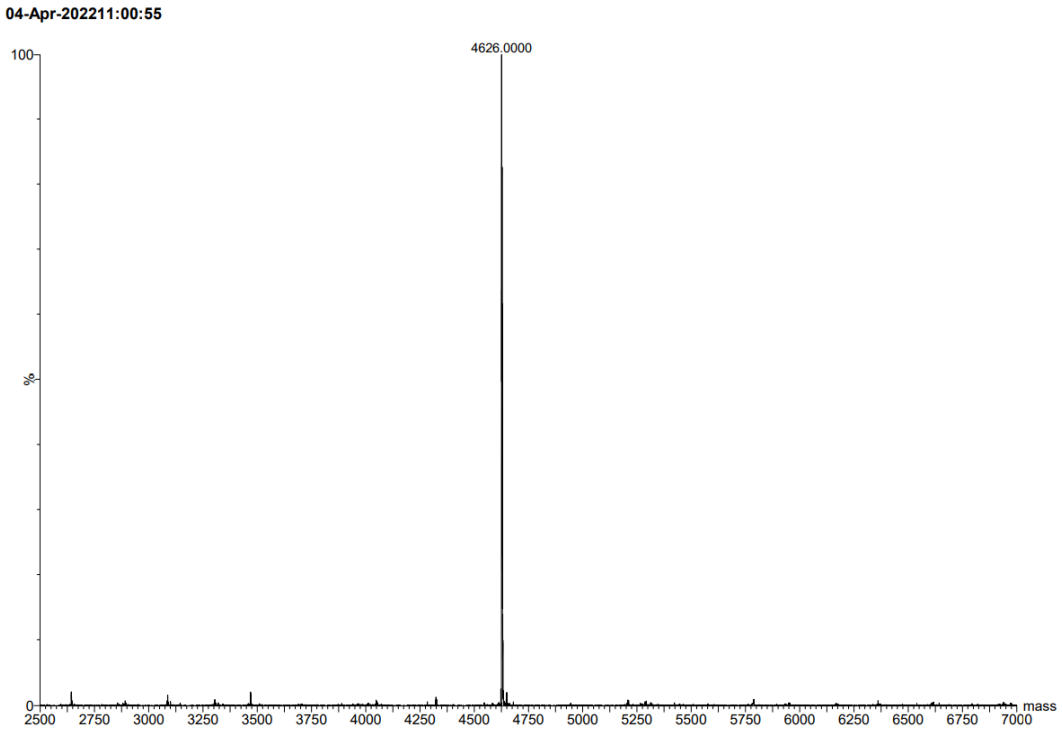

Figure S26. Mass spectrum of ODN7. The calculated molecular weight is 4625.4 Da, and observed molecular weight is 4626 Da.

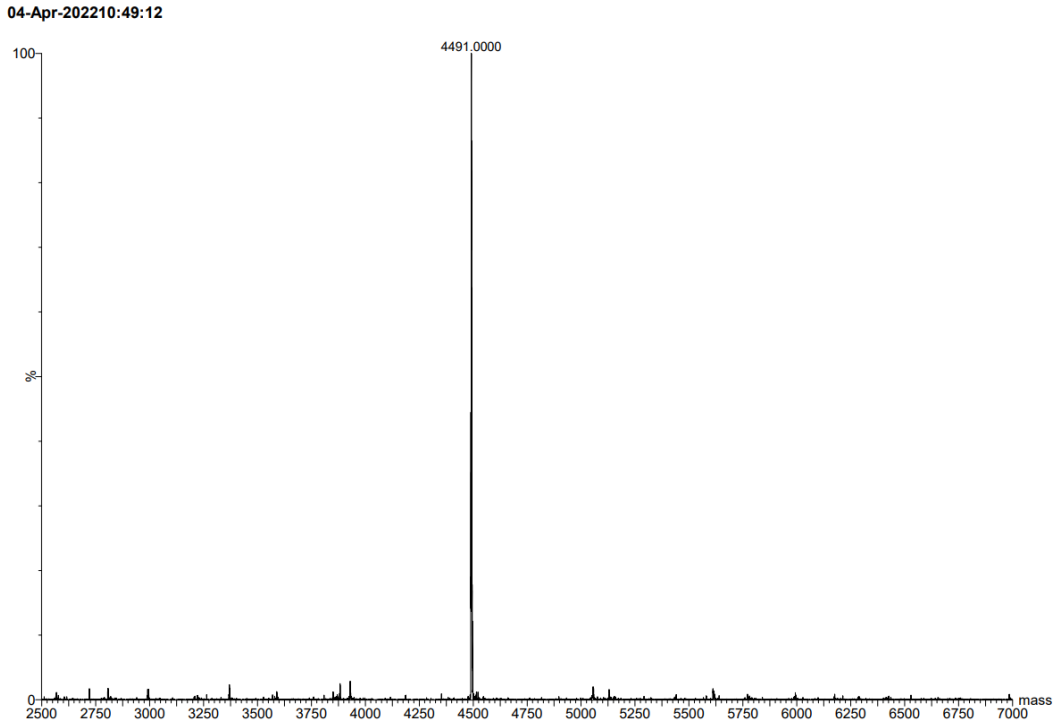

Figure S27. Mass spectrum of ODN7UV. The calculated molecular weight is 4490.3 Da, and observed molecular weight is 4491 Da.

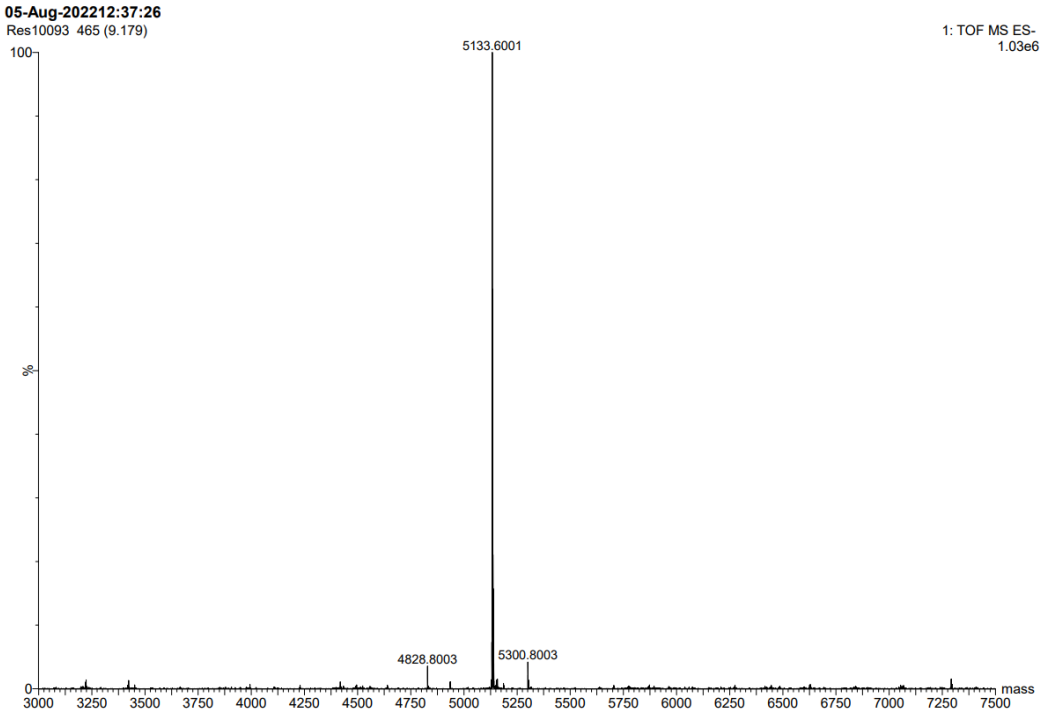

Figure S28. Mass spectrum of Cy3-ODN7. The calculated molecular weight is 5132 Da, and observed molecular weight is 5133.6 Da.

Figure S29. Mass spectrum of Cy3-ODN7UV. The calculated molecular weight is 4998.9 Da, and observed molecular weight is 5000 Da.

4. Synthesis of phosphoramidites

4.1 Synthesis of benzyl phosphoramidite

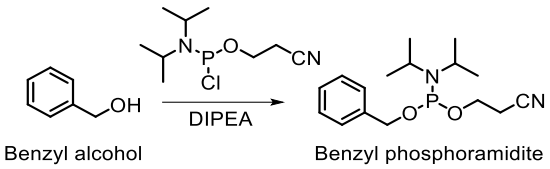

Figure S30. Synthesis of benzyl phosphoramidite.

Benzyl alcohol (0.2 g, 1.85 mmol) was dissolved in 20 mL anhydrous dichloromethane under argon gas protection, and 0.96 mL N,N-diisopropylethylamine (DIPEA) (0.71 g, 5.54 mmol) was added. The mixture was cooled down under ice bath. Then, 0.61 mL 2-cyanoethyl N,N-diisopropylchlorophosphoramidite (0.65 g, 2.74 mmol) was added dropwise. The reaction was monitored by thin-layer chromatography. When the reaction was completed, the mixture was diluted with 50 mL dichloromethane and washed successively with saturated $NaHCO_3$ and brine. The organic layer was collected and dried by anhydrous sodium sulfate. After purification by silica gel column chromatography (elution solvents: ethyl acetate/petroleum ether 1:3 to 1:1 v/v and 1% triethylamine was added), 0.18 g benzyl phosphoramidite was obtained as colorless oily. ^{1}H NMR (400 MHz, DMSO-*d*6) δ 7.40 – 7.32 (m, 4H), 7.29 (tt, *J* = 5.4, 4.3 Hz, 1H), 4.69 (qd, *J* = 12.7, 8.6 Hz, 2H), 3.87 – 3.69 (m, 2H), 3.69 – 3.55 (m, 2H), 2.78 (t, *J* = 5.9 Hz, 2H), 1.16 (dd, *J* = 8.4, 6.8 Hz, 12H). ^{31}P NMR (162 MHz, DMSO-*d*6) δ 147.31.

4.2 Synthesis of PAB phosphoramidite

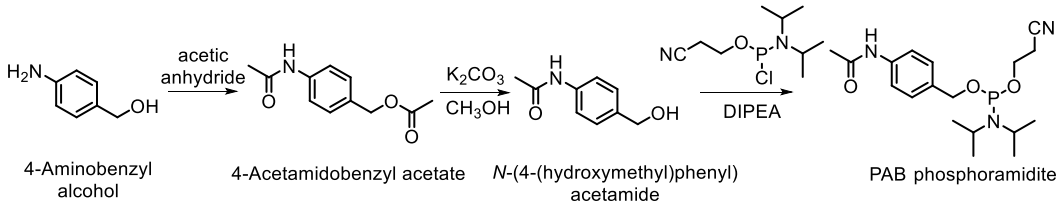

Figure S31. Synthesis of PAB phosphoramidite.

Synthesis of 4-acetamidobenzyl acetate

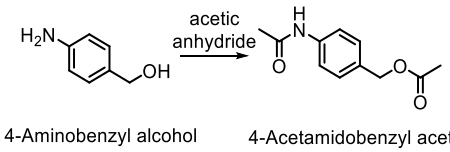

4-Aminobenzyl alcohol (0.51 g, 4.14 mmol) was dissolved in 30 mL dichloromethane. Triethylamine (1.44 mL, 10.3 mmol) and 1.69 g acetic anhydride (16.5 mmol) were added. The reaction was stirred at room temperature overnight. Then, the mixture was diluted with 100 mL dichloromethane and washed successively by saturated $NaHCO_3$ and brine. The organic layer was collected and dried by anhydrous Na_2SO_4. After removing organic solvent under reduced pressure, the residue was treated with 50 mL hexane, and the white precipitates were collected and dried under high vacuum. After drying, 0.73 g 4-acetamidobenzyl acetate was obtained as

white solid (85% yield). ^{1}H NMR (400 MHz, $CDCl_3$) δ 7.69 (s, 1H), 7.44 (d, *J* = 8.4 Hz, 2H), 7.22 (d, *J* = 8.4 Hz, 2H), 4.98 (s, 2H), 2.09 (s, 3H), 2.01 (s, 3H). ^{13}C NMR (101 MHz, $CDCl_3$) δ 170.99, 168.63, 138.06, 131.71, 129.17, 119.92, 65.95, 24.53, 21.05.

Synthesis of N-(4-(hydroxymethyl)phenyl)acetamide

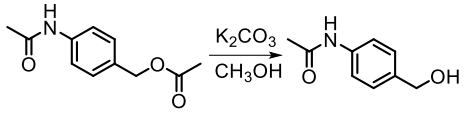

4-Acetamidobenzyl acetate *N*-(4-(hydroxymethyl)phenyl) acetamide

4-Acetamidobenzyl acetate (0.25 g, 1.2 mmol) was dissolved in 10 mL methanol, and 0.5 g K_2CO_3 (3.61 mmol) was added. The mixture was stirred overnight. Then, the solvent was removed under reduced pressure, and the residue was dissolved in 50 mL dichloromethane and washed with saturated brine. The organic layer was collected and dried with anhydrous Na_2SO_4. After drying under high vacuum, 114 mg N-(4-(hydroxymethyl)phenyl)acetamide was obtained (57.5% yield). ^{1}H NMR (400 MHz, DMSO-*d*6) δ 9.84 (s, 1H), 7.48 (d, *J* = 8.5 Hz, 2H), 7.18 (d, *J* = 8.5 Hz, 2H), 5.04 (s, 1H), 4.38 (s, 2H), 1.99 (s, 3H). ^{13}C NMR (101 MHz, DMSO-*d*6) δ 168.11, 137.95, 137.07, 126.90, 118.70, 62.63, 23.96.

Synthesis of PAB phosphoramidite

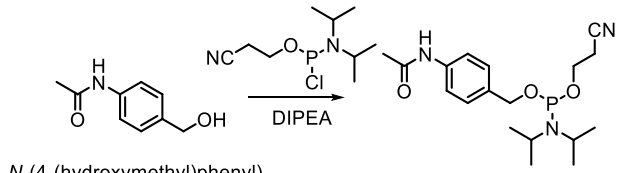

N-(4-(hydroxymethyl)phenyl) acetamide PAB phosphoramidite

N-(4-(hydroxymethyl)phenyl)acetamide (105 mg, 0.63 mmol) was dissolved in 20 mL anhydrous dichloromethane under argon gas protection, and 0.32 mL DIPEA (0.24 g, 1.9 mmol) was added. The mixture was cooled down under ice bath. Then, 0.25 mL 2-cyanoethyl N,N-diisopropylchlorophosphoramidite (0.23 g, 0.97 mmol) was added dropwise. The reaction was monitored by thin-layer chromatography. When the reaction was completed, the mixture was diluted with 50 mL dichloromethane and washed successively with saturated $NaHCO_3$ and brine. The organic layer was collected and dried by anhydrous Na_2SO_4. After purification by silica gel column chromatography (elution solvents: ethyl acetate and 1% triethylamine was added), 80 mg PAB phosphoramidite was obtained as colorless oily. ^{1}H NMR (400 MHz, DMSO-*d*6) δ 9.94 (s, 1H), 7.55 (d, *J* = 8.5 Hz, 2H), 7.25 (d, *J* = 8.5 Hz, 2H), 4.61 (ddd, *J* = 27.9, 12.4, 8.7 Hz, 2H), 3.81 – 3.66 (m, 2H), 3.66 – 3.53 (m, 2H), 2.77 (t, *J* = 5.9 Hz, 2H), 2.03 (s, 3H), 1.14 (dd, *J* = 8.7, 6.8 Hz, 12H). ^{31}P NMR (162 MHz, DMSO-*d*6) δ 147.17.

4.3 Synthesis of N-methylated PAB (mPAB) phosphoramidite

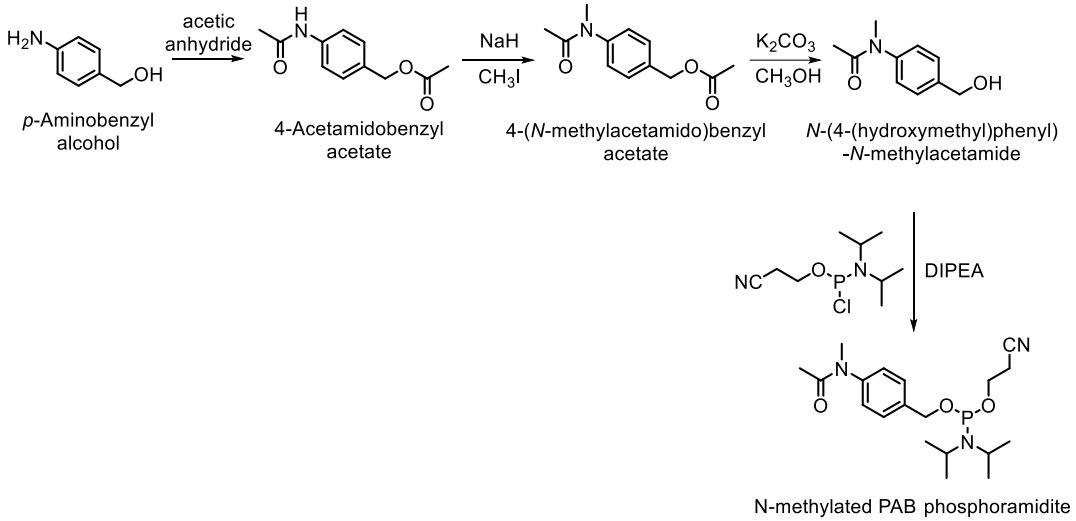

Figure S32. Synthesis of N-methylated PAB (mPAB) phosphoramidite.

Synthesis of 4-(N-methylacetamido)benzyl acetate

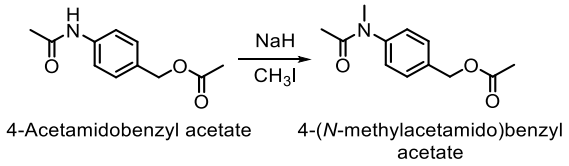

4-acetamidobenzyl acetate (0.442 g, 2.13 mmol) was dissolved in 10 mL dry tetrahydrofuran under argon gas protection. The mixture was cooled down under ice bath, and 84 mg NaH (60% dispersion in mineral oil) was added. The reaction was warmed to room temperature. When the hydrogen evolution ceased, 0.12 mL CH_3I was added, and the mixture was stirred for 30 minutes. Then, the mixture was poured into 40 mL saturated ammonium chloride and washed with ethyl acetate twice. The organic layer was collected and dried by anhydrous Na_2SO_4. After purification by silica gel column chromatography (elution solvent: ethyl acetate), 0.31 g 4-(N-methylacetamido)benzyl acetate was obtained (65.7% yield). ^{1}H NMR (400 MHz, $CDCl_3$) δ 7.34 (d, *J* = 8.3 Hz, 2H), 7.12 (d, *J* = 8.2 Hz, 2H), 5.05 (s, 2H), 3.19 (s, 3H), 2.06 (s, 3H), 1.81 (s, 3H). ^{13}C NMR (101 MHz, $CDCl_3$) δ 170.75, 170.45, 144.47, 135.61, 129.50, 127.24, 65.48, 37.13, 22.44, 20.97.

Synthesis of N-(4-(hydroxymethyl)phenyl)-N-methylacetamide

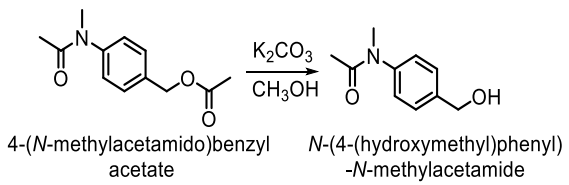

4-(N-methylacetamido)benzyl acetate (0.29 g, 1.31 mmol) was dissolved in 20 mL methanol, 0.54 g K_2CO_3 (3.91 mmol) was added. The mixture was stirred overnight under room

temperature. Then, the organic solvent was removed under reduced pressure, and the residue was dissolved in 100 mL dichloromethane and washed successively with saturated $NaHCO_3$ and brine. The organic layer was collected and dried by anhydrous Na_2SO_4. After purification by silica gel column chromatography (elution solvent: ethyl acetate), 185 mg of N-(4-(hydroxymethyl)phenyl)-N-methylacetamide was obtained (78.6% yield). ^{1}H NMR (400 MHz, $CDCl_3$) δ 7.36 (d, *J* = 8.2 Hz, 2H), 7.11 (d, *J* = 8.2 Hz, 2H), 4.67 (s, 2H), 3.18 (s, 3H), 2.28 (s, 1H), 1.80 (s, 3H). ^{13}C NMR (101 MHz, $CDCl_3$) δ 170.72, 143.77, 140.70, 128.19, 127.11, 64.49, 37.21, 22.37.

Synthesis of mPAB phosphoramidite

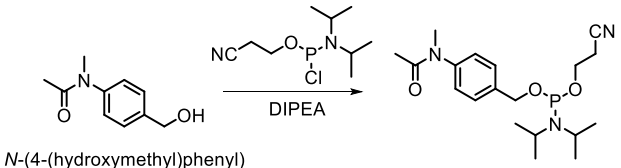

N-(4-(hydroxymethyl)phenyl)-*N*-methylacetamide

mPAB phosphoramidite

N-(4-(hydroxymethyl)phenyl)-N-methylacetamide (170 mg, 0.95 mmol) was dissolved in 20 mL anhydrous dichloromethane under argon gas protection, and 0.5 mL DIPEA (2.84 mmol) was added. The mixture was cooled down under ice bath. Then, 0.32 mL 2-cyanoethyl N,N-diisopropylchlorophosphoramidite (1.42 mmol) was added dropwise. The reaction was monitored by thin-layer chromatography. When the reaction was completed, the mixture was diluted with 50 mL dichloromethane and washed successively with saturated $NaHCO_3$ and brine. The organic layer was collected and dried by anhydrous Na_2SO_4. After purification by silica gel column chromatography (elution solvents: ethyl acetate and 1% triethylamine was added), 150 mg mPAB phosphoramidite was obtained as colorless oily (42.1% yield). ^{1}H NMR (400 MHz, $CDCl_3$) δ 7.39 (d, *J* = 8.3 Hz, 2H), 7.16 (d, *J* = 8.3 Hz, 2H), 4.73 (ddd, *J* = 36.9, 12.8, 8.3 Hz, 2H), 3.97 – 3.78 (m, 2H), 3.75 – 3.60 (m, 2H), 3.25 (s, 3H), 2.65 (t, *J* = 6.4 Hz, 2H), 1.87 (s, 3H), 1.20 (dd, *J* = 8.4, 6.8 Hz, 12H). ^{31}P NMR (162 MHz, $CDCl_3$) δ 148.71. ^{13}C NMR (101 MHz, $CDCl_3$) δ 170.56, 144.04, 143.81, 128.24, 127.01, 117.57, 64.95, 64.77, 58.55, 58.36, 43.28, 43.16, 37.17, 24.70, 24.63, 24.57, 22.43, 20.45, 20.38.

4.4 Synthesis of Val-Ala(NB) phosphoramidite

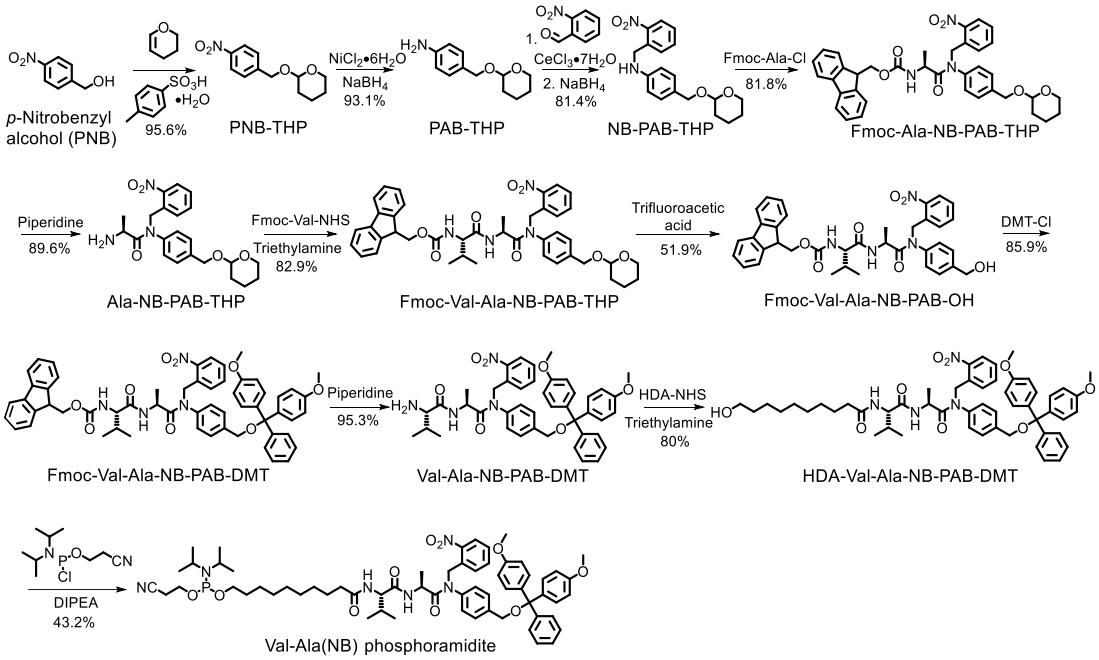

Figure S33. Synthesis of Val-Ala(NB) phosphoramidite.

Synthesis of PNB-THP

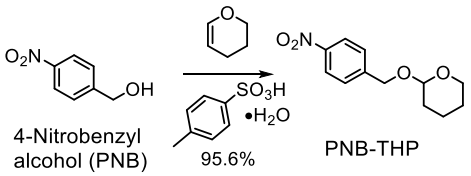

4-Nitrobenzyl alcohol (5.0 g, 32.6 mmol) was dissolved in 100 mL dichloromethane. 3,4-Dihydro-2H-pyran (4.12 g, 48.9 mmol) and 0.93 g *p*-toluenesulfonic acid monohydrate (4.9 mmol) were added. The mixture was stirred under room temperature for 1.5 hours. Then, the mixture was washed with saturated $NaHCO_3$. The organic layer was collected and dried over anhydrous Na_2SO_4. After purification by silica gel column chromatography (elution solvents: ethyl acetate/petroleum ether 1:5 to 1:2 v/v), 7.4 g PNB-THP was obtained as yellow oily (95.6% yield). ^{1}H NMR (400 MHz, $CDCl_3$) δ 8.20 (d, *J* = 8.8 Hz, 2H), 7.53 (d, *J* = 8.9 Hz, 2H), 4.88 (d, *J* = 13.5 Hz, 1H), 4.73 (t, *J* = 3.5 Hz, 1H), 4.60 (d, *J* = 13.5 Hz, 1H), 3.94 – 3.82 (m, 1H), 3.62 – 3.52 (m, 1H), 1.90 – 1.75 (m, 2H), 1.69 – 1.50 (m, 4H). ^{13}C NMR (101 MHz, $CDCl_3$) δ 147.29, 146.12, 127.77, 123.60, 98.31, 67.64, 62.29, 30.46, 25.36, 19.27.

Synthesis of PAB-THP

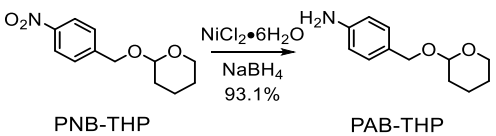

PNB-THP (1.18 g, 4.97 mmol) was dissolved in 20 mL CH_3CN in 150 mL flask. H_2O (2 mL) and 0.2 g nickel (II) chloride hexahydrate (0.84 mmol) were added. The mixture was stirred

under room temperature for 5 minutes. Then, 0.63 g sodium borohydride (16.8 mmol) was added (*keeping the flask opened to balance gas pressure*), and the mixture was stirred for 30 minutes under room temperature. Then, the mixture was diluted with 30 mL H_2O and extracted with dichloromethane (100 mL). The organic layer was collected and dried by Na_2SO_4. The solvents were removed under reduced pressure, and the residue was dried under high vacuum. 0.96 g PAB-THP was obtained as oily (93.1% yield). ^{1}H NMR (400 MHz, $CDCl_3$) δ 7.17 (d, *J* = 8.4 Hz, 2H), 6.68 (d, *J* = 8.4 Hz, 2H), 4.67 (dd, *J* = 7.7, 3.9 Hz, 2H), 4.39 (d, *J* = 11.5 Hz, 1H), 3.92 (ddd, *J* = 11.5, 8.2, 3.4 Hz, 1H), 3.62 – 3.45 (m, 1H), 1.90 – 1.79 (m, 1H), 1.76 – 1.66 (m, 1H), 1.64 – 1.50 (m, 4H). ^{13}C NMR (101 MHz, $CDCl_3$) δ 145.48, 129.63, 128.43, 115.21, 97.35, 68.73, 62.17, 30.64, 25.53, 19.48.

Synthesis of NB-PAB-THP

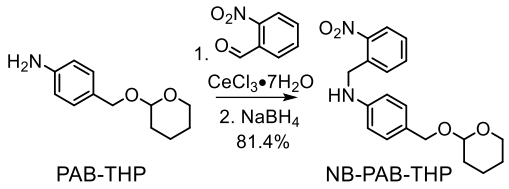

PAB-THP (0.95 g, 4.58 mmol) was dissolved in 25 mL methanol in 150 mL flask. 2-Nitrobenzaldehyde (0.76 g, 5.03 mmol) and 68 mg cerium (III) chloride heptahydrate (0.18 mmol) were added. The mixture was stirred at room temperature for 30 minutes. Then, 0.433 g sodium borohydride (11.45 mmol) was added (*keeping the flask opened to balance gas pressure*) and stirred for further 2 hours. The residue was diluted with 100 mL ethyl acetate and washed with saturated $NaHCO_3$. The organic layer was collected and dried over anhydrous Na_2SO_4. After purification by silica gel column chromatography (elution solvents: ethyl acetate/petroleum ether 1:4 to 1:3 v/v), 1.28 g NB-PAB-THP was obtained as orange oily (81.4% yield). ^{1}H NMR (400 MHz, $CDCl_3$) δ 7.98 (dd, *J* = 8.1, 1.3 Hz, 1H), 7.57 (d, *J* = 7.8 Hz, 1H), 7.47 (td, *J* = 7.6, 1.3 Hz, 1H), 7.37 – 7.16 (m, 2H), 7.08 (d, *J* = 8.5 Hz, 2H), 6.49 – 6.43 (m, 2H), 4.64 (s, 2H), 4.61 – 4.54 (m, 2H), 4.28 (d, *J* = 11.4 Hz, 1H), 3.84 (ddd, *J* = 11.4, 8.1, 3.1 Hz, 1H), 3.49 – 3.42 (m, 1H), 1.82 – 1.71 (m, 1H), 1.64 – 1.58 (m, 1H), 1.56 – 1.42 (m, 4H). ^{13}C NMR (101 MHz, $CDCl_3$) δ 147.02, 135.69, 133.77, 129.89, 129.81, 128.92, 128.09, 125.28, 121.33, 112.88, 97.56, 68.90, 62.27, 45.89, 30.73, 25.61, 19.58.

Synthesis of Fmoc-Ala-NB-PAB-THP

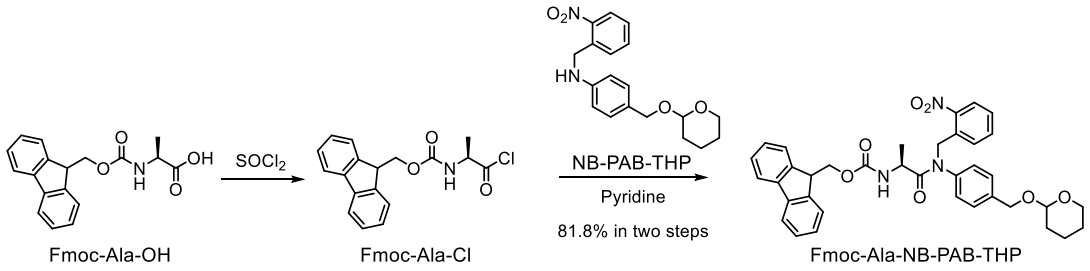

Fmoc-Ala-OH (1.5 g, 4.8 mmol) was dissolved in anhydrous dichloromethane (30 mL) in a two-neck flask under argon gas protection, and excess $SOCl_2$ (2.8 mL, 38.5 mmol) was added

dropwise. The mixture was heated at reflux for 30 min. Then, the solvent was evaporated under reduced pressure, and the residue was purified by crystallization from anhydrous *n*-hexane. After drying, Fmoc-Ala-Cl was obtained as white solid and used for the next step without further purification.

NB-PAB-THP (3.7 g, 10.8 mmol) was dissolved in 30 mL anhydrous dichloromethane under argon gas protection, and dry pyridine (0.78 mL, 9.6 mmol) was added. Then, Fmoc-Ala-Cl (4.8 mmol) in dry dichloromethane was added dropwise. The mixture was stirred under room temperature for 24 hours. Then, the organic solvents were removed under reduced pressure, and the residue was purified by silica gel column chromatography (elution solvents: ethyl acetate/petroleum ether 1:4 to 1:1 v/v). After purification, 2.5 g Fmoc-Ala-NB-PAB-THP was obtained as foam solid (81.8% yield in two steps). ^{1}H NMR (400 MHz, CDCl3) δ 7.95 (d, *J* = 8.1 Hz, 1H), 7.76 (d, *J* = 7.5 Hz, 2H), 7.65 – 7.55 (m, 4H), 7.40 (t, *J* = 8.4 Hz, 5H), δ 7.31 (t, *J* = 7.5 Hz, 2H), 7.22 (d, *J* = 8.2 Hz, 2H), 5.55 (d, *J* = 8.0 Hz, 1H), 5.43 (dd, *J* = 16.5, 3.4 Hz, 1H), 5.17 (dd, *J* = 16.5, 2.9 Hz, 1H), 4.78 (d, *J* = 12.6 Hz, 1H), 4.71 (dd, *J* = 6.8, 3.4 Hz, 1H), 4.52 – 4.43 (m, 2H), 4.40 – 4.30 (m, 2H), 4.22 (t, *J* = 7.1 Hz, 1H), 3.88 (t, *J* = 10.4 Hz, 1H), 3.54 (d, *J* = 11.1 Hz, 1H), 1.85 (ddd, *J* = 13.7, 10.0, 4.0 Hz, 1H), 1.77 – 1.70 (m, 1H), 1.69 – 1.52 (m, 4H), 1.25 (d, *J* = 6.9 Hz, 3H). ^{13}C NMR (101 MHz, CDCl3) δ 173.83, 155.77, 143.90, 143.79, 141.27, 140.07, 139.35, 133.51, 132.21, 129.62, 129.05, 128.16, 127.89, 127.69, 127.06, 125.15, 124.92, 119.96, 99.97, 98.10, 98.00, 67.91, 67.03, 62.14, 51.00, 47.67, 47.11, 30.47, 25.39, 19.25, 18.66.

Synthesis of Ala-NB-PAB-THP

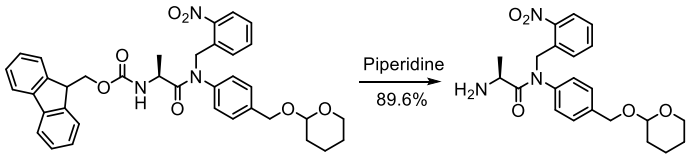

Fmoc-Ala-NB-PAB-THP Ala-NB-PAB-THP

Fmoc-Ala-NB-PAB-THP (1.41 g, 2.21 mmol) was dissolved in 24 mL N,N-dimethylformamide (DMF), and 6 mL piperidine was added. The mixture was stirred under room temperature for 30 minutes. Then, the organic solvents were removed under high vacuum, and the residue was purified by silica gel column chromatography (elution solvents: ethyl acetate/petroleum ether 1:1 to dichloromethane/methanol 10:1 v/v). After drying, 0.82 g Ala-NB-PAB-THP was obtained (89.6% yield). ^{1}H NMR (400 MHz, $CDCl_3$) δ 7.92 (d, *J* = 8.0 Hz, 1H), 7.63 – 7.55 (m, 2H), 7.43 – 7.37 (m, 1H), 7.35 (d, *J* = 8.3 Hz, 2H), 7.10 (d, *J* = 8.3 Hz, 2H), 5.35 – 5.19 (m, 2H), 4.77 (d, *J* = 12.5 Hz, 1H), 4.72 – 4.67 (m, 1H), 4.47 (d, *J* = 12.5 Hz, 1H), 3.93 – 3.84 (m, 1H), 3.55 (ddd, *J* = 15.8, 11.9, 5.7 Hz, 2H), 1.88 – 1.80 (m, 3H), 1.76 – 1.70 (m, 1H), 1.65 – 1.50 (m, 4H), 1.18 (d, *J* = 6.7 Hz, 3H). ^{13}C NMR (101 MHz, $CDCl_3$) δ 177.13, 148.79, 140.75, 139.16, 133.50, 132.66, 129.89, 129.12, 128.28, 127.86, 124.98, 98.20, 98.14, 68.07, 62.35, 50.61, 47.58, 30.62, 25.51, 21.98, 19.44.

Synthesis of Fmoc-Val-Ala-NB-PAB-THP

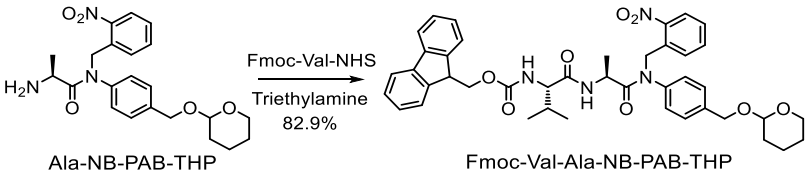

Ala-NB-PAB-THP (0.8 g, 1.93 mmol) and 1.26 g Fmoc-Val-NHS[1] (2.90 mmol) were dissolved in 40 mL dichloromethane, and 0.3 mL triethylamine was added. The mixture was stirred under room temperature overnight. Then, the organic solvents were removed under reduced pressure. After purification by silica gel column chromatography (elution solvents: ethyl acetate/petroleum ether 1:3 to 2:1 v/v), 1.18 g Fmoc-Val-Ala-NB-PAB-THP was obtained as solid foam (82.9% yield). ^{1}H NMR (400 MHz, $CDCl_3$) δ 7.96 (d, *J* = 8.1 Hz, 1H), 7.75 (d, *J* = 7.5 Hz, 2H), 7.60 (dt, *J* = 11.4, 7.1 Hz, 4H), 7.38 (dd, *J* = 7.0, 4.1 Hz, 5H), 7.33 – 7.23 (m, 4H), 6.62 (d, *J* = 6.9 Hz, 1H), 5.44 (dd, *J* = 16.9, 14.1 Hz, 2H), 5.08 (d, *J* = 18.3 Hz, 1H), 4.77 (d, *J* = 12.5 Hz, 1H), 4.70 (dd, *J* = 6.6, 3.1 Hz, 1H), 4.62 (p, *J* = 6.9 Hz, 1H), 4.47 (d, *J* = 12.5 Hz, 1H), 4.38 (dt, *J* = 17.5, 10.5 Hz, 2H), 4.20 (t, *J* = 7.0 Hz, 1H), 4.06 (dd, *J* = 8.5, 6.3 Hz, 1H), 3.88 (t, *J* = 10.0 Hz, 1H), 3.60 – 3.50 (m, 1H), 2.13 (td, *J* = 13.1, 6.6 Hz, 1H), 1.91 – 1.80 (m, 1H), 1.71 (m, 1H), 1.68 – 1.51 (m, 4H), 1.21 (d, *J* = 6.9 Hz, 3H), 0.97 (dd, *J* = 10.3, 6.9 Hz, 6H). ^{13}C NMR (101 MHz, $CDCl_3$) δ 173.37, 170.93, 156.30, 148.41, 143.94, 143.78, 141.30, 140.22, 139.39, 139.36, 133.49, 132.27, 129.49, 129.08, 128.12, 127.89, 127.70, 127.07, 125.11, 124.99, 119.98, 119.96, 98.12, 98.02, 68.00, 67.94, 67.07, 62.16, 62.14, 59.93, 51.29, 47.21, 46.40, 33.97, 31.58, 30.50, 25.63, 25.42, 24.96, 19.29, 19.27, 19.10, 17.95, 17.84.

Synthesis of Fmoc-Val-Ala-NB-PAB-OH

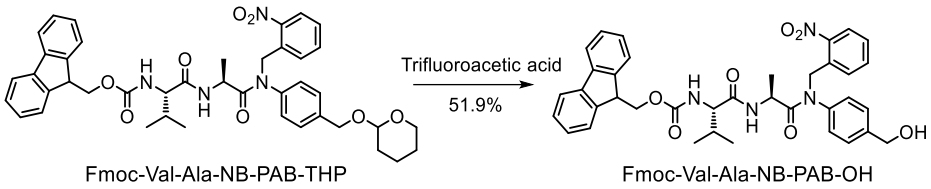

1.09 g Fmoc-Val-Ala-NB-PAB-THP (1.56 mmol) was dissolved in 10 mL dichloromethane, and 10 mL trifluoroacetic acid was added. The mixture was stirred under room temperature for two hours. Then, the organic solvents were removed under high vacuum. The residue was purified by silica gel column chromatography (elution solvents: ethyl acetate/petroleum ether 1:1 v/v to ethyl acetate). After purification, 0.53 g Fmoc-Val-Ala-NB-PAB-OH was obtained (51.9% yield). ^{1}H NMR (400 MHz, $CDCl_3$) δ 7.94 (d, *J* = 8.0 Hz, 1H), 7.75 (d, *J* = 7.5 Hz, 2H), 7.58 (dd, *J* = 11.4, 6.3 Hz, 4H), 7.38 (t, *J* = 7.7 Hz, 5H), 7.27 (dt, *J* = 17.2, 8.1 Hz, 4H), 6.65 (d, *J* = 4.7 Hz, 1H), 5.53 – 5.37 (m, 2H), 5.10 (d, *J* = 16.5 Hz, 1H), 4.67 (s, 2H), 4.57 (p, *J* = 6.8 Hz, 1H), 4.37 (dt, *J* = 17.2, 10.4 Hz, 2H), 4.18 (t, *J* = 6.9 Hz, 1H), 4.07 – 4.00 (m, 1H), 2.49 – 2.30 (m, 1H), 2.12 (dt, *J* = 15.5, 8.7 Hz, 1H), 1.20 (d, *J* = 6.8 Hz, 3H), 0.96 (dd, *J* = 9.6, 7.1 Hz, 6H). ^{13}C NMR (101 MHz, $CDCl_3$) δ 173.47, 171.19, 156.49, 148.62, 144.03, 143.87, 141.91, 141.42, 133.61,

132.19, 129.81, 128.52, 128.35, 128.18, 127.84, 127.20, 125.21, 125.08, 120.10, 67.23, 64.49, 60.17, 60.14, 51.18, 47.30, 46.55, 31.57, 19.25, 18.05, 17.96, 17.93.

Synthesis of Fmoc-Val-Ala-NB-PAB-DMT

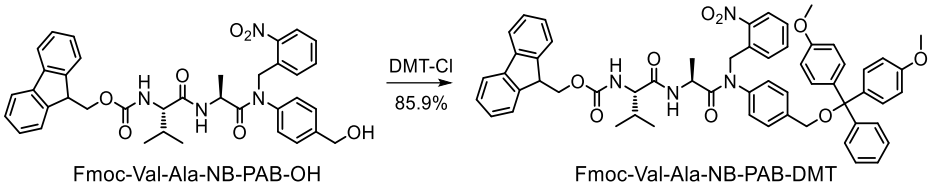

Fmoc-Val-Ala-NB-PAB-OH　　Fmoc-Val-Ala-NB-PAB-DMT

Fmoc-Val-Ala-NB-PAB-OH (0.51 g, 0.78 mmol) was dissolved in 20 mL anhydrous pyridine under argon gas protection. 4,4'-Dimethoxytrityl chloride (DMT-Cl) (0.53 g, 1.56 mmol) was added, and the mixture was stirred overnight. Then, the solvent was removed under high vacuum, and the residue was purified by silica gel column chromatography (elution solvents: ethyl acetate/petroleum ether 1:2 to 1:1 v/v and 1% triethylamine was added). After purification, 0.64 g Fmoc-Val-Ala-NB-PAB-DMT was obtained as solid foam (85.9% yield). ^{1}H NMR (400 MHz, $CDCl_3$) δ 7.98 (d, *J* = 8.1 Hz, 1H), 7.75 (d, *J* = 7.4 Hz, 2H), 7.67 – 7.55 (m, 4H), 7.49 (dd, *J* = 5.2, 3.4 Hz, 2H), 7.44 – 7.34 (m, 9H), 7.33 – 7.25 (m, 5H), 7.25 – 7.18 (m, 2H), 6.87 – 6.77 (m, 4H), 6.55 (d, *J* = 7.0 Hz, 1H), 5.44 (dd, *J* = 22.9, 12.8 Hz, 2H), 5.09 (d, *J* = 16.7 Hz, 1H), 4.64 (p, *J* = 6.9 Hz, 1H), 4.39 (ddd, *J* = 17.5, 10.5, 7.5 Hz, 2H), 4.24 – 4.16 (m, 3H), 4.06 (dd, *J* = 8.6, 6.2 Hz, 1H), 3.78 (s, 6H), 2.19 – 2.09 (m, 1H), 1.23 (d, *J* = 7.0 Hz, 3H), 0.98 (dd, *J* = 9.8, 7.0 Hz, 6H). ^{13}C NMR (101 MHz, $CDCl_3$) δ 173.52, 158.66, 156.42, 148.51, 144.94, 144.04, 143.90, 141.43, 140.42, 139.93, 136.13, 133.64, 132.47, 130.15, 129.53, 128.38, 128.25, 128.03, 127.83, 127.20, 126.98, 120.10, 113.32, 86.69, 67.18, 64.81, 60.08, 55.35, 51.55, 47.33, 46.56, 31.70, 19.24, 18.13, 17.96.

Synthesis of Val-Ala-NB-PAB-DMT

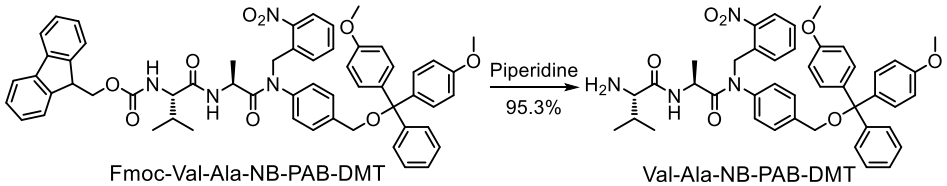

Fmoc-Val-Ala-NB-PAB-DMT　　Val-Ala-NB-PAB-DMT

Fmoc-Val-Ala-NB-PAB-DMT (0.61 g, 0.64 mmol) was dissolved in 8 mL DMF, and 2 mL piperidine was added. The mixture was stirred under room temperature for 30 minutes. Then, the solvent was removed under high vacuum, and the residue was purified by silica gel column chromatography (elution solvents: ethyl acetate/petroleum ether 1:1 to dichloromethane/methanol 5:1 v/v and 1% triethylamine were added). After purification, 0.45 g Val-Ala-NB-PAB-DMT was obatined as solid foam (95.3% yield). ^{1}H NMR (400 MHz, $CDCl_3$) δ 7.96 (d, *J* = 8.9 Hz, 1H), 7.73 (d, *J* = 7.8 Hz, 1H), 7.69 – 7.58 (m, 2H), 7.48 (dd, *J* = 5.2, 3.3 Hz, 2H), 7.43 – 7.33 (m, 7H), 7.31 – 7.18 (m, 5H), 6.87 – 6.78 (m, 4H), 5.42 (d, *J* = 16.7 Hz, 1H), 5.14 (d, *J* = 16.7 Hz, 1H), 4.69 (p, *J* = 7.0 Hz, 1H), 4.16 (s, 2H), 3.78 (s, 6H), 3.24 (d, *J* = 3.9

Hz, 1H), 2.24 (dtd, *J* = 13.8, 6.9, 4.0 Hz, 1H), 1.24 (d, *J* = 6.9 Hz, 3H), 0.98 (d, *J* = 7.0 Hz, 3H), 0.82 (d, *J* = 6.9 Hz, 3H). ^{13}C NMR (101 MHz, $CDCl_3$) δ 174.40, 174.03, 158.65, 148.53, 144.95, 140.21, 140.02, 136.15, 133.75, 132.61, 130.15, 129.62, 128.34, 128.26, 128.17, 128.02, 127.91, 126.96, 125.08, 113.31, 86.66, 64.82, 60.28, 55.35, 51.39, 46.22, 45.96, 31.16, 19.81, 18.55, 16.28.

Synthesis of HDA-Val-Ala-NB-PAB-DMT

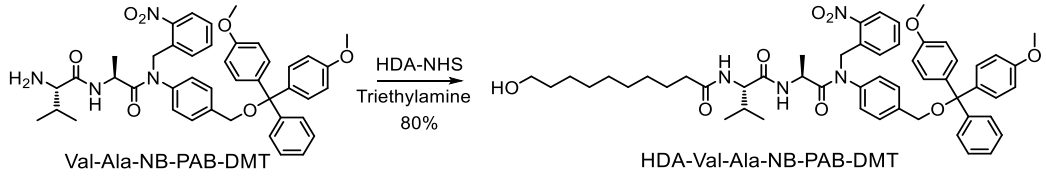

Val-Ala-NB-PAB-DMT (0.43 g, 0.59 mmol) and 0.25 g NHS-protected 10-hydroxydecanoic acid (HDA-NHS)[1] were dissolved in 25 mL dichloromethane, and 0.25 mL triethylamine was added. The mixture was stirred under room temperature overnight. Then, the organic solvents were removed under reduced pressure. After purification by silica gel column chromatography (elution solvents: ethyl acetate/petroleum ether 1:1 to dichloromethane/ methanol 10:1 v/v and 1% triethylamine was added), 0.43 g HDA-Val-Ala-NB-PAB-DMT was obtained as solid foam (80% yield). ^{1}H NMR (400 MHz, $CDCl_3$) δ 7.97 – 7.84 (m, 1H), 7.61 – 7.50 (m, 2H), 7.44 – 7.37 (m, 2H), 7.38 – 7.26 (m, 7H), 7.17 (dddd, *J* = 9.2, 7.3, 6.2, 1.4 Hz, 5H), 6.76 (dd, *J* = 9.4, 2.5 Hz, 4H), 6.54 (d, *J* = 7.1 Hz, 1H), 6.03 (d, *J* = 8.7 Hz, 1H), 5.38 (d, *J* = 16.8 Hz, 1H), 5.02 (d, *J* = 16.8 Hz, 1H), 4.53 (p, *J* = 6.9 Hz, 1H), 4.26 (dd, *J* = 8.7, 6.4 Hz, 1H), 4.10 (s, 2H), 3.71 (s, 6H), 3.60 – 3.50 (m, 2H), 2.13 (t, *J* = 7.6 Hz, 2H), 2.02 (dt, *J* = 17.1, 5.2 Hz, 1H), 1.50 (ddd, *J* = 20.8, 12.8, 5.6 Hz, 4H), 1.28 – 1.12 (m, 13H), 0.89 (t, *J* = 7.1 Hz, 6H). ^{13}C NMR (101 MHz, $CDCl_3$) δ 173.37, 173.05, 171.05, 158.53, 148.38, 144.81, 140.25, 139.87, 136.00, 133.51, 132.39, 130.02, 129.40, 128.23, 128.12, 128.09, 127.89, 127.70, 126.85, 125.03, 113.19, 86.56, 64.68, 62.96, 57.78, 55.22, 51.42, 46.41, 36.74, 32.74, 31.58, 29.29, 29.24, 29.16, 29.11, 25.64, 19.12, 18.13, 17.87.

Synthesis of Val-Ala(NB) phosphoramidite

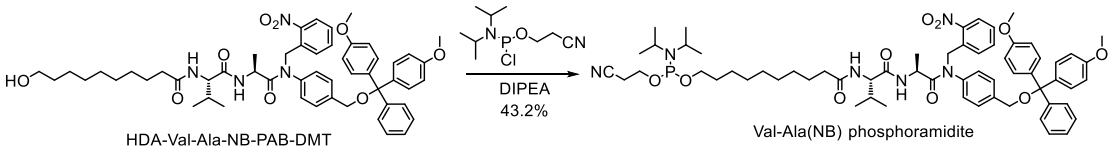

HDA-Val-Ala-NB-PAB-DMT (0.4 g, 0.44 mmol) was dissolved in 20 mL anhydrous dichloromethane under argon gas protection, and 0.4 mL DIPEA was added. The mixture was cooled down under ice bath. Then, 0.2 mL 2-cyanoethyl N,N-diisopropylchlorophosphoramidite (0.9 mmol) was added dropwise. The reaction was monitored by thin-layer chromatography. When the reaction was completed, the mixture was diluted with 50 mL dichloromethane and

washed with saturated KCl. The organic layer was collected and dried by anhydrous Na_2SO_4. After purification by silica gel column chromatography (elution solvents: ethyl acetate with 1% triethylamine), 0.21 g Val-Ala(NB) phosphoramidite was obtained as solid foam (43.2% yield). ^{1}H NMR (400 MHz, $CDCl_3$) δ 7.98 (d, *J* = 7.9 Hz, 1H), 7.67 – 7.58 (m, 2H), 7.48 (dd, *J* = 5.2, 3.3 Hz, 2H), 7.45 – 7.34 (m, 7H), 7.32 – 7.27 (m, 2H), 7.26 – 7.19 (m, 3H), 6.86 – 6.80 (m, 4H), 6.33 (d, *J* = 7.1 Hz, 1H), 5.99 (d, *J* = 8.6 Hz, 1H), 5.44 (d, *J* = 16.7 Hz, 1H), 5.10 (d, *J* = 16.8 Hz, 1H), 4.61 (p, *J* = 6.8 Hz, 1H), 4.29 (dd, *J* = 8.6, 6.3 Hz, 1H), 4.17 (s, 2H), 3.90 – 3.79 (m, 2H), 3.78 (s, 6H), 3.67 – 3.53 (m, 4H), 2.63 (t, *J* = 6.6 Hz, 2H), 2.20 (t, *J* = 7.6 Hz, 2H), 2.16 – 2.05 (m, 1H), 1.66 – 1.53 (m, 4H), 1.35 – 1.22 (m, 13H), 1.18 (dd, *J* = 6.8, 4.9 Hz, 12H), 0.97 (t, *J* = 6.5 Hz, 6H). ^{31}P NMR (162 MHz, $CDCl_3$) δ 147.17.

4.5 Synthesis of CA4 phosphoramidite

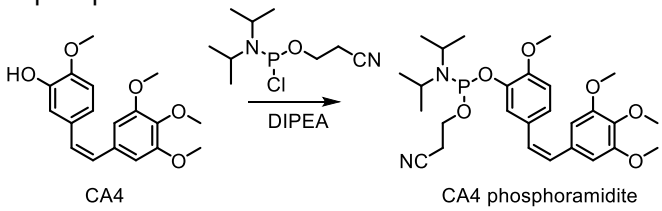

Figure S34. Synthesis of CA4 phosphoramidite.

Combretastatin A-4 (CA4) (0.5 g, 1.58 mmol) was dissolved in 20 mL anhydrous dichloromethane under argon gas protection, and 0.55 mL DIPEA (3.16 mmol) was added. The mixture was cooled down under ice bath. Then, 0.5 mL 2-cyanoethyl N,N-diisopropylchlorophosphoramidite was added dropwise. The reaction was monitored by thin-layer chromatography. When the reaction was completed, the mixture was diluted with 50 mL dichloromethane and washed with saturated KCl. The organic layer was collected and dried by anhydrous Na_2SO_4. After purification by silica gel column chromatography (elution solvents: ethyl acetate/petroleum ether 1:4 to 1:2 v/v and 1% triethylamine was added), 0.78 g CA4 phosphoramidite was obtained (95.5% yield). ^{1}H NMR (400 MHz, $CDCl_3$) δ 7.02 (t, *J* = 1.7 Hz, 1H), 6.95 (dd, *J* = 8.4, 2.1 Hz, 1H), 6.78 (d, *J* = 8.4 Hz, 1H), 6.50 (s, 2H), 6.43 (dd, *J* = 12.1 Hz, 2H), 3.96 – 3.86 (m, 2H), 3.83 (s, 3H), 3.81 (s, 3H), 3.74 – 3.64 (m, 8H), 2.67 (t, *J* = 6.6 Hz, 2H), 1.19 (d, *J* = 6.8 Hz, 6H), 1.10 (d, *J* = 6.8 Hz, 6H). ^{31}P NMR (162 MHz, $CDCl_3$) δ 149.01. ^{13}C NMR (101 MHz, $CDCl_3$) δ 153.06, 150.78, 150.75, 143.06, 142.98, 137.16, 132.92, 130.03, 129.39, 129.09, 124.47, 121.98, 121.88, 117.82, 111.94, 106.05, 60.99, 59.39, 59.21, 56.03, 55.91, 43.96, 43.82, 24.76, 24.68, 24.36, 24.29, 20.33, 20.27.

4.6 Synthesis of 4MU phosphoramidite

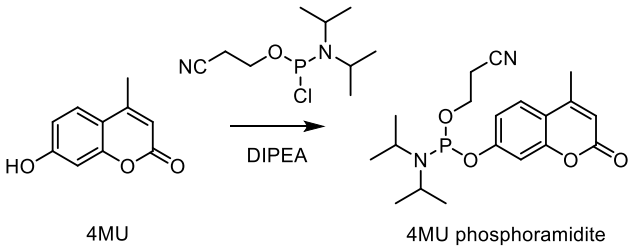

Figure S35. Synthesis of 4MU phosphoramidite.

4-Methylumbelliferone (4MU) (0.5 g, 2.83 mmol) was dissolved in a mixed solvents with 10 mL dry tetrahydrofuran and 20 mL dry dichloromethane under argon gas protection, and 0.9 mL DIPEA (0.66 g, 5.16 mmol) was added. The mixture was cooled down under ice bath. Then, 0.75 mL 2-cyanoethyl N,N-diisopropylchlorophosphoramidite (0.79 g, 3.36 mmol) was added dropwise. The reaction was monitored by thin-layer chromatography. When the reaction was completed, the mixture was diluted with 100 mL dichloromethane and washed with 50 mL saturated KCl. The organic layer was collected and dried by anhydrous sodium sulfate. After purification by silica gel column chromatography (elution solvents: ethyl acetate/petroleum ether 1:1 v/v and 1% triethylamine was added), 0.637 g 4MU phosphoramidite was obtained as colorless oily (59.7% yield). ^{1}H NMR (400 MHz, $CDCl_3$) δ 7.43 (d, *J* = 8.3 Hz, 1H), 6.93 (dtd, *J* = 3.7, 2.4, 1.5 Hz, 2H), 6.10 (d, *J* = 1.2 Hz, 1H), 3.95 – 3.84 (m, 2H), 3.73 – 3.61 (m, 2H), 2.63 (t, *J* = 6.4 Hz, 2H), 2.34 (d, *J* = 1.2 Hz, 3H), 1.18 (d, *J* = 6.8 Hz, 6H), 1.11 (d, *J* = 6.8 Hz, 6H). ^{31}P NMR (162 MHz, $CDCl_3$) δ 147.45. ^{13}C NMR (101 MHz, $CDCl_3$) δ 161.16, 157.69, 157.61, 154.76, 152.39, 125.52, 117.31, 116.49, 116.40, 115.00, 112.76, 107.48, 107.37, 59.21, 59.03, 43.98, 43.85, 24.65, 24.58, 24.46, 24.39, 20.41, 20.33, 18.71.

5. NMR spectra

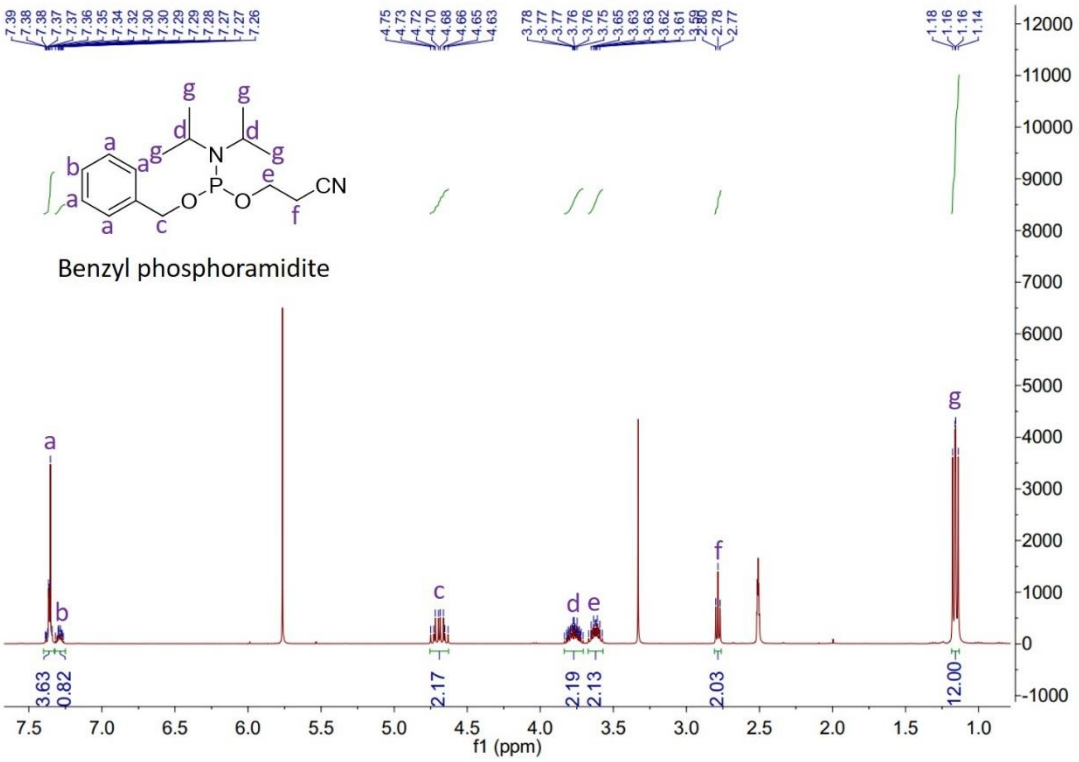

Figure S36. ^{1}H NMR of benzyl phosphoramidite.

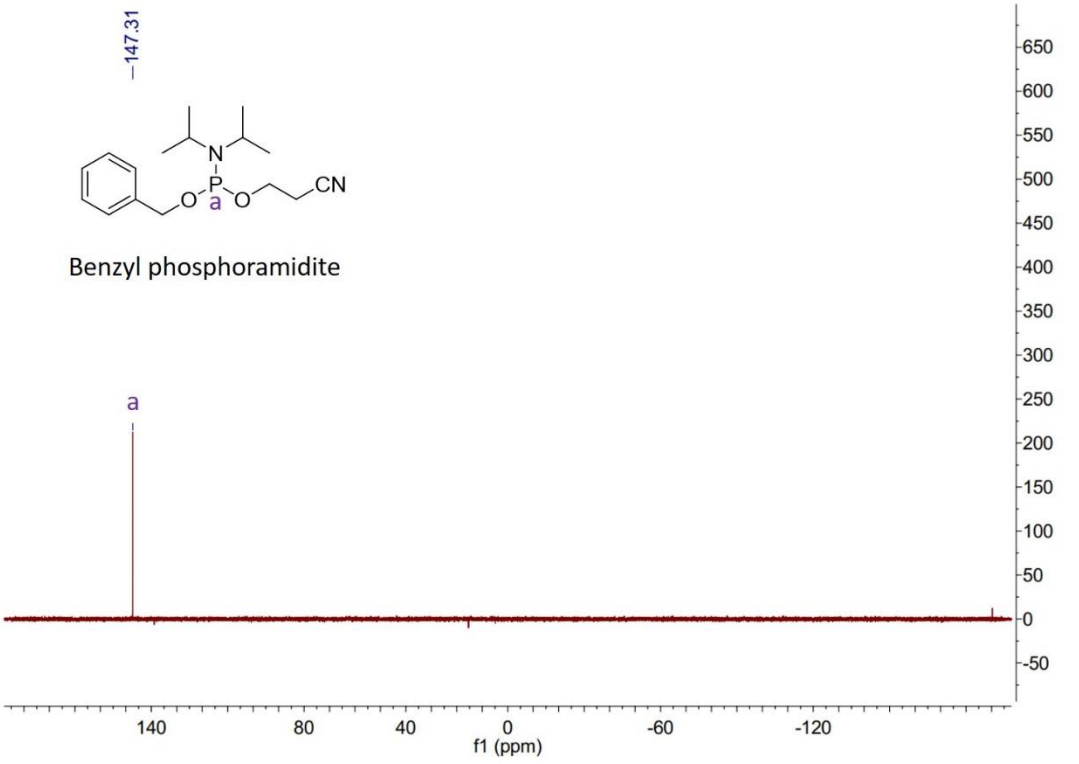

Figure S37. ^{31}P NMR of benzyl phosphoramidite.

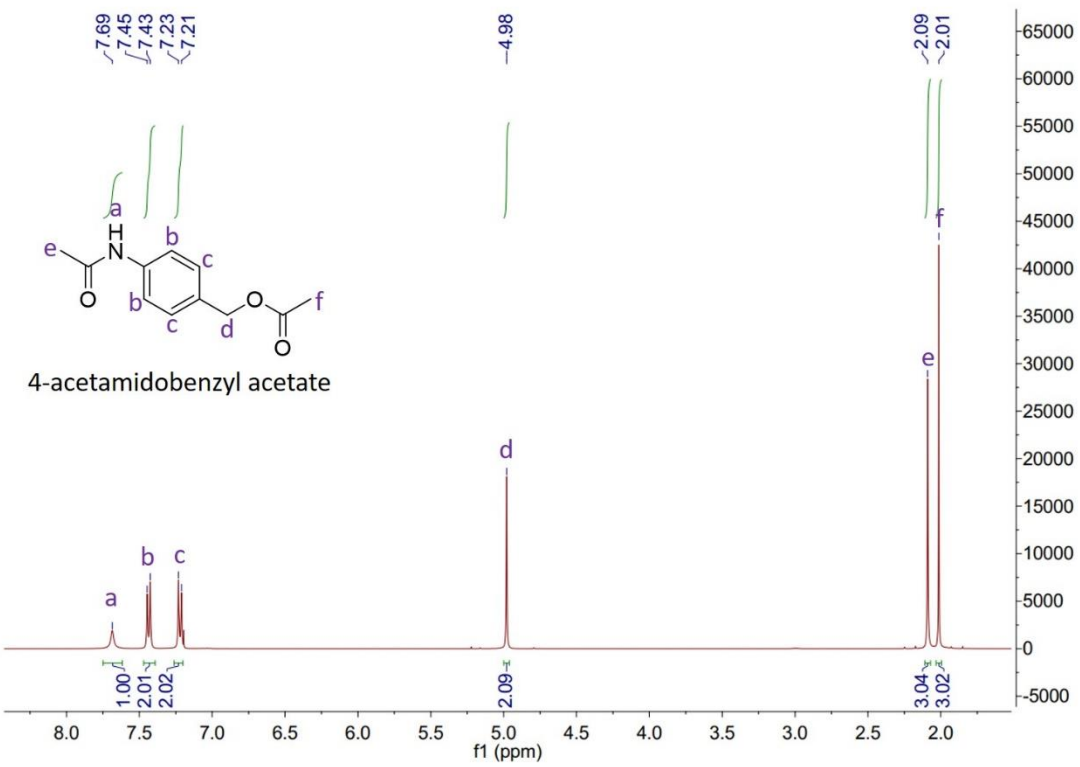

Figure S38. ^{1}H NMR of 4-acetamidobenzyl acetate.

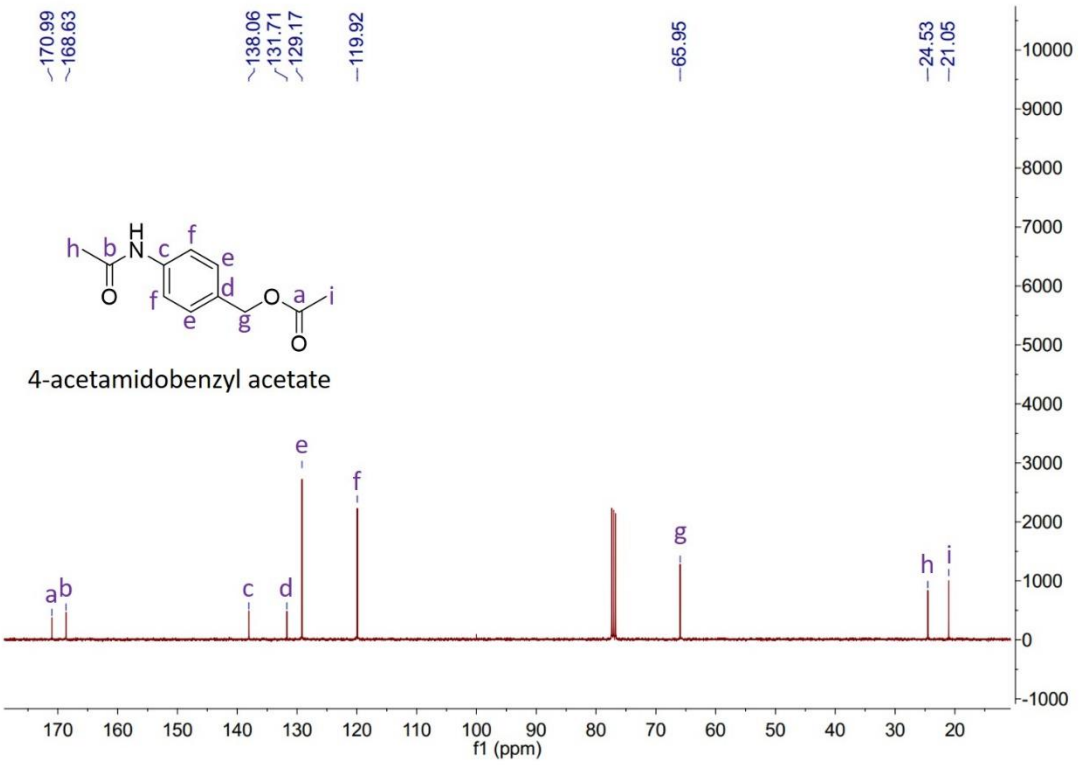

Figure S39. ^{13}C NMR of 4-acetamidobenzyl acetate.

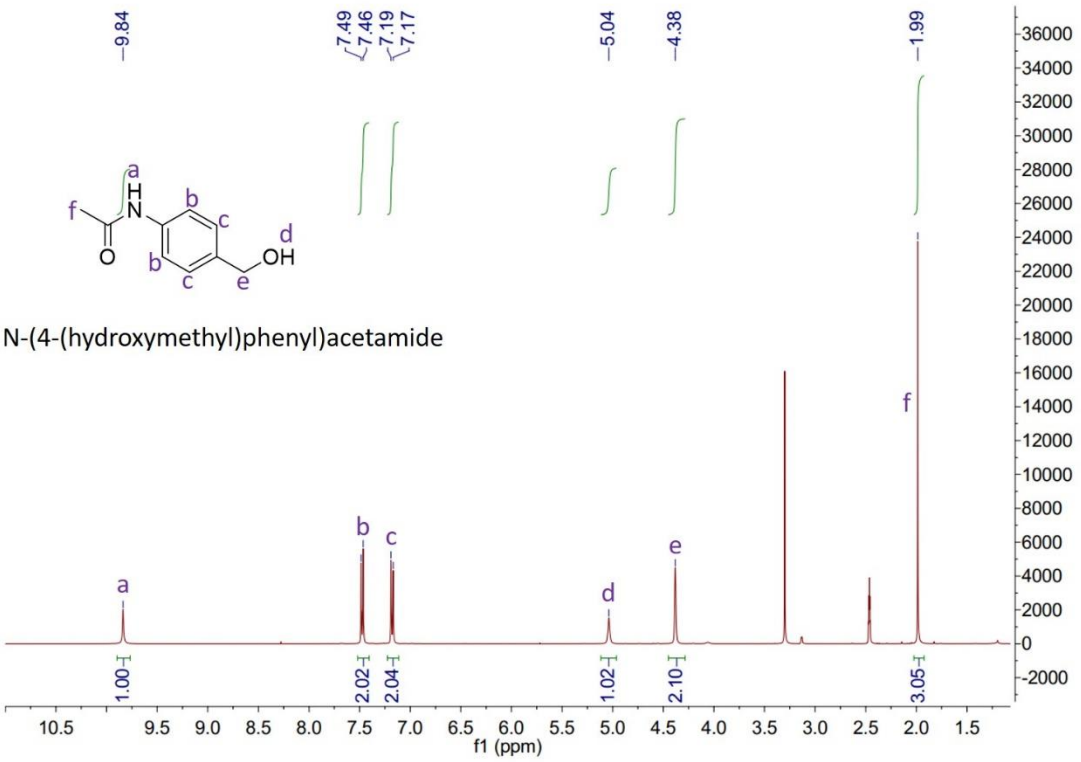

Figure S40. ^{1}H NMR of N-(4-(hydroxymethyl)phenyl)acetamide.

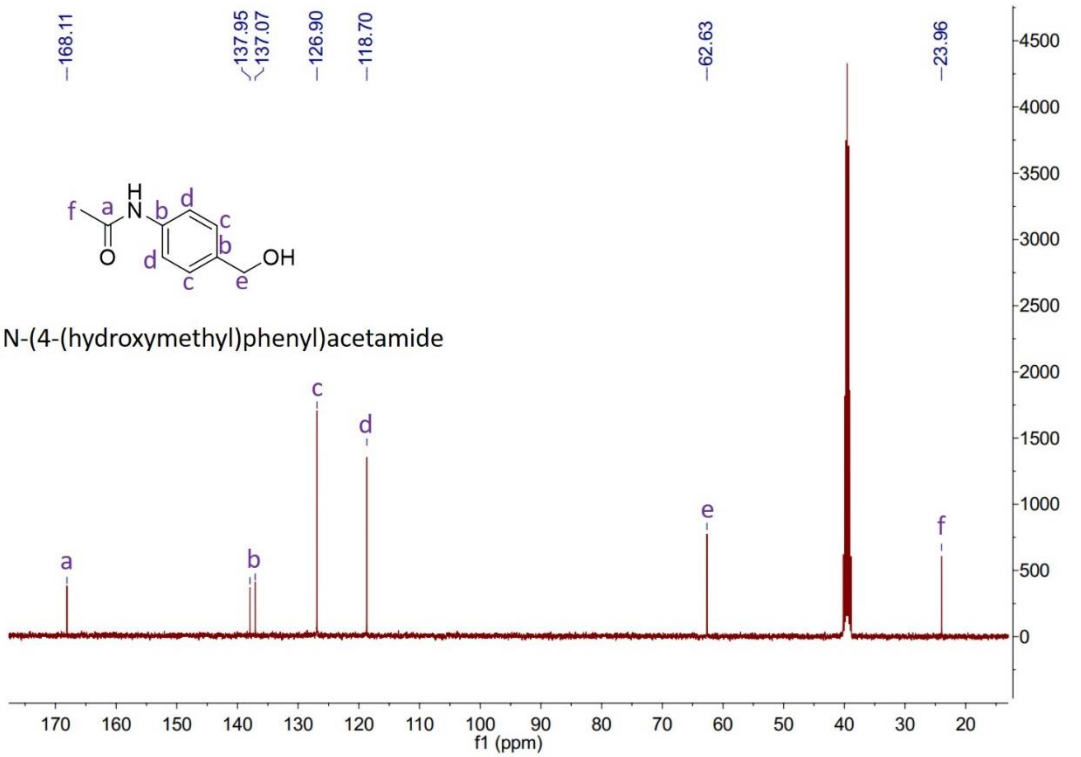

Figure S41. ^{13}C NMR of N-(4-(hydroxymethyl)phenyl)acetamide.

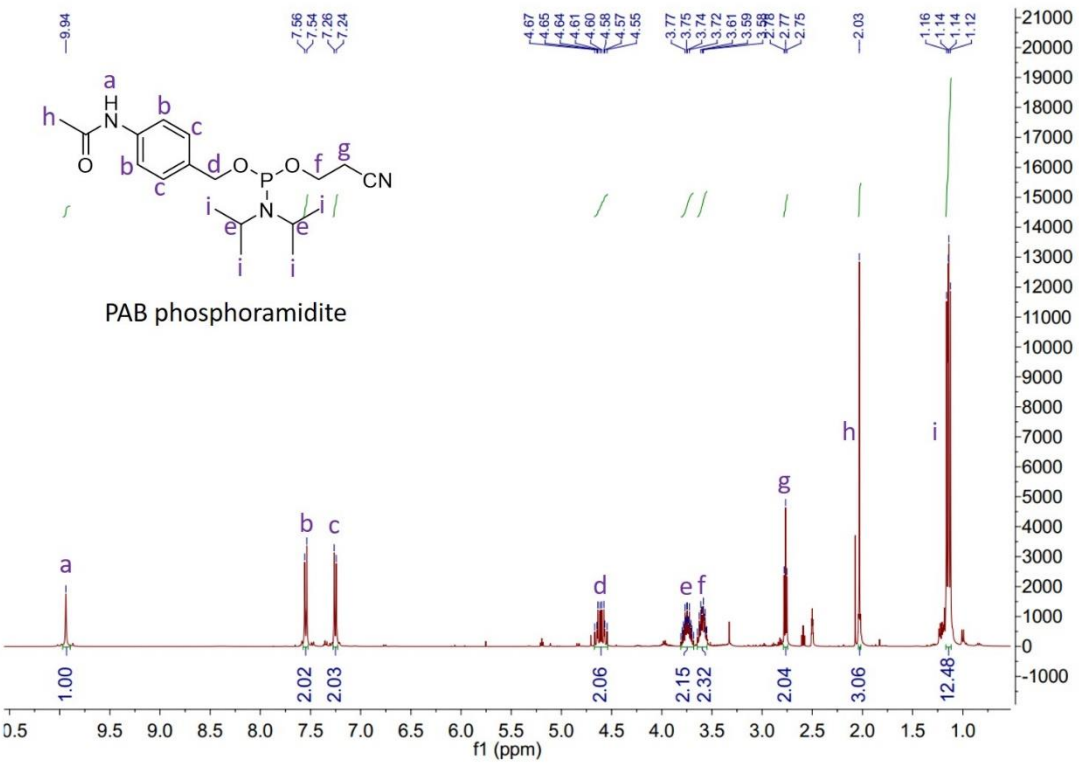

Figure S42. ^{1}H NMR of PAB phosphoramidite.

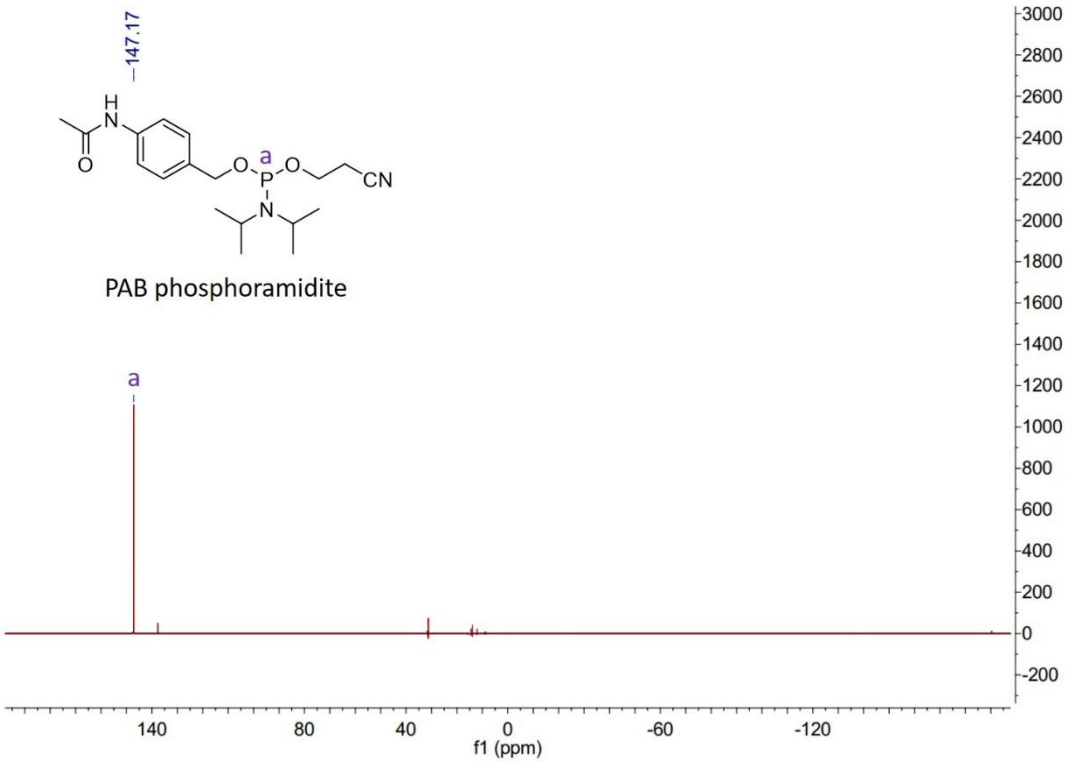

Figure S43. ^{31}P NMR of PAB phosphoramidite.

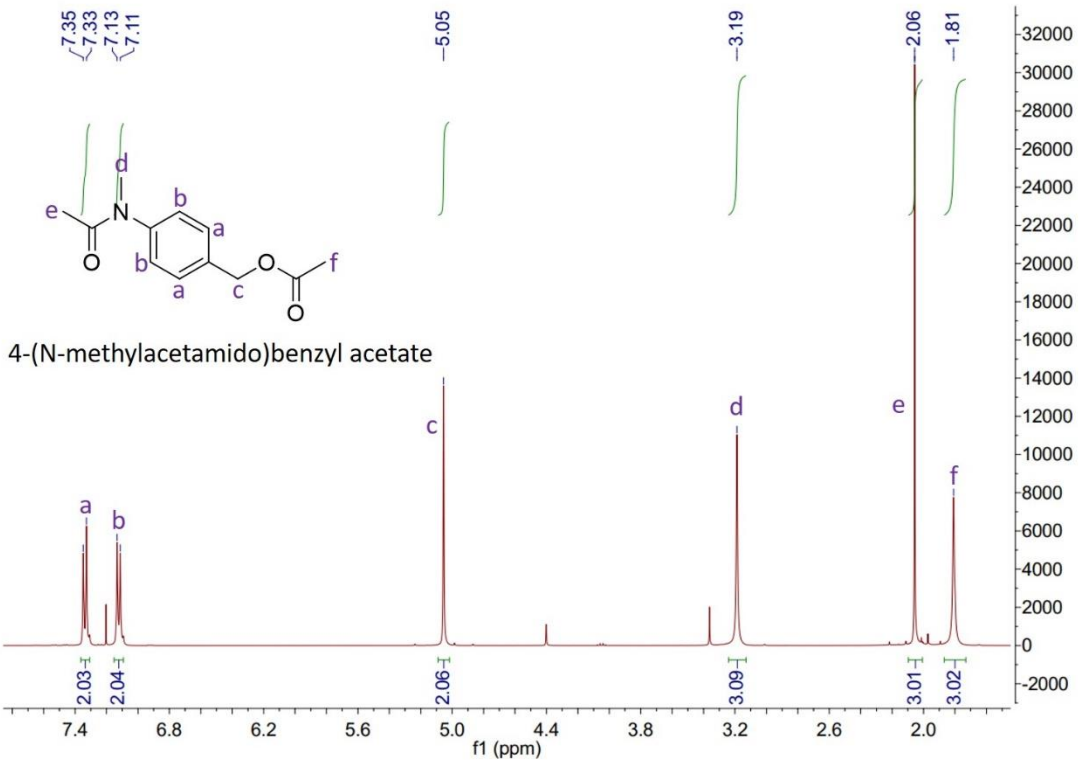

Figure S44. ^{1}H NMR of 4-(N-methylacetamido)benzyl acetate.

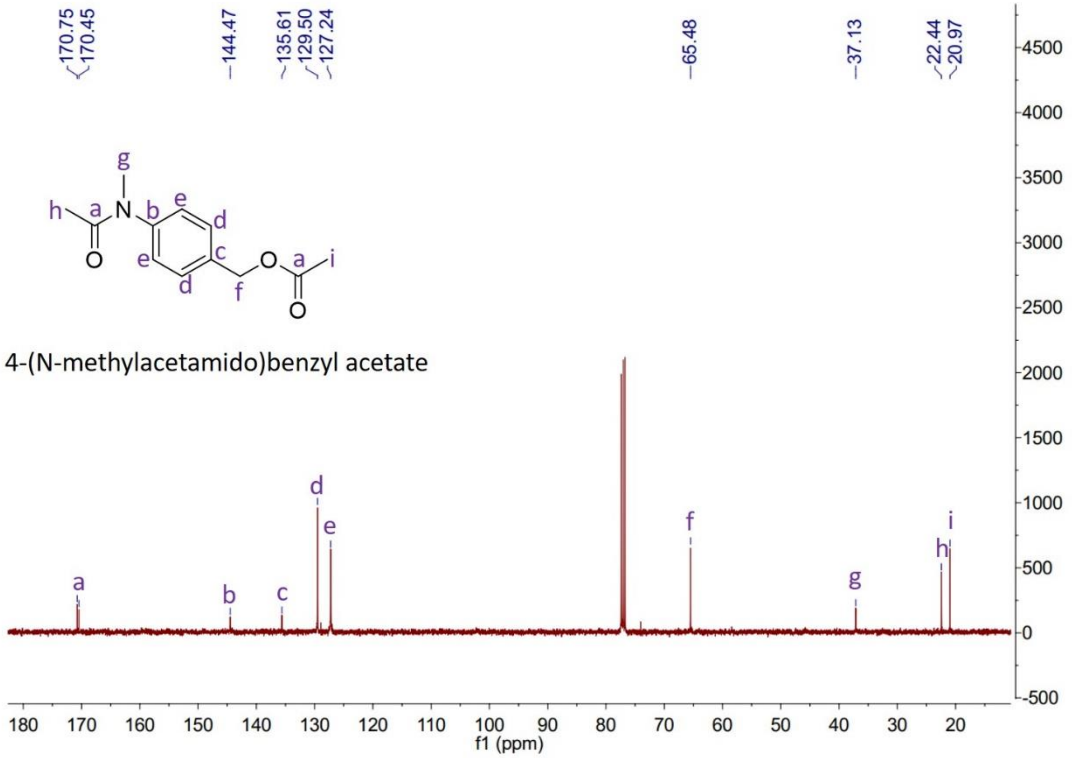

Figure S45. ^{13}C NMR of 4-(N-methylacetamido)benzyl acetate.

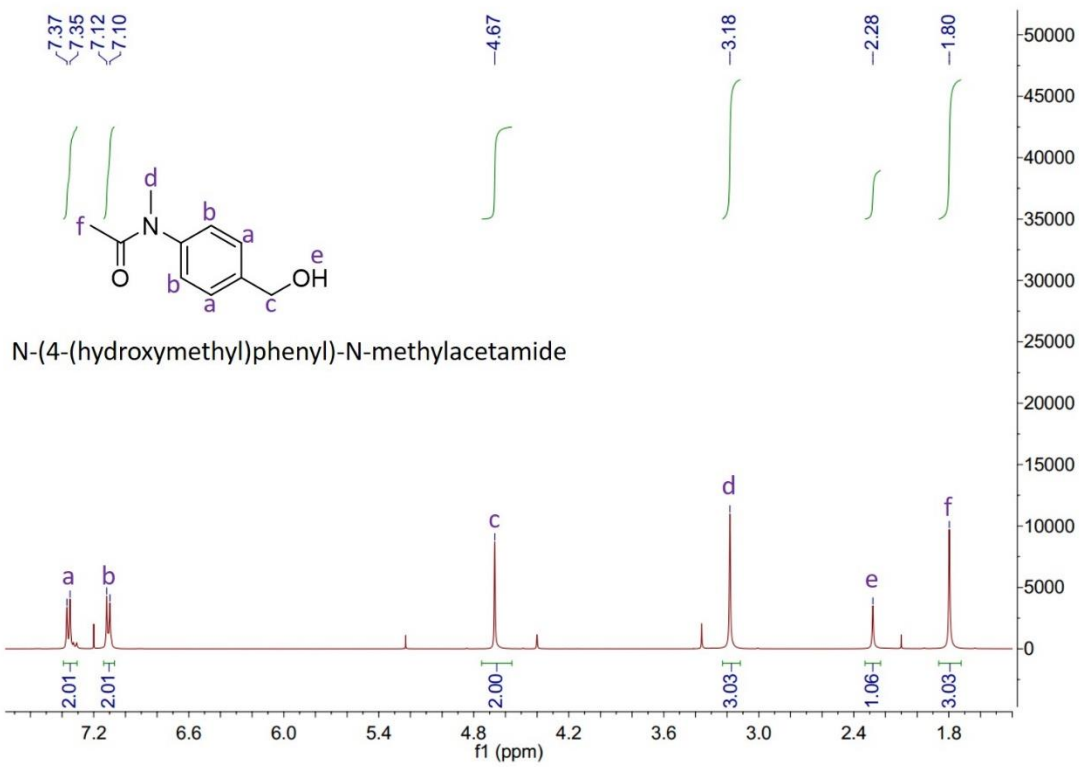

Figure S46. ^{1}H NMR of N-(4-(hydroxymethyl)phenyl)-N-methylacetamide.

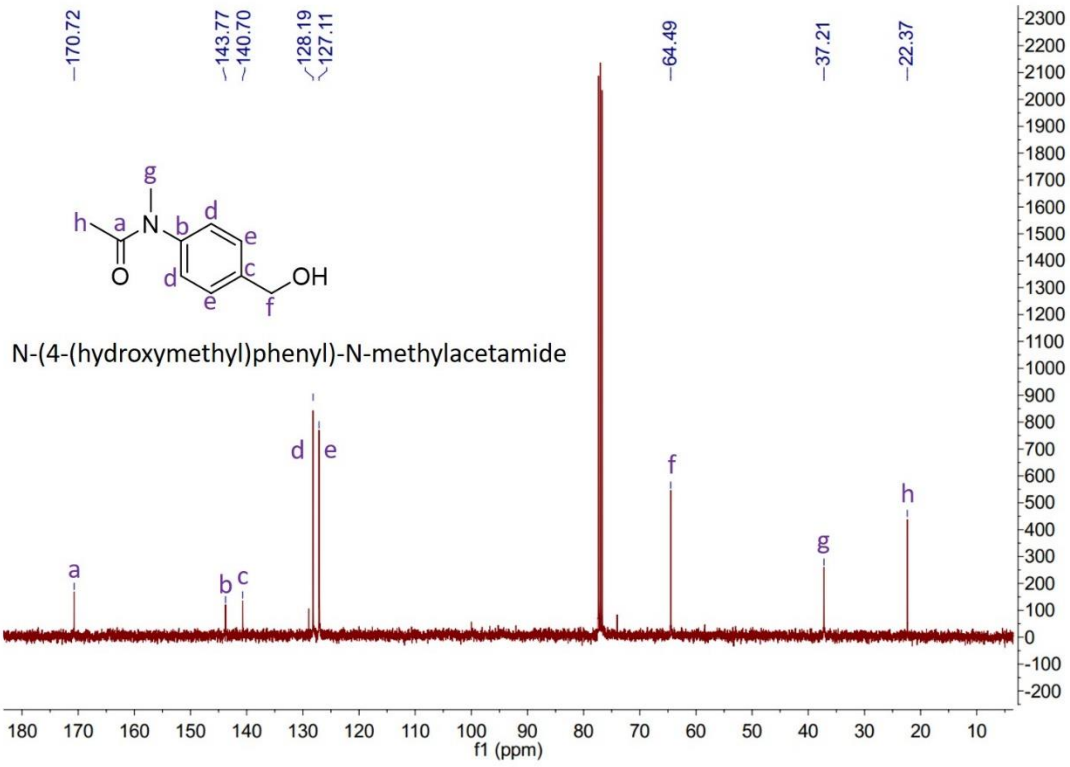

Figure S47. ^{13}C NMR of N-(4-(hydroxymethyl)phenyl)-N-methylacetamide.

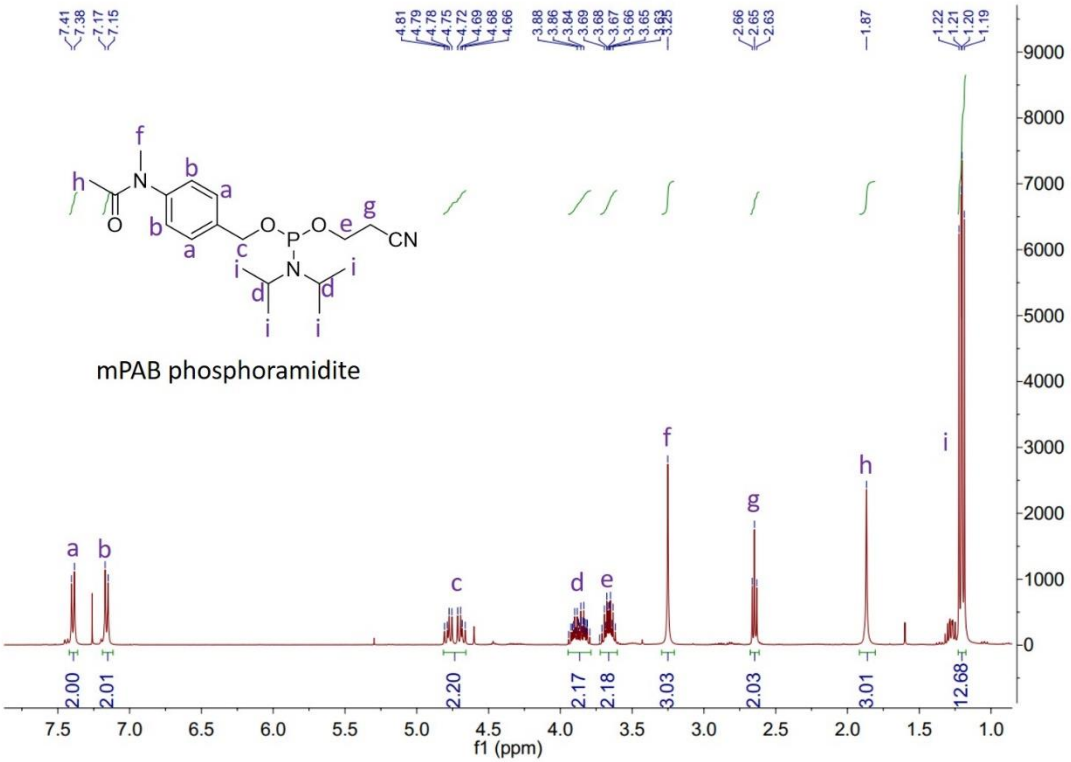

Figure S48. ^{1}H NMR of mPAB phosphoramidite.

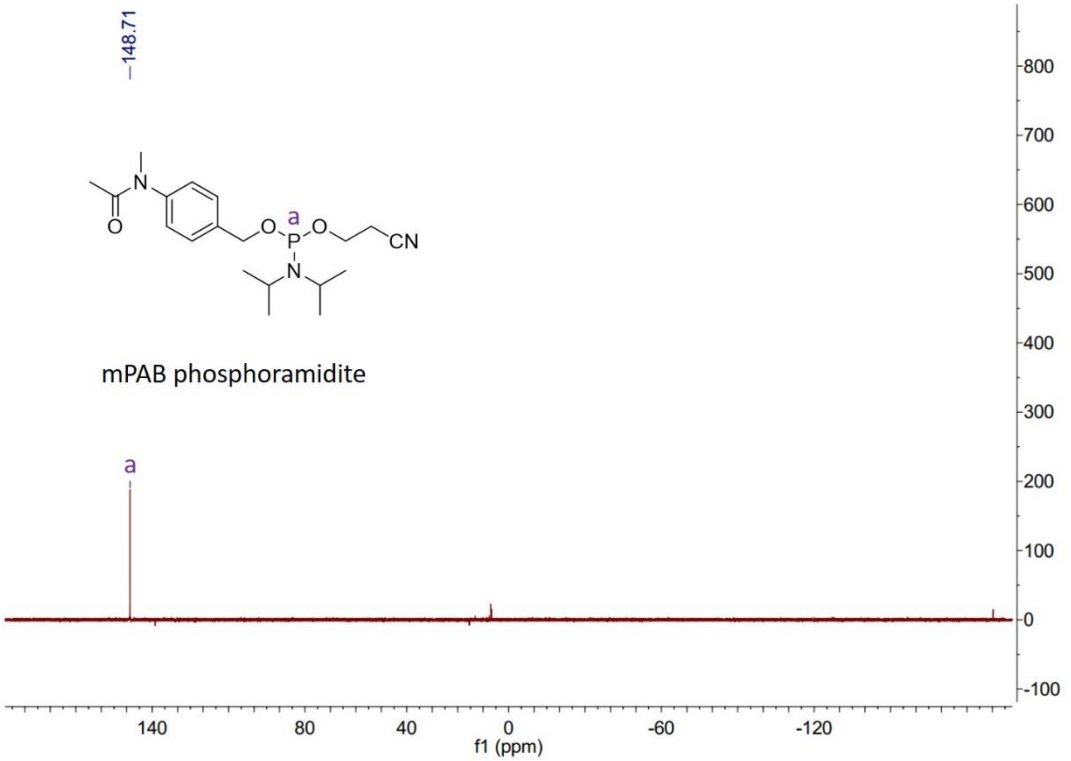

Figure S49. ^{31}P NMR of mPAB phosphoramidite.

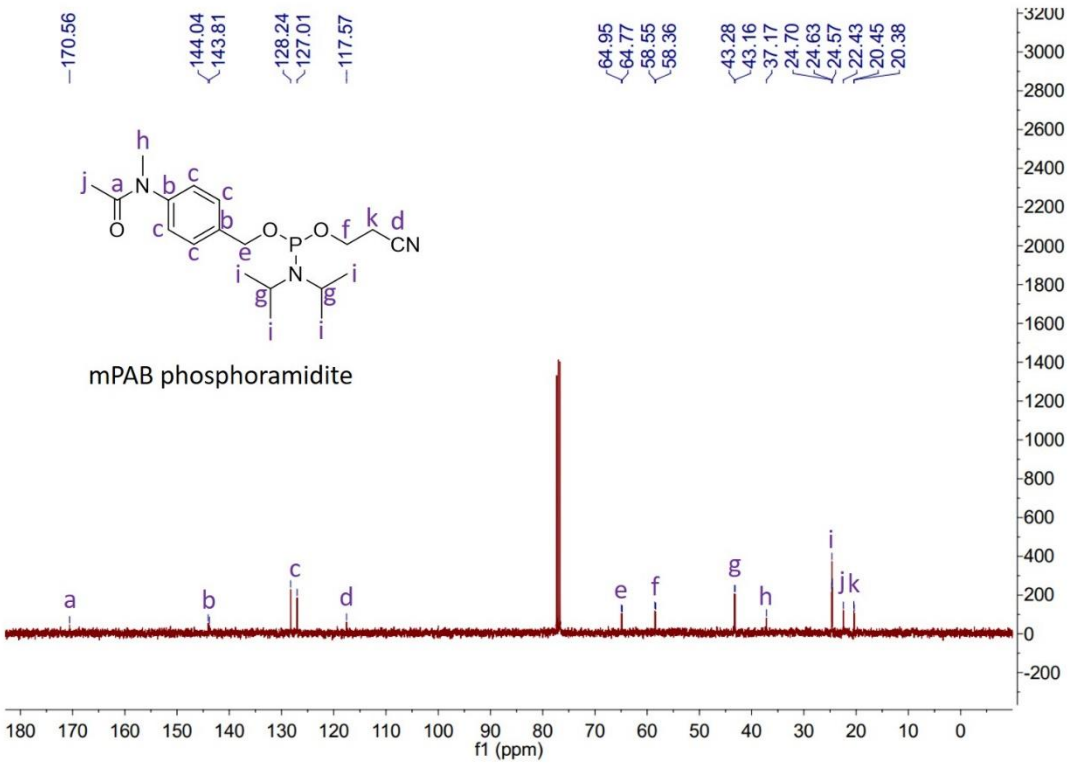

Figure S50. ^{13}C NMR of mPAB phosphoramidite.

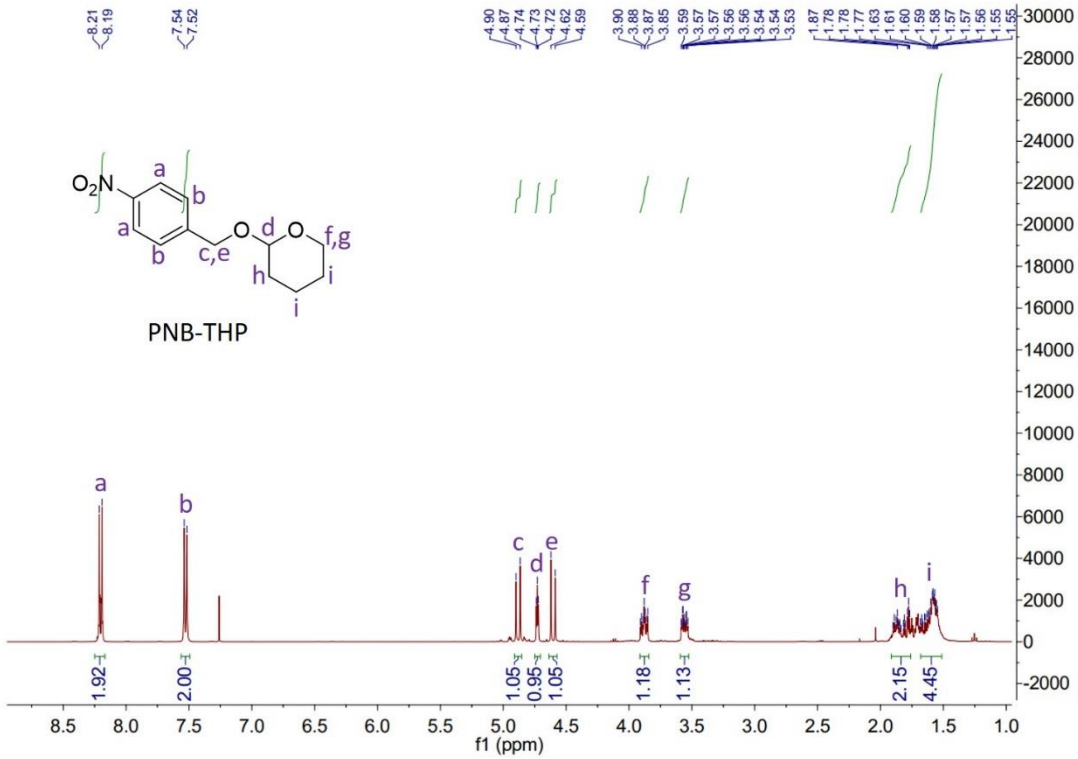

Figure S51. ^{1}H NMR of PNB-THP.

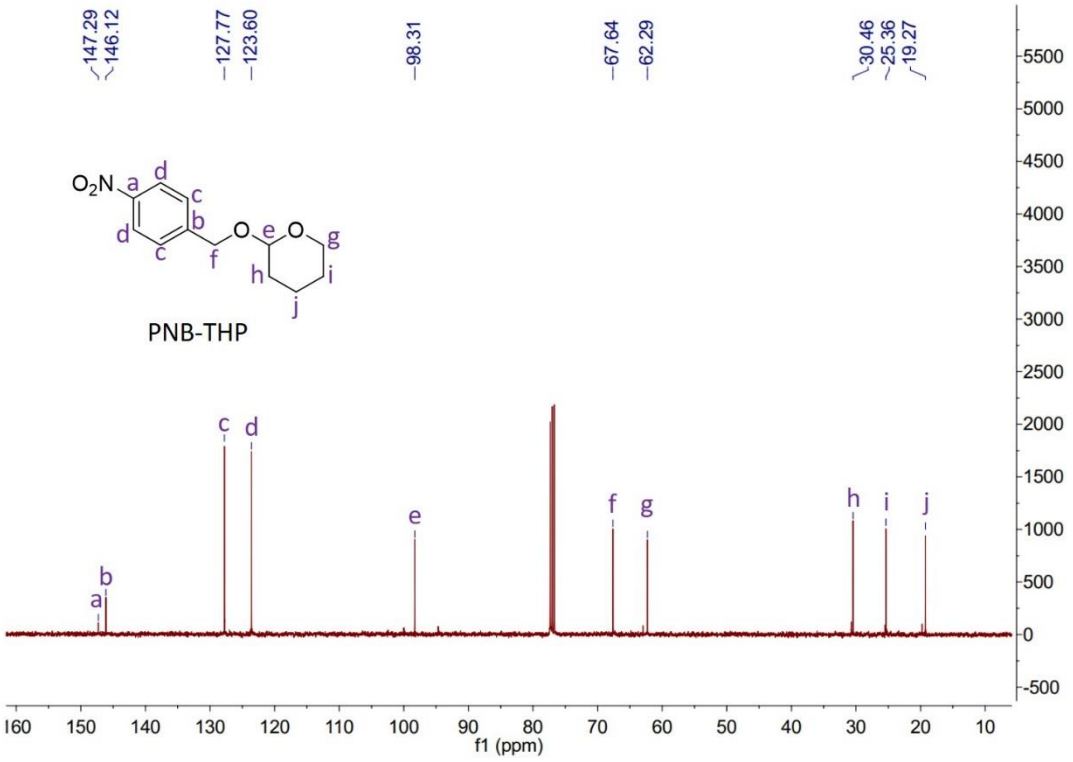

Figure S52. ^{13}C NMR of PNB-THP.

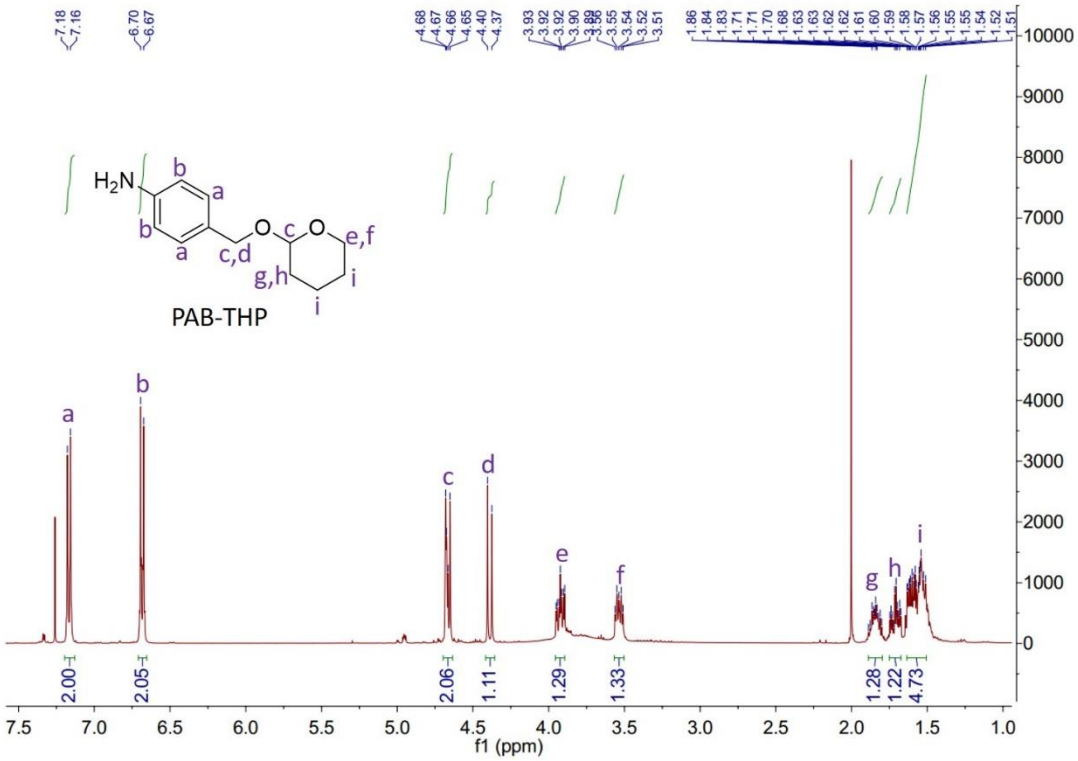

Figure S53. ^{1}H NMR of PAB-THP.

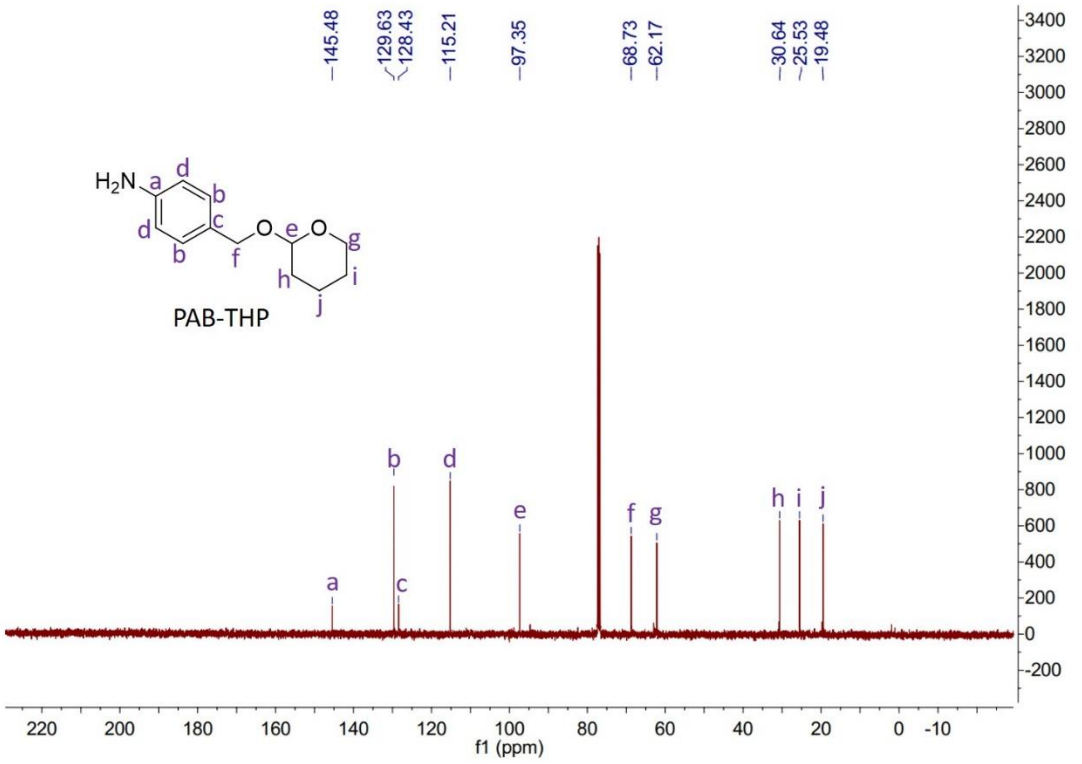

Figure S54. ^{13}C NMR of PAB-THP.

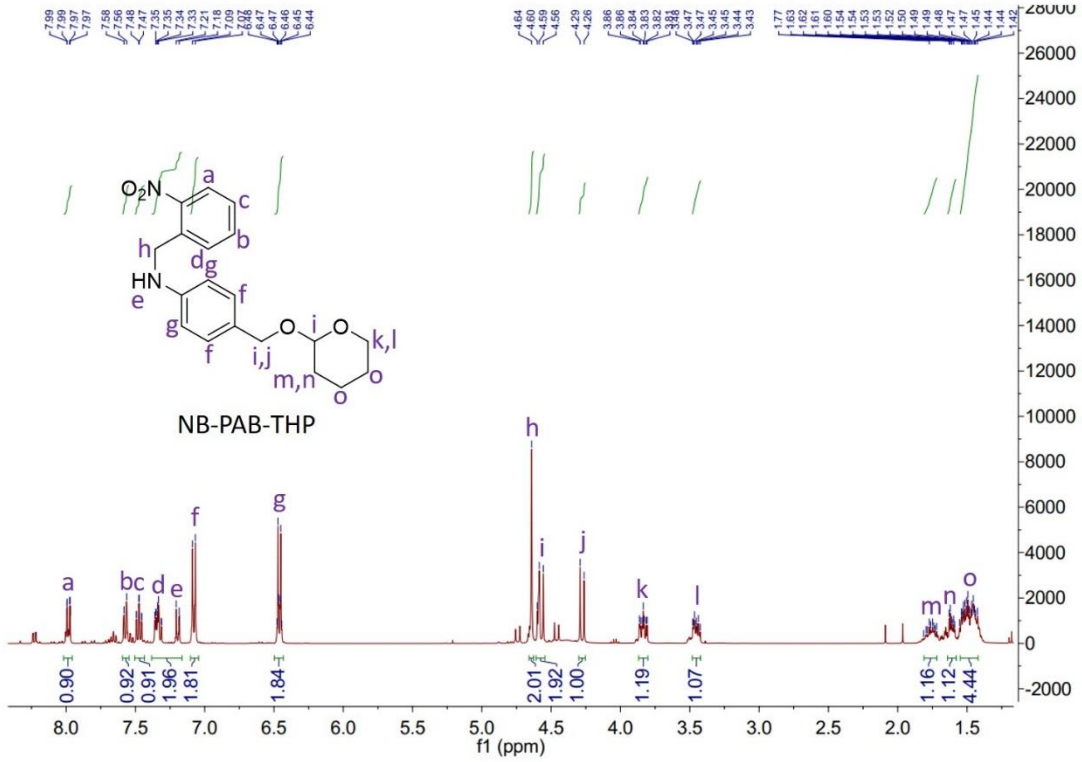

Figure S55. ^{1}H NMR of NB-PAB-THP.

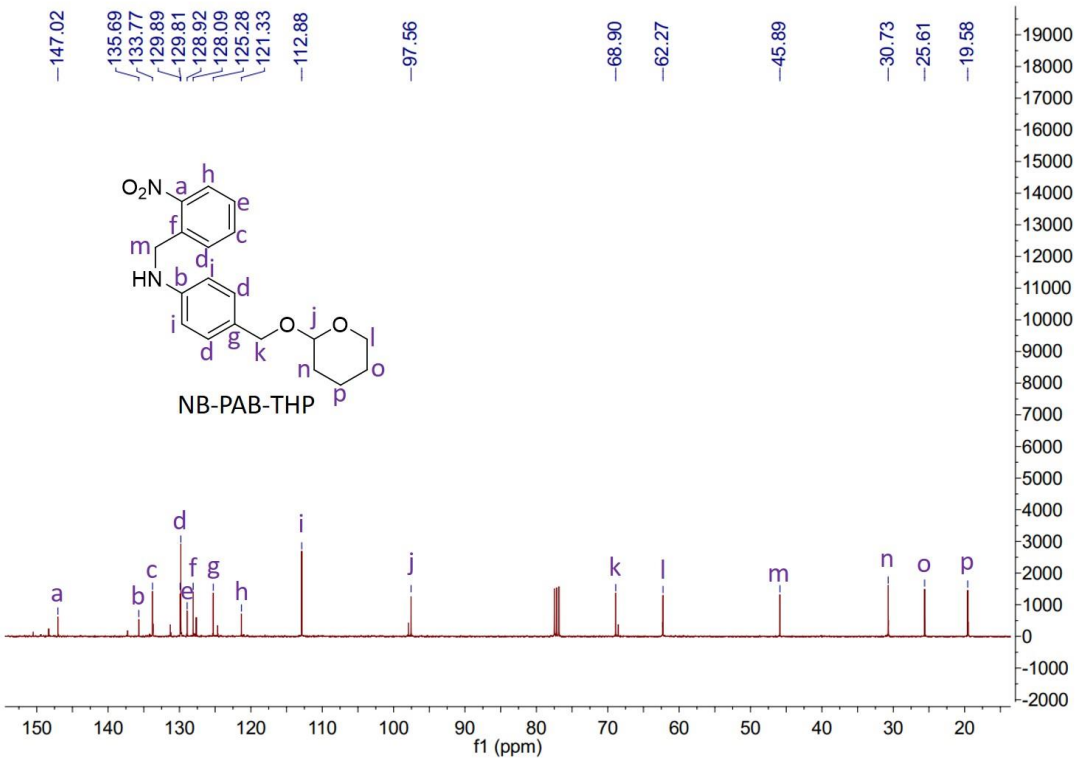

Figure S56. ^{13}C NMR of NB-PAB-THP.

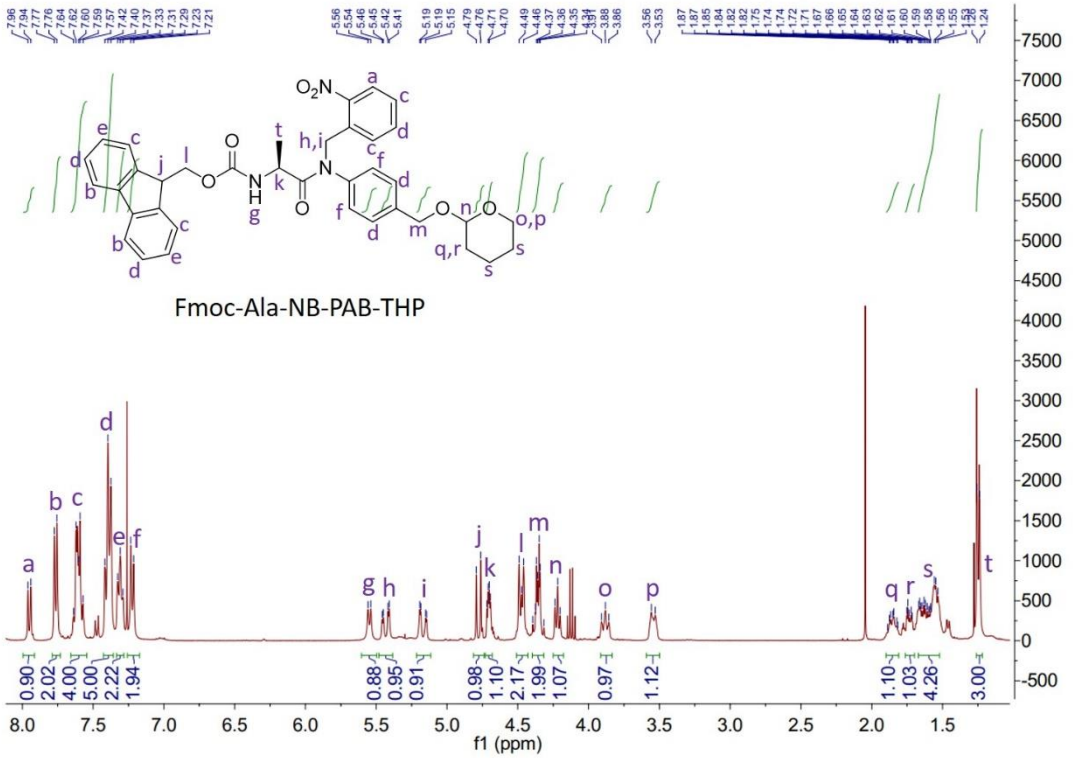

Figure S57. ^{1}H NMR of Fmoc-Ala-NB-PAB-THP.

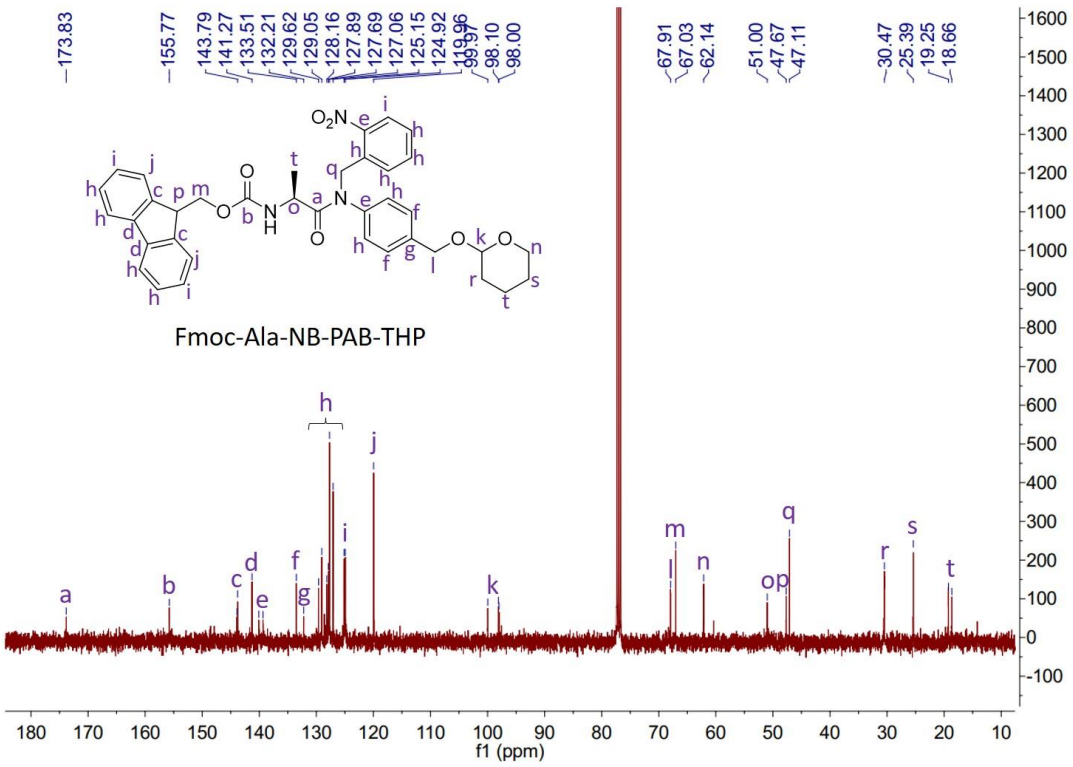

Figure S58. ^{13}C NMR of Fmoc-Ala-NB-PAB-THP.

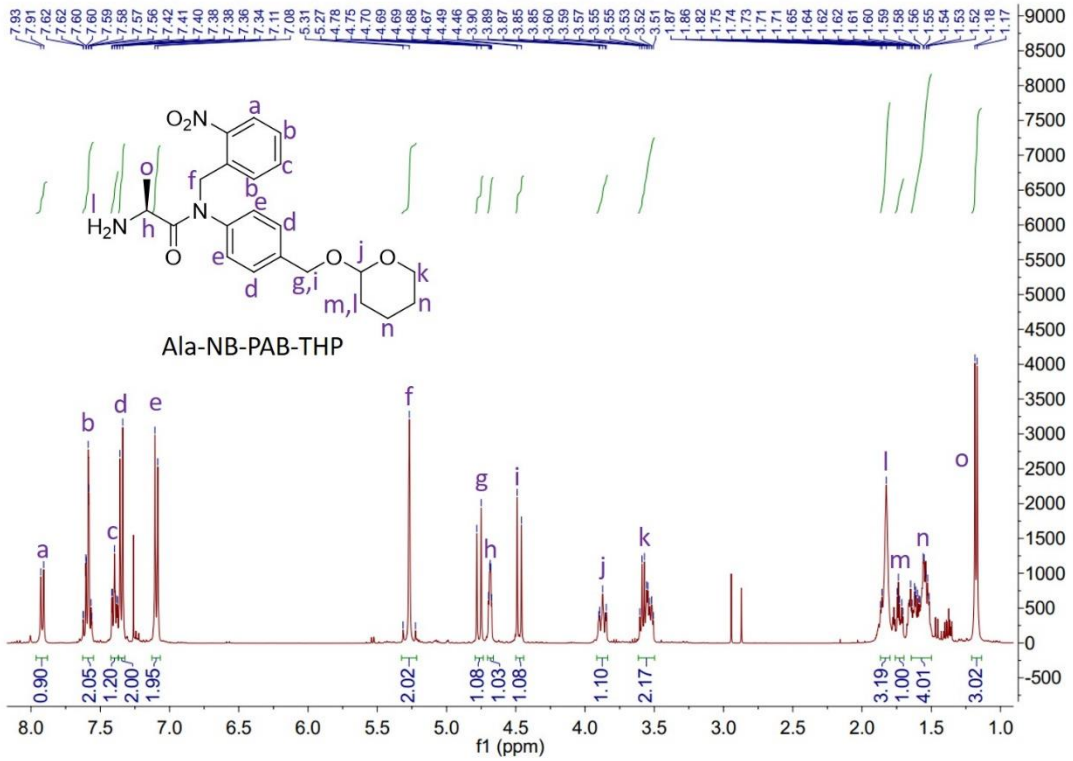

Figure S59. ^{1}H NMR of Ala-NB-PAB-THP.

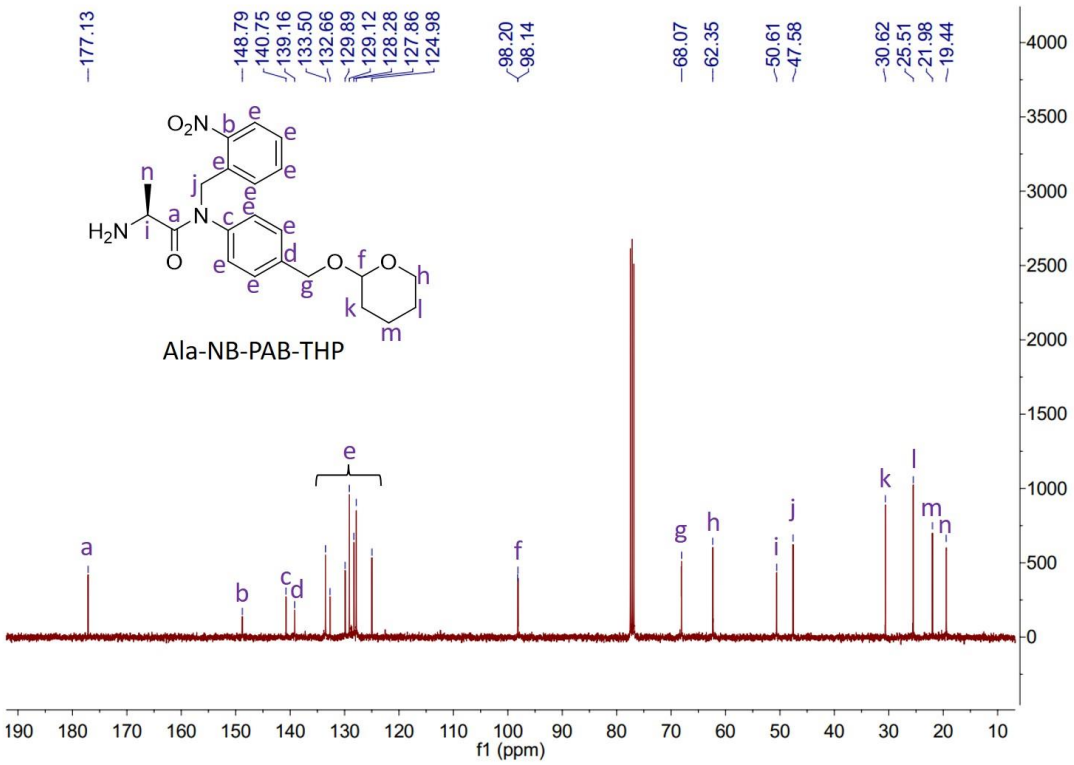

Figure S60. ^{13}C NMR of Ala-NB-PAB-THP.

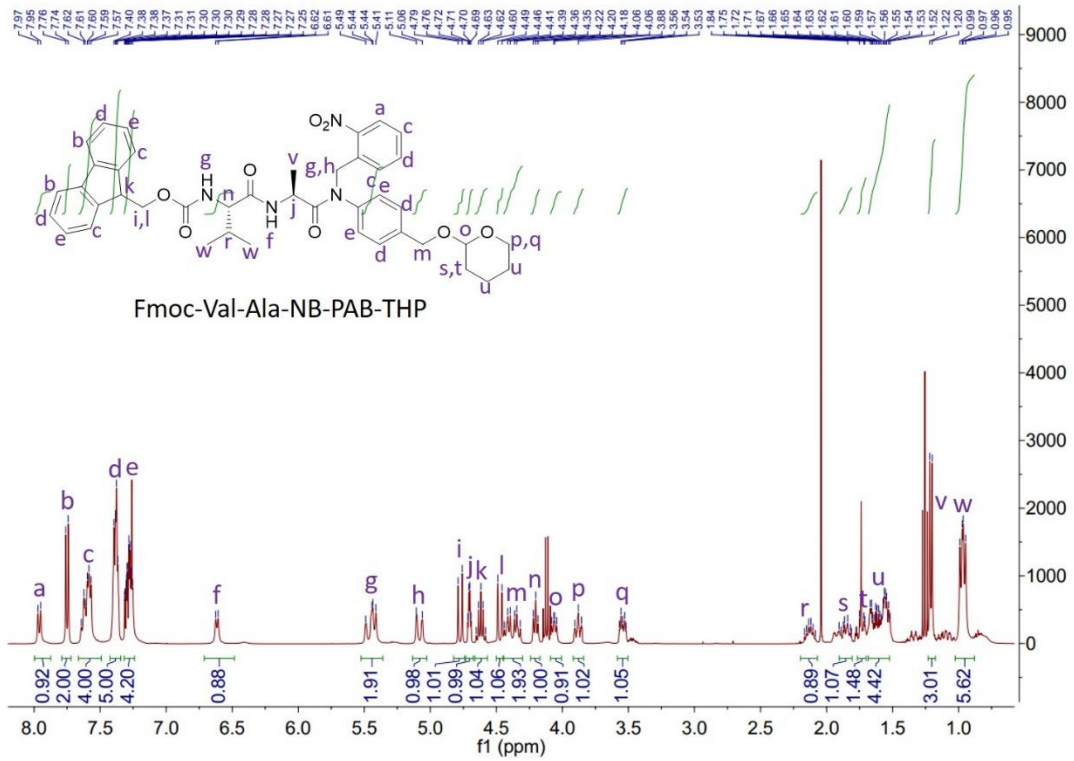

Figure S61. ^{1}H NMR of Fmoc-Val-Ala-NB-PAB-THP.

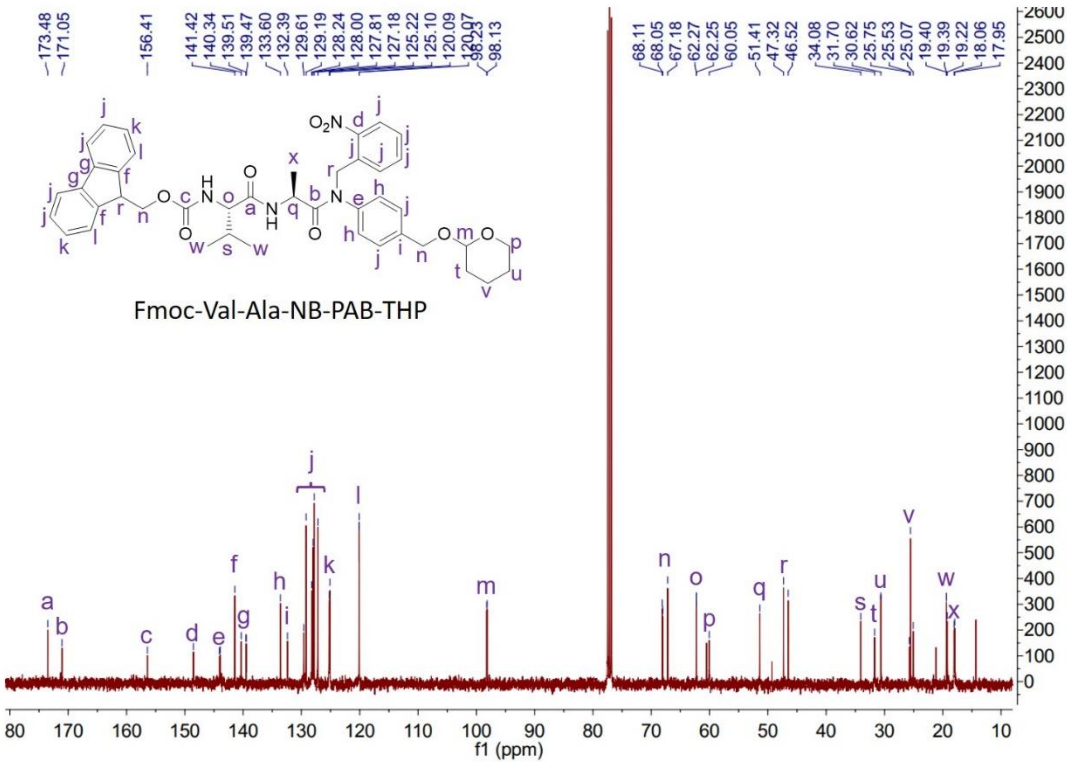

Figure S62. ^{13}C NMR of Fmoc-Val-Ala-NB-PAB-THP.

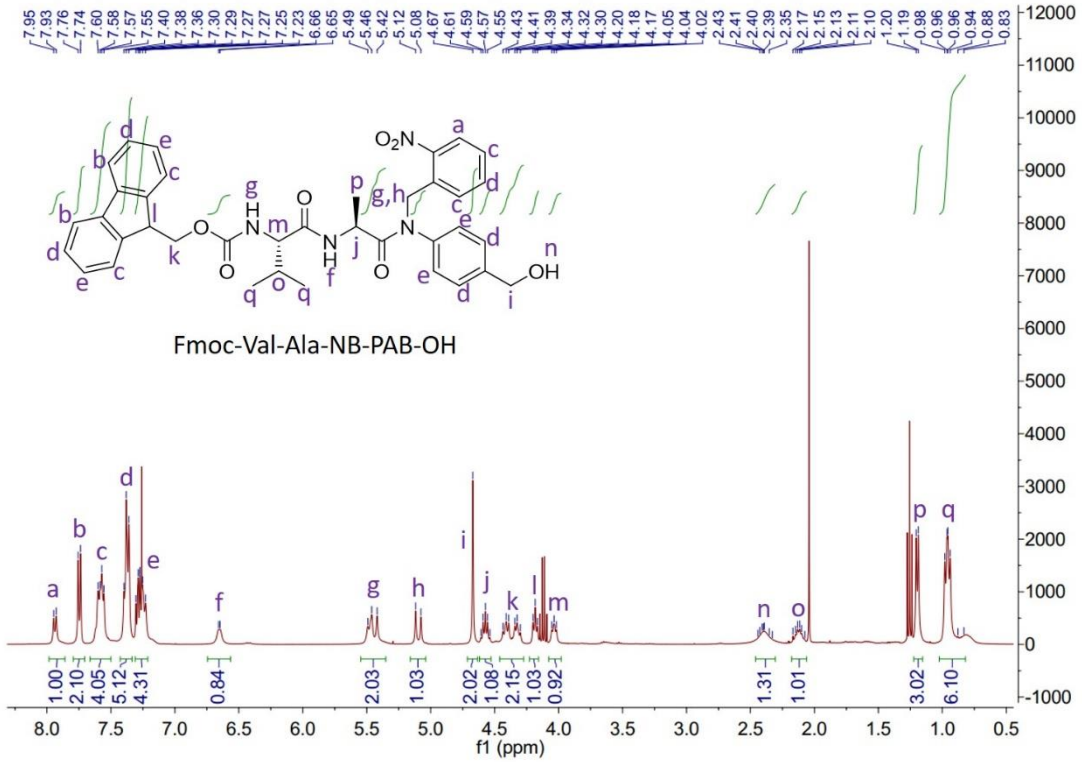

Figure S63. ^{1}H NMR of Fmoc-Val-Ala-NB-PAB-OH.

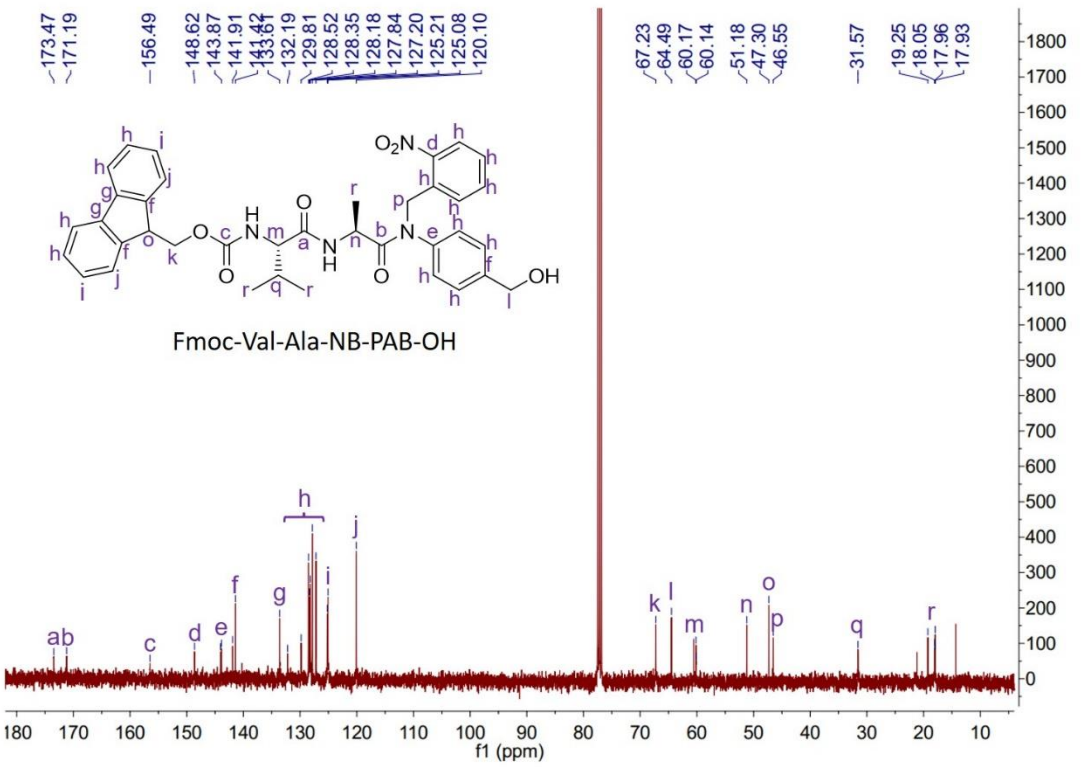

Figure S64. ^{13}C NMR of Fmoc-Val-Ala-NB-PAB-OH.

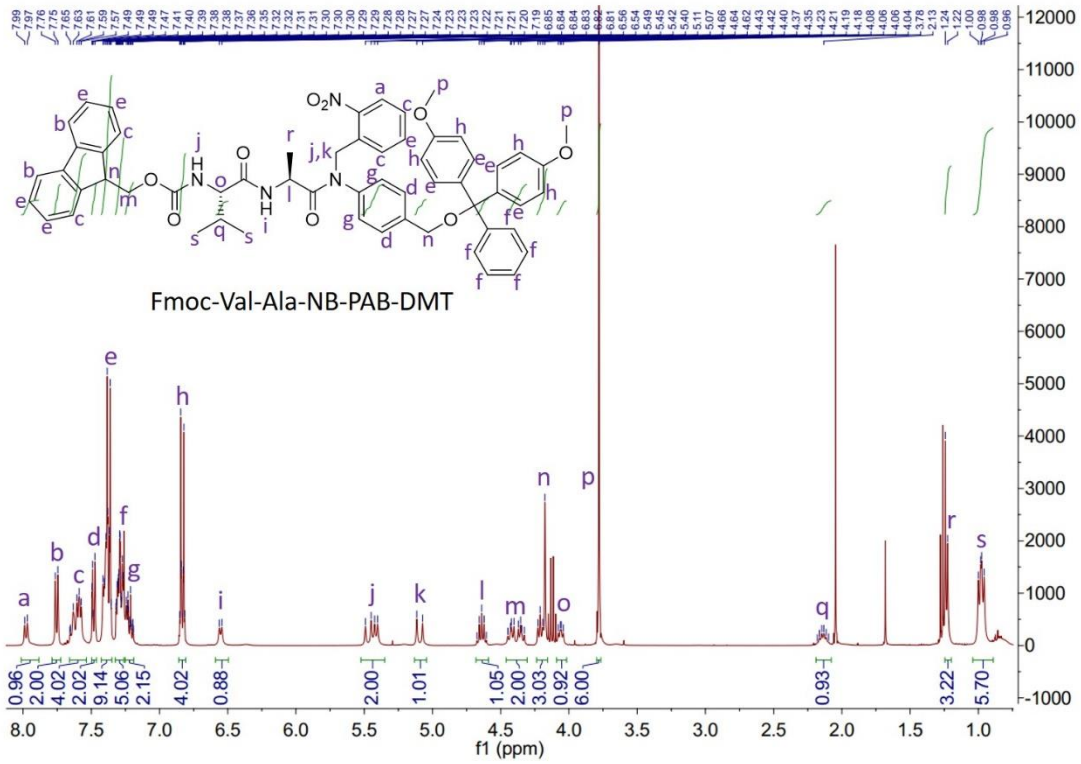

Figure S65. ^{1}H NMR of Fmoc-Val-Ala-NB-PAB-DMT.

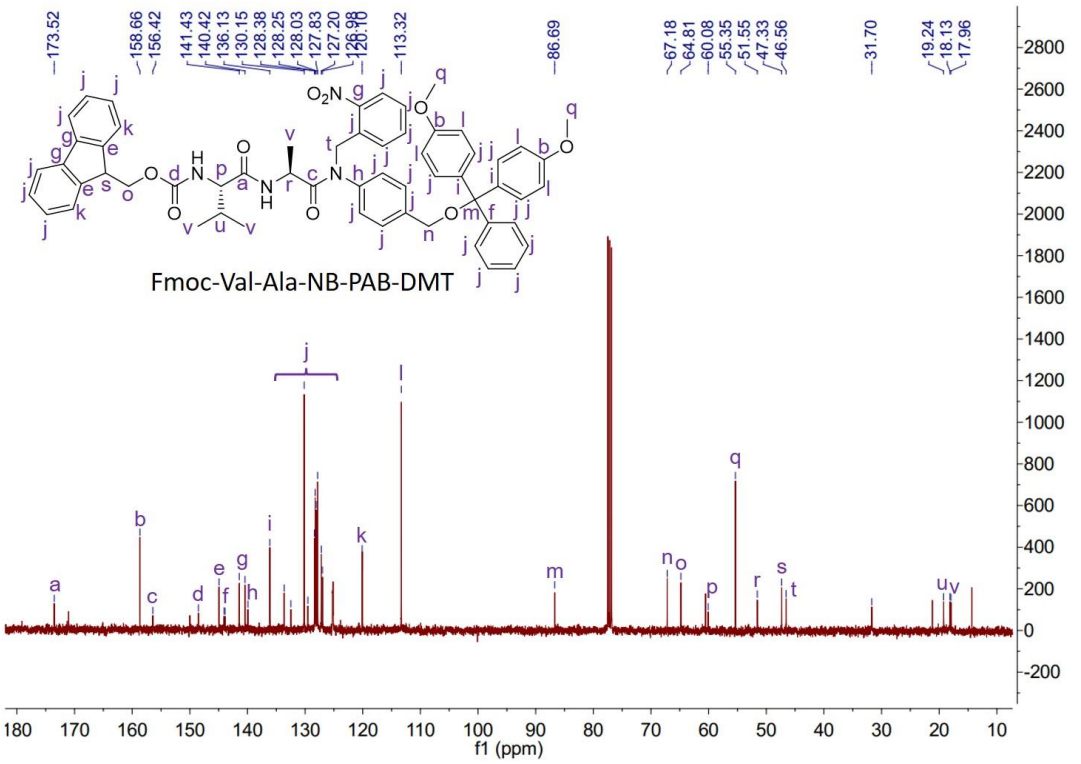

Figure S66. ^{13}C NMR of Fmoc-Val-Ala-NB-PAB-DMT.

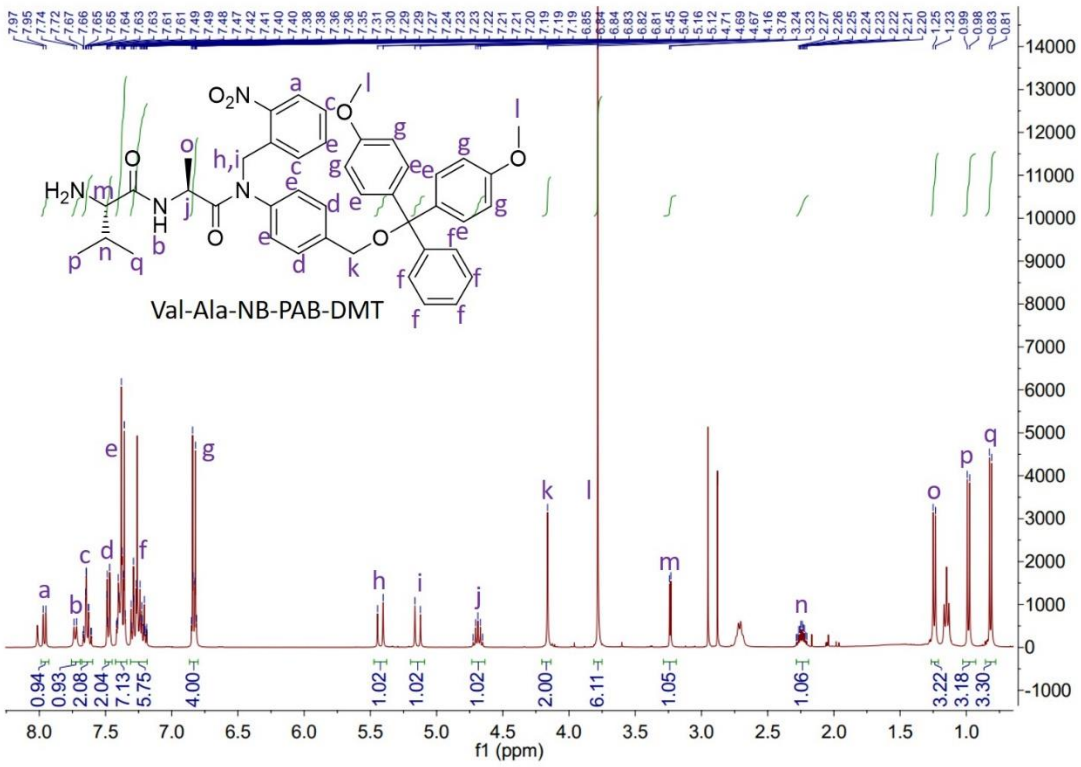

Figure S67. ^{1}H NMR of Val-Ala-NB-PAB-DMT.

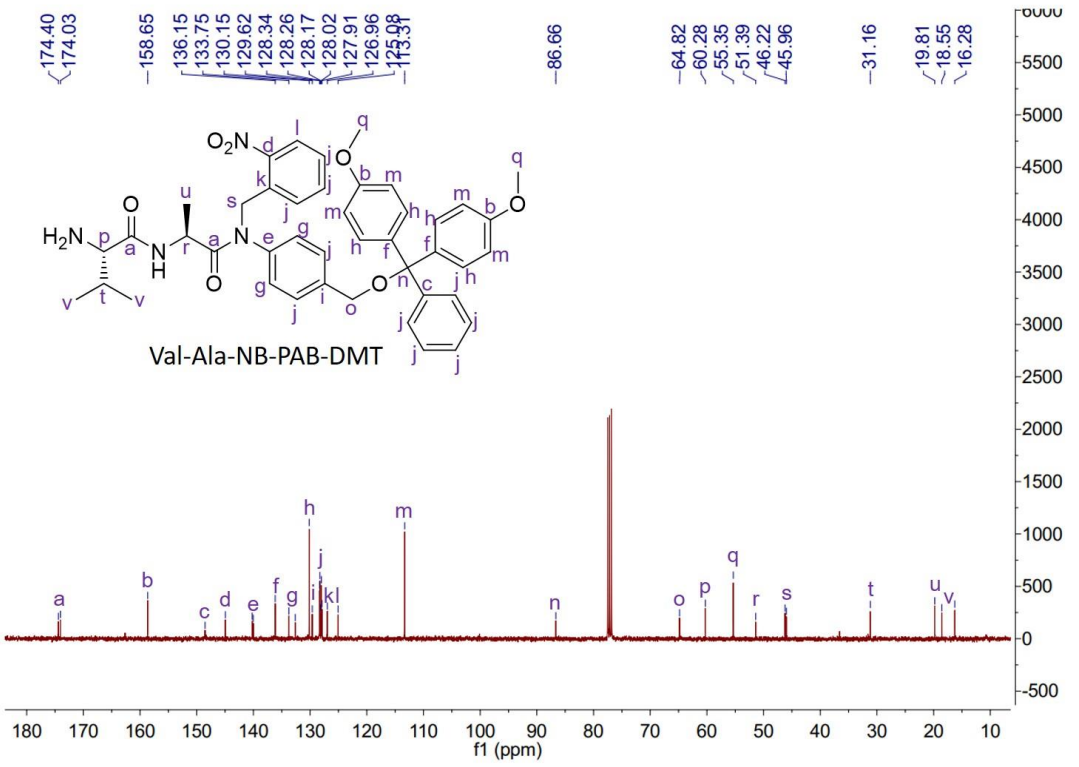

Figure S68. ^{13}C NMR of Val-Ala-NB-PAB-DMT.

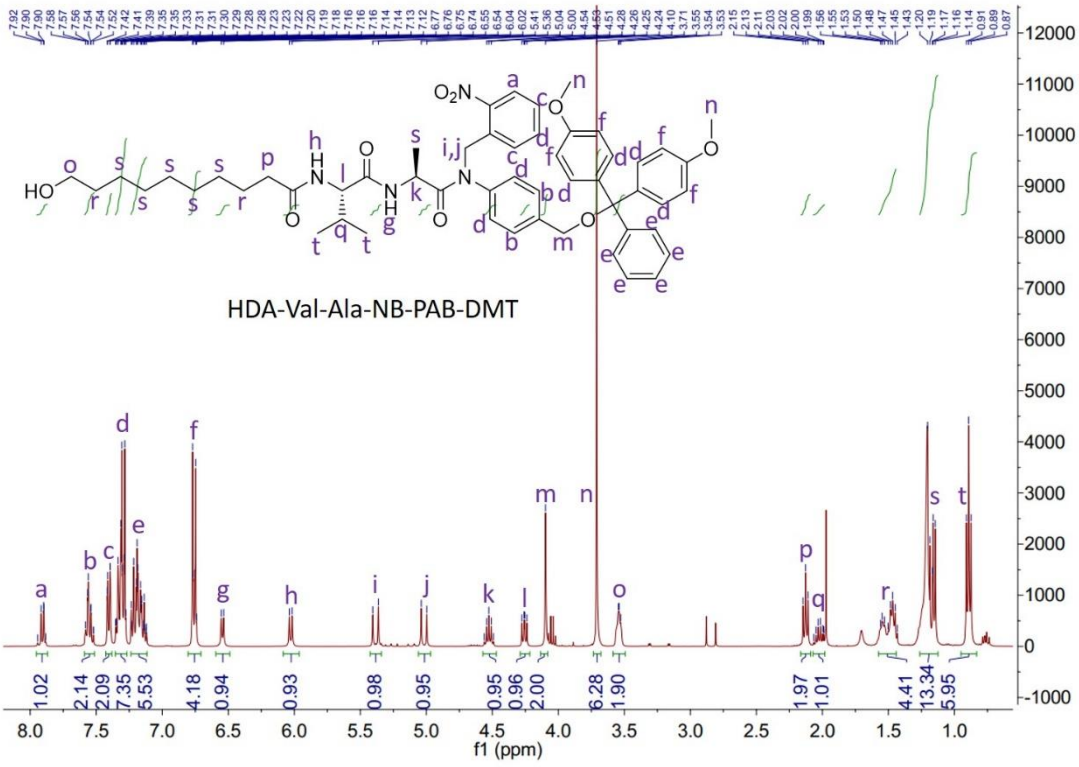

Figure S69. ^{1}H NMR of HDA-Val-Ala-NB-PAB-DMT.

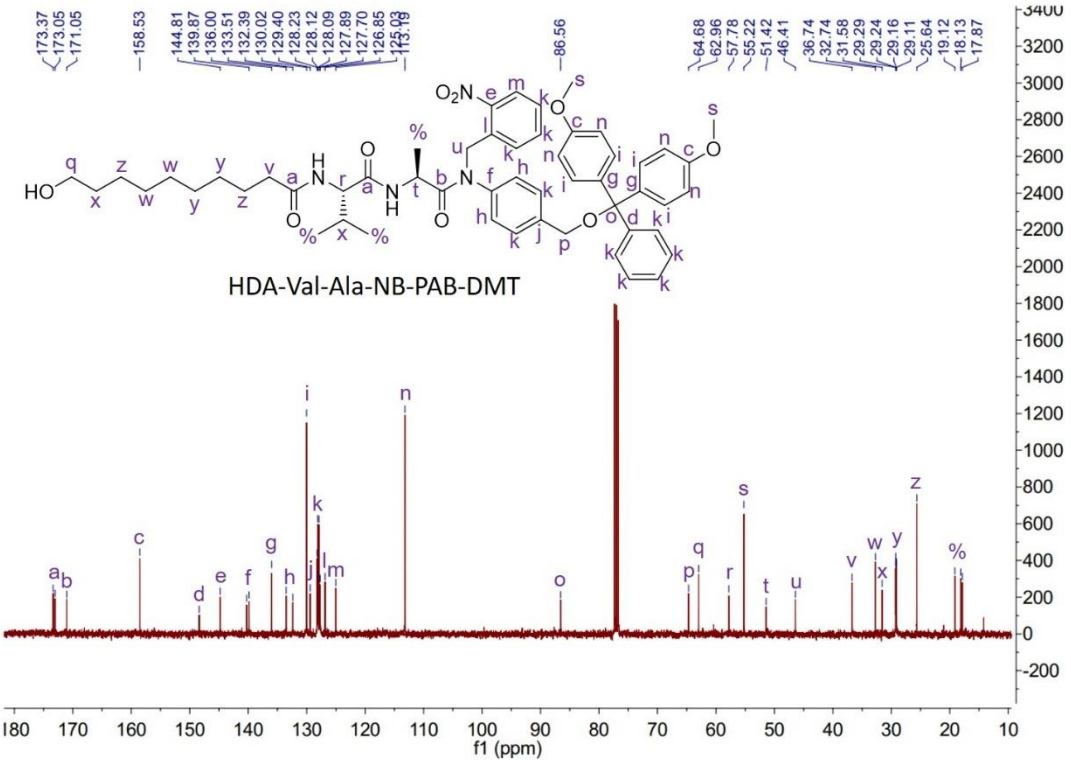

Figure S70. ^{13}C NMR of HDA-Val-Ala-NB-PAB-DMT.

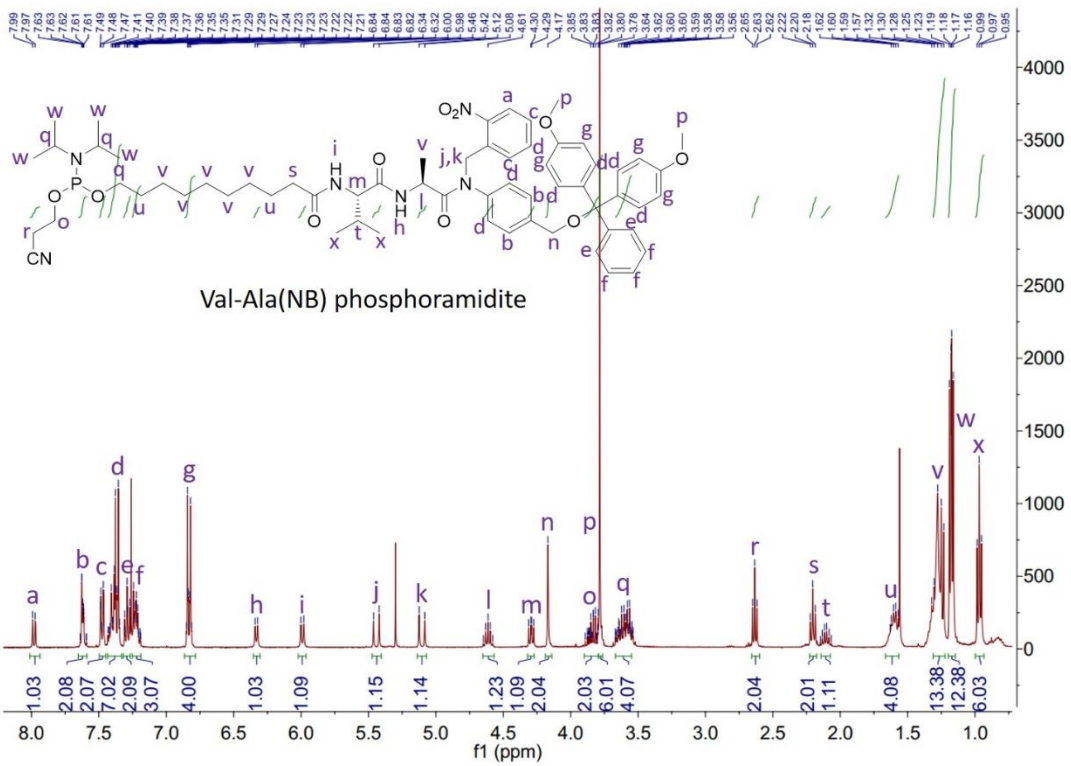

Figure S71. ^{1}H NMR of Val-Ala(NB) phosphoramidite.

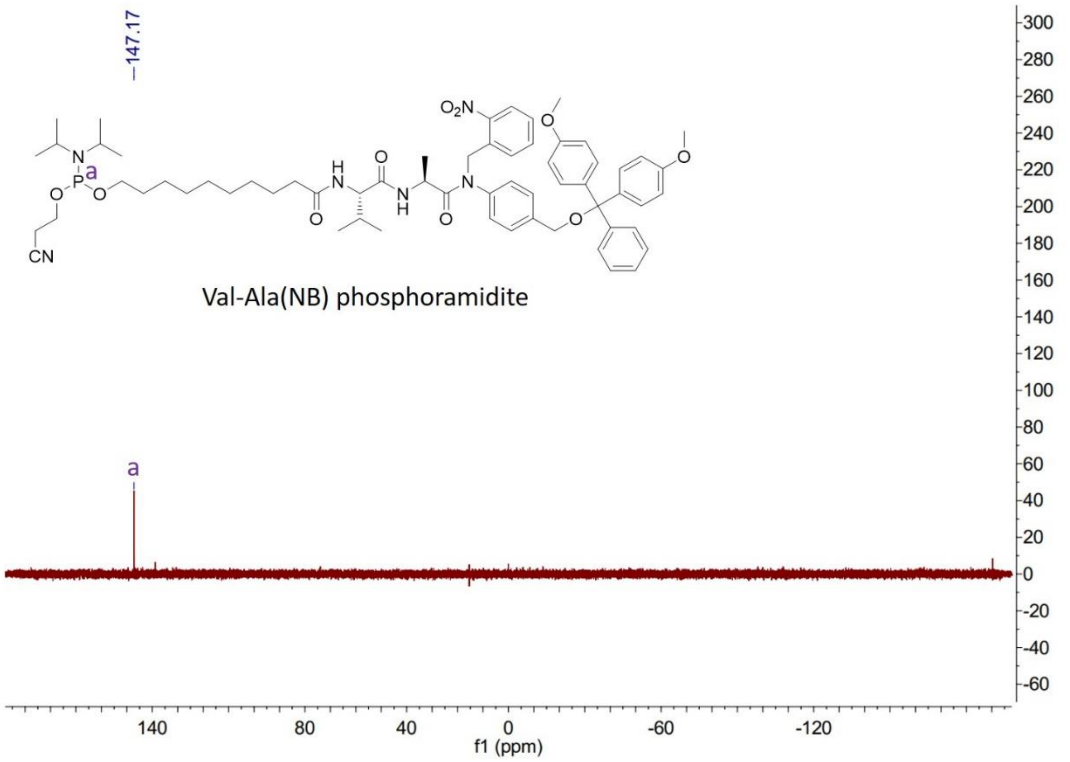

Figure S72. ^{31}P NMR of Val-Ala(NB) phosphoramidite.

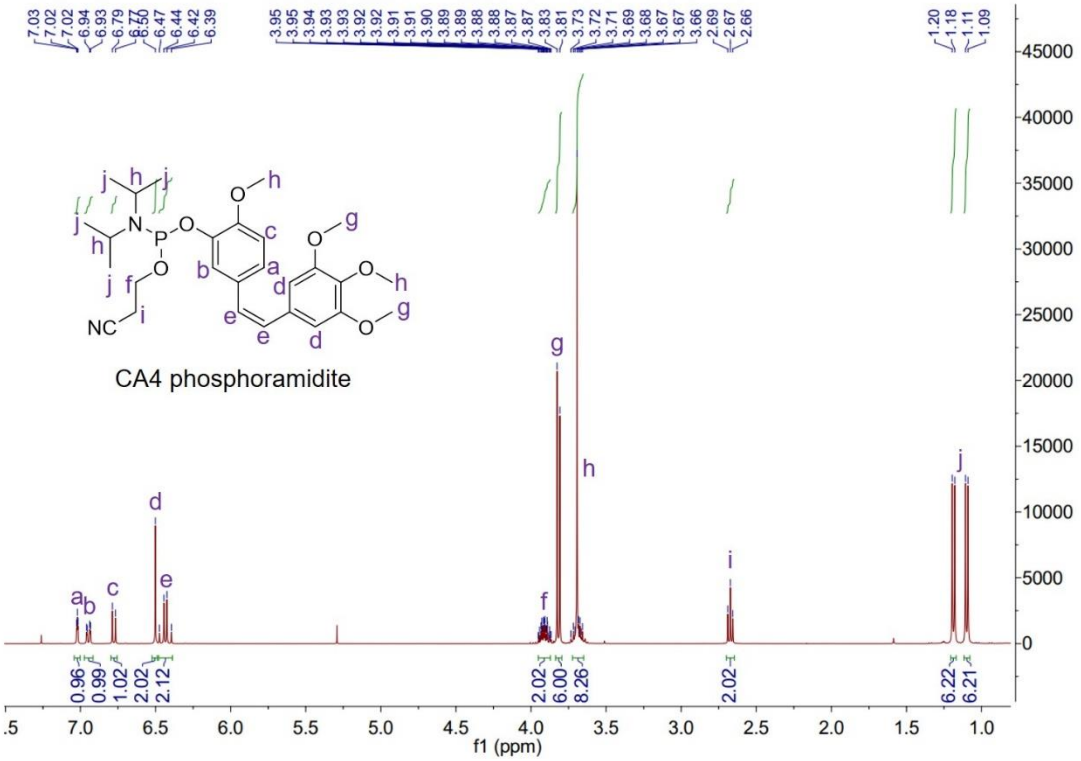

Figure S73. ^{1}H NMR of CA4 phosphoramidite.

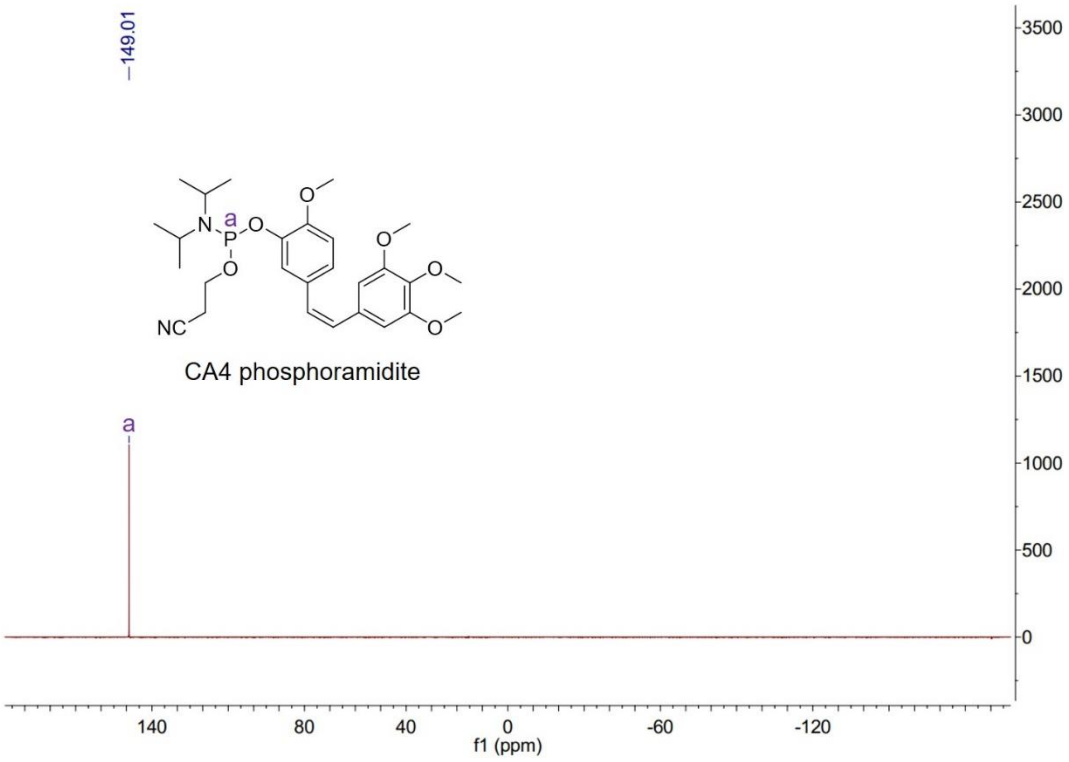

Figure S74. ^{31}P NMR of CA4 phosphoramidite.

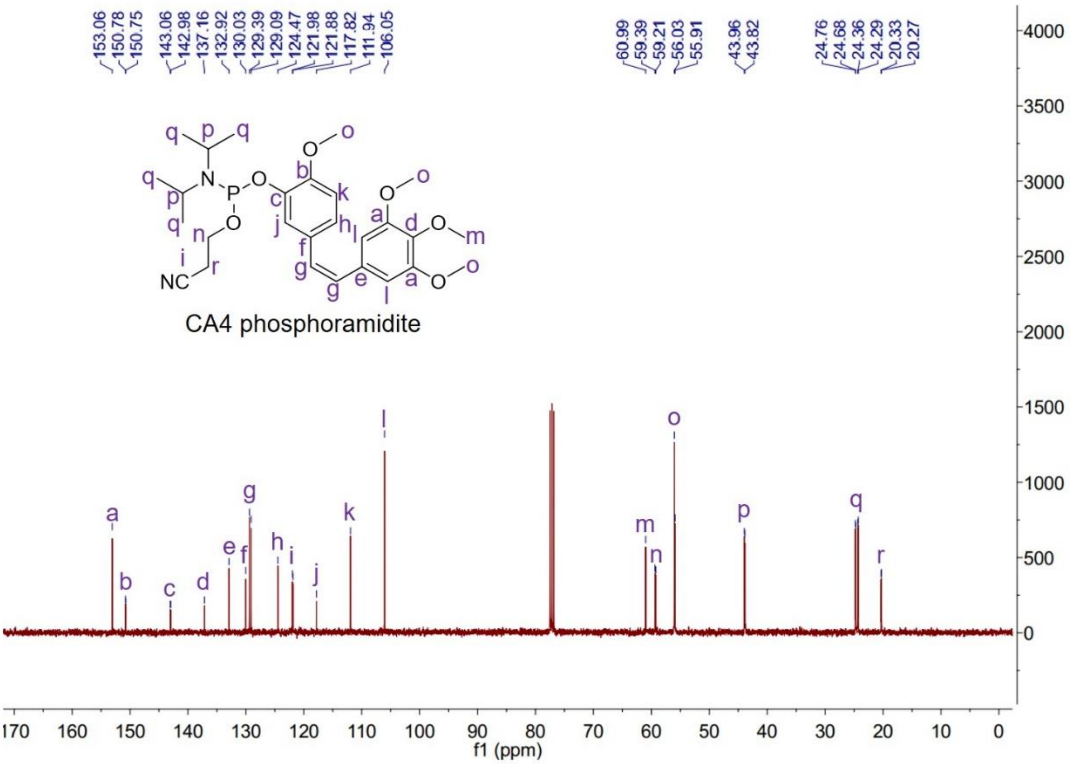

Figure S75. ^{13}C NMR of CA4 phosphoramidite.

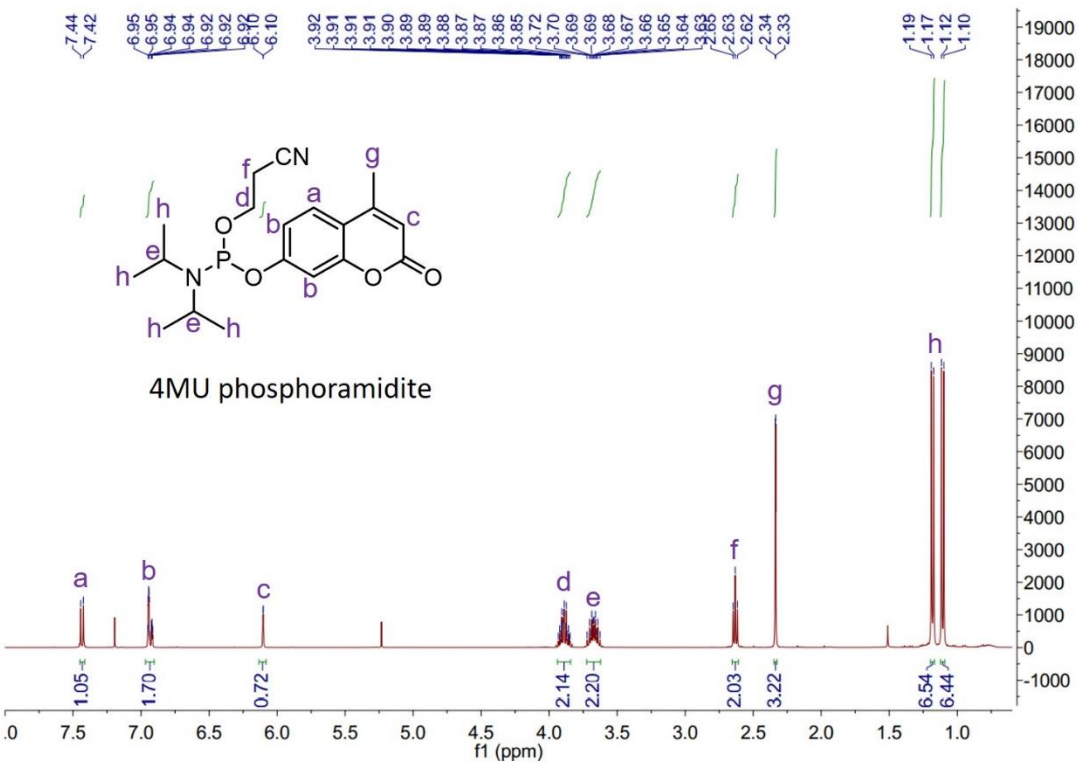

Figure S76. ^{1}H NMR of 4MU phosphoramidite.

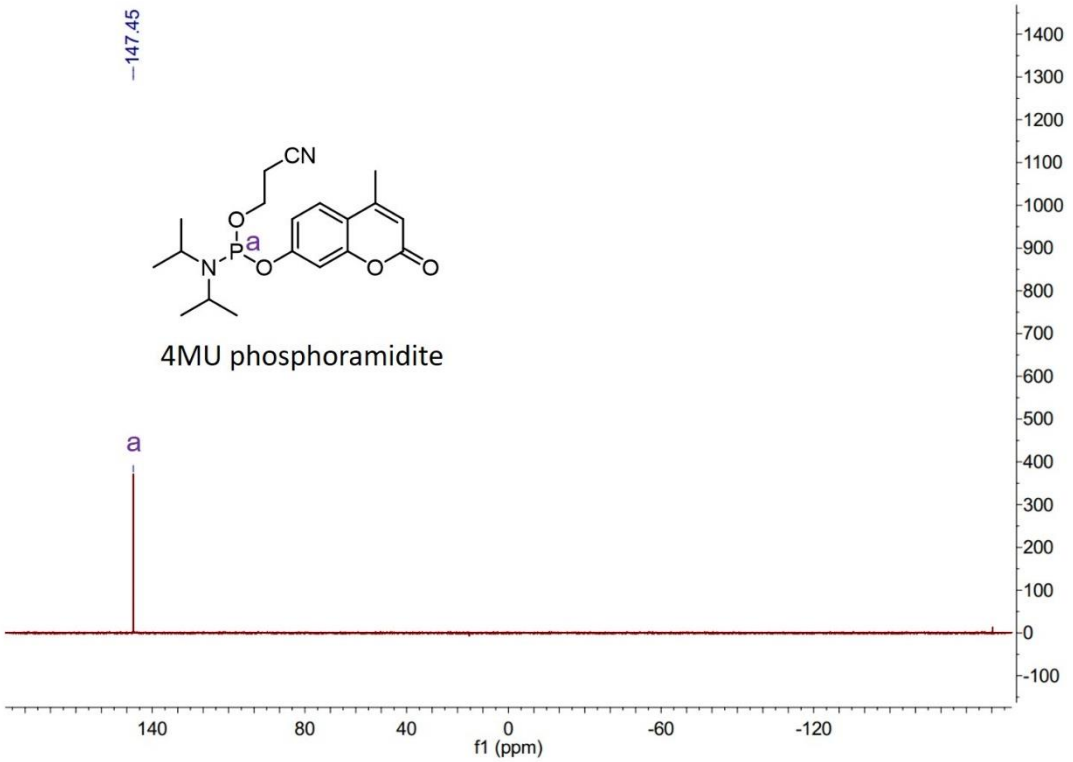

Figure S77. ^{31}P NMR of 4MU phosphoramidite.

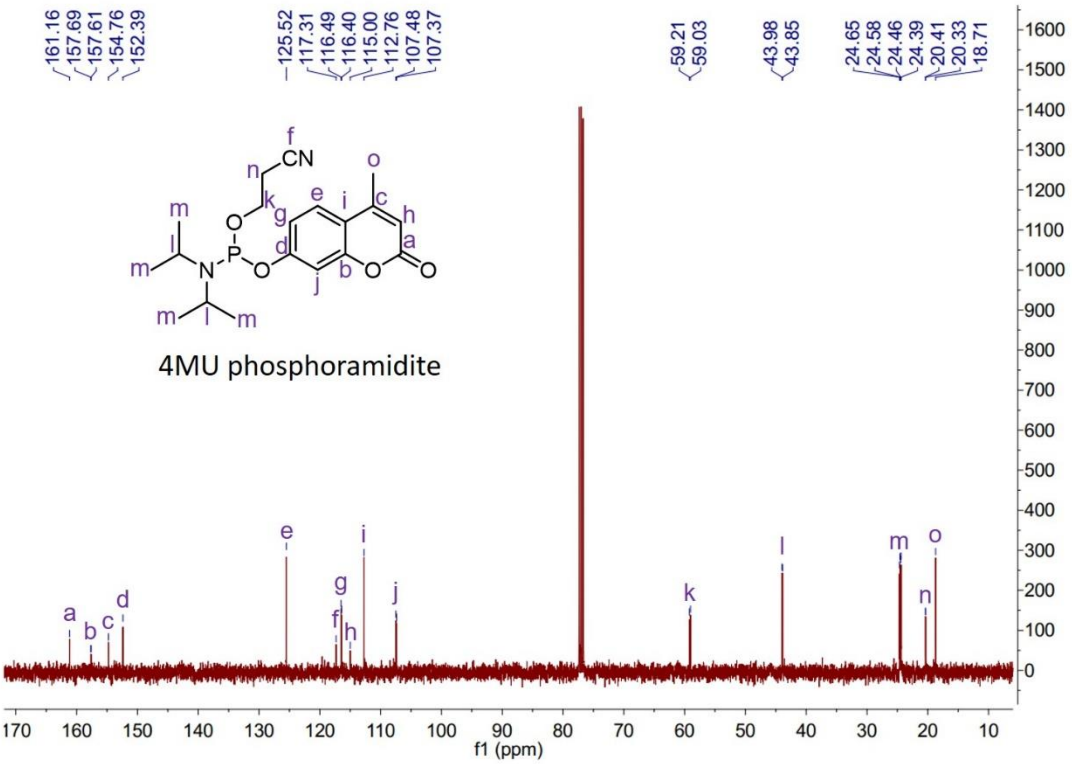

Figure S78. ^{13}C NMR of 4MU phosphoramidite.

6. References

1. C. Jin, A. H. Ei-Sagheer, S. Q. Li, K. A. Vallis, W. H. Tan and T. Brown, *Angew. Chem. Int. Ed.*, 2022, **61**, e202114016.